Diese Arbeit wurde vorgelegt am
Lehr- und Forschungsgebiet Theorie der hybriden Systeme

Optimale Gebäudesteuerung mittels Systemlinearisierung auf Basis eines verallgemeinerten physikalischen Modells

Optimal building control using system linearization based on a generalized physics model

Masterarbeit
Informatik

März 2021

Vorgelegt von Presented by	Stefan Leachu Königstraße 32 52064 Aachen Matrikelnummer: 354435 Stefan.Leachu@rwth-aachen.de
Erstprüfer First examiner	Prof. Dr. rer. nat. Erika Ábrahám Lehr- und Forschungsgebiet: Theorie der hybriden Systeme RWTH Aachen University
Zweitprüfer Second examiner	Prof. Dr. rer. nat. Christina Büsing Lehrstuhl II für Mathematik RWTH Aachen University
Betreuer Supervisor	M. Sc. Ahmed Abida Lehr- und Forschungsgebiet: Theorie der hybriden Systeme RWTH Aachen University

Eigenständigkeitserklärung

Hiermit versichere ich, dass ich diese Masterarbeit selbständig verfasst und keine anderen als die angegebenen Quellen und Hilfsmittel benutzt habe. Die Stellen meiner Arbeit, die dem Wortlaut oder dem Sinn nach anderen Werken entnommen sind, habe ich in jedem Fall unter Angabe der Quelle als Entlehnung kenntlich gemacht. Dasselbe gilt sinngemäß für Tabellen und Abbildungen. Diese Arbeit hat in dieser oder einer ähnlichen Form noch nicht im Rahmen einer anderen Prüfung vorgelegen.

Aachen, im März 2021

Stefan Leachu

Contents

Nomenclature

$\alpha_{W_i,ex}$	Solar absorptivity of external wall surface i	-
β	Tilting angle of the surface to the horizontal	$^\circ$
$\dot{m}$	Mass flow of water in radiator	kgs^{-1}
$\dot{Q}$	Rate of heat	W
$\dot{Q}_{floor}$	Heat flow of floor heating	W
$\dot{Q}_{j,\mathrm{Rad}}$	Rate of heat from internal radiation source j	W
$\dot{Q}_{radiator}$	Heat flow of radiator	W
$\dot{Q}_{W_i}$	Heat flow of wall i	W
γ	Surface azimuth angle	$^\circ$
ω	Hour angle	$^\circ$
ρ_g	Ground reflectance	-
ρ_{A}	Density of air	kgm^{-3}
ρ_{W}	Density of water	kgm^{-3}
σ	Stefan-Boltzmann constant	$5.67 \cdot 10^{-8}\ \mathrm{Wm}^{-2}\mathrm{K}^{-4}$
$\tau_{\mathrm{D},j}$	Direct solar radiation transmissivity of window j	-
$\tau_{\mathrm{d},j}$	Diffuse solar radiation transmissivity of window j	-
θ	Solar beam angle	$^\circ$
θ_{h}	Solar beam angle to the horizontal plane	$^\circ$
ε	Emissivity	-
$\varepsilon_{\mathrm{MRT},i}$	Emissivity of MRT-surface considering object i	-
$\varepsilon_{\mathrm{WG_i}}$	Emissivity of window i	-
$\varepsilon_{W_i,ex}$	Long wave emissivity of external wall surface i	-
$\varepsilon_{W_i,in}$	Long wave emissivity of interior wall surface i	-
A	Area	m^2
$A_{\mathrm{MRT},i}$	Area of MRT-surface considering object i	m^2

A_{tot}	Sum of all area of all enclosed surfaces within a zone	m^2
$A_{\mathrm{WG},j}$	Area of window j	m^2
A_{floor}	Area of floor	m^2
C	Overall heat capacity $c_{\mathrm{A}}\rho_{\mathrm{A}}V$	JK^{-1}
c_{W}	Specific heat capacity of water	$\mathrm{JK}^{-1}\mathrm{kg}^{-1}$
C_t	Turbulent natural convection constant	$0.84\ \mathrm{Wm}^{-2}\mathrm{K}^{-4/3}$
c_{A}	Specific heat capacity of air	$\mathrm{JK}^{-1}\mathrm{kg}^{-1}$
d	Declination angle	$^\circ$
$F_{\mathrm{MRT},i}$	Shape factor between MRT-surface and object i	-
$F_{W_i,A}$	Shape factor between external wall surface i and outdoor air	-
$F_{W_i,G}$	Shape factor between external wall surface i and ground	-
$F_{W_i,S}$	Shape factor between external wall surface i and sky	-
H	Characteristical length	m
h	Heat transfer coefficient	$\mathrm{Wm}^{-2}\mathrm{K}^{-1}$
$h_{W_i,\mathrm{RadG},ex}$	Radiant heat transfer coefficient for ground	$\mathrm{Wm}^{-2}\mathrm{K}^{-1}$
$h_{W_i,\mathrm{RadO},ex}$	Radiant heat transfer coefficient for outdoor air	$\mathrm{Wm}^{-2}\mathrm{K}^{-1}$
$h_{W_i,\mathrm{RadS},ex}$	Radiant heat transfer coefficient for sky	$\mathrm{Wm}^{-2}\mathrm{K}^{-1}$
$h_{W_i,conv,ex}$	Convective heat transfer coefficient at exterior wall surface i	$\mathrm{Wm}^{-2}\mathrm{K}^{-1}$
$h_{W_i,conv,in}$	Convective heat transfer coefficient at interior wall surface i	$\mathrm{Wm}^{-2}\mathrm{K}^{-1}$
I_0	Solar constant	$1367\ \mathrm{Wm}^{-2}$
$I_{\mathrm{D,h}}$	Intensitiy of direct radiation to the horizontal plane	Wm^{-2}
I_{d}	Intensity of diffuse radiation	Wm^{-2}
I_{el}	Electrical current	A
I_{E}	Extraterrestrial radiation	Wm^{-2}
$I_{\mathrm{T,h}}$	Horizontal intensity of solar radiation	Wm^{-2}
$I_{j,\ \mathrm{d}}$	Diffuse radiation intensity on a surface in the same direction as window j	Wm^{-2}

$I_{j,D}$	Direct radiation intensity on a surface in the same direction as window j	$\mathrm{Wm^{-2}}$
$I_{W_i,T,ex}$	Total intensity of solar radiation at external wall surface i	$\mathrm{Wm^{-2}}$
k	Thermal conductivity	$\mathrm{Wm^{-1}K^{-1}}$
k_{C}	Clearness index of the sky	-
L	Thickness of material	m
l	Latitude angle with positive values for northern position	$^\circ$
L_0	Longitude of standard meridian (west positive)	$^\circ$
L_{loc}	Longitude of investigated location (west positive)	$^\circ$
n_{day}	Number of day in the year	-
P	Electrical power	W
Q	Heat	J
q	Heat flux	$\mathrm{Wm^{-2}}$
q_{Bal}	Balance heat flux for MRT-method	$\mathrm{Wm^{-2}}$
$q_{W_i,conv,ex}$	Convective heat flux at exterior wall surface i	$\mathrm{Wm^{-2}}$
$q_{W_i,conv,in}$	Convective eat flux at interior wall surface i	$\mathrm{Wm^{-2}}$
$q_{W_i,rad,ex}$	Radiant heat flux at exterior wall surface i	$\mathrm{Wm^{-2}}$
$q_{W_i,radInt,in}$	Radiant heat flux at interior wall surface i from internal sources	$\mathrm{Wm^{-2}}$
$q_{W_i,radS,in}$	Radiant heat flux at interior wall surface i from long wave radiation by enclosed surfaces	$\mathrm{Wm^{-2}}$
$q_{W_i,sol,ex}$	Solar heat flux at exterior wall surface i	$\mathrm{Wm^{-2}}$
$q_{W_i,sol,in}$	Solar flux at interior wall surface i	$\mathrm{Wm^{-2}}$
$q_{WG_i,ex}$	Heat flux at exterior window surface i	$\mathrm{Wm^{-2}}$
$q_{WG_i,in}$	Heat flux at interior window surface i	$\mathrm{Wm^{-2}}$
$q_{WG_i,radInt,in}$	Radiant heat flux at interior window surface i from internal sources	$\mathrm{Wm^{-2}}$
$q_{WG_i,radS,in}$	Radiant heat flux at interior window surface i from long wave radiation by enclosed surfaces	$\mathrm{Wm^{-2}}$
R_{el}	Electrical resistance	Ω

SLF_j	Fraction of area of window j with direct solar radiation contact	-
T	Temperature	°C
t	Time	s
T_G	Ground temperature	°C
T_i	Interior ai temperature	°C
T_o	Outside air temperature	°C
T_S	Sky temperature	°C
$T_{\mathrm{Avg,G,o}}$	Average temperature between ground and outside air	°C
$T_{\mathrm{Avg,o,W_i}}$	Average temperature between outside air and wall i	°C
$T_{\mathrm{Avg,S,o}}$	Average temperature between sky and outside air i	°C
t_{Clock}	Local time	
$T_{\mathrm{MRT},i}$	Temperature of MRT-surface considering object i	°C
t_{Sol}	Solar time	
T_{air}	Air temperature	°C
T_{in}	Inlet water temperatur of radiator	°C
T_{out}	Outlet watet temperatur of radiator	°C
$T_{W_i,ex}$	Exterior wall surface temperature	°C
$T_{W_i,in}$	Interior wall surface temperature	°C
T_{WG_i}	Window glazing temperature	°C
v_0	Wind speed	ms^{-1}
V_{el}	Electrical voltage	V
W_i	Wall i	
WG_i	Window i	
Z_i	Zone i	
HVAC	Heating, Ventilation and Air Conditioning	

1. Introduction

1.1. Motivation and problem definition

Climate change is on everyone's lips. Year after year, more and more electrical energy is consumed (cf. [54]). In 2020, the total energy consumption was dominated by the commercial and residential sector, which accounted for 40% (cf. [15]). Thereby, 50% of energy demand in buildings is caused by HVAC-systems (Heating Ventilation Air Conditioning). The situation in the USA is comparable. The buildings create an amount of 70% of the electricity consumption, where the HVAC-system of buildings uses 30% of the total energy consumption (cf. [54]), and a stagnation of these values is not detectable.

Moreover, studies have pointed out that HVAC-systems have equipment and operational problems, leading to side effects (cf. [54]). In fact, besides the lower indoor comfort within buildings, in the case of HVAC, it provokes the waste of around 4% to 20% of consumed energy.

Additionally, the changing climate conditions put the main focus on sustainability. That is why there is much research in the context of building optimization to avoid wasting and help saving energy. In general, there are three approaches used in practice to model characteristics of buildings (cf. [13]). Their insight possibilities name these models. The most non-transparent one is the black-box model. It uses statistic approaches to extract relations from already gathered data. White-box models are the most transparent ones because they are based on physics equations describing the relations. Between these two, the grey-box model is combing both of them. The rise of the artificial intelligence trend has especially pushed data-driven optimization used in grey-box and black-box modeled approaches. But just like that, through the computational strength of modern computer also the physics-based, white-box, approach gained more attention (cf. [41]). Next to the artificial intelligence methodology, rc-networks (analogy to resistor and capacitance from electric circuits (cf. [13])) are the most popular for grey-box modeling (cf. [30]). However, white-box approaches capture the whole dynamics in buildings accurately and are favored when representing processing signals of HVAC-systems (cf. [54, 41]). In comparison, white-box models are identified to lead to 50% less energy consumption than in the same grey-box modeled building when regulating temperature (cf. [69]).

Furthermore, white-box models do not rely on specific building data when training the model compared to black-box and grey-box approaches. Therefore, it is more suitable when the model should generally be applicable to more buildings, i.e. it is a more generalized and flexible model. However, since it is based on physical relations, they are well known as non-linear in most cases.

When considering non-linear functions in the context of mathematical optimization, they can lead to problems. As known from mathematical analysis, non-linear functions have got local and global optima. In the case of optimization, this differentiation leads to problems: It can not be guaranteed that a global optimum can be found in finite time, which could lead to no solution at all (cf. [64]). In contrast, linear functions

do not exhibit this behavior so that they enable finding global optima efficiently in polynomial time (cf. [44]). This class of optimization is called linear programming.
For applying linear programming to non-linear functions, the investigated function can be linearized to obtain the desired goal. Nevertheless, this approximation results in an error and can be concluded into a tradeoff between accuracy and simplicity. However, Picard et al. [68] have pointed out that linearized building optimization can be performed with a minor error of ± 1K in temperature.
On this basis, optimal control for buildings is focused. This means that building optimization in terms of energy consumption combined with a white-box model and linearization is investigated in this thesis to predict an optimal control strategy for a building.

1.2. Related work

With the focus of the thesis, this section considers related work in the area of linear building optimization based on white-box models. This contains the three steps of building modeling, linearization and optimization.

Building modeling

Author	Objective
Ashouri et al. [17]	optimization of linear grey-box model
Skruch [76]	modeling framework for white-box model
Underwood and Yik [80]	derivation of white-box model based on physical explanations
Clemens [29]	white-box model of solar impact on buildings

Table 1: Summary table of building modeling.

Harish and Kumar review 52 paper about building modeling including optimization on ten categories. For example, they distinguish between the modeled subsystem of buildings (walls, doors, etc.), the modeling approach and the optimization method. It is noticeable that only seven paper make white-box models a subject of discussion, while Ashouri et al. [17] presents the only paper which deals with linear optimization for energy minimization. But, they do not model the building itself. They consider the building a basic single zone in a 1R1C thermal model. Additionally, building services, such as pumps and storages, are added. In fact, all used relations are linear. So, linearization is not needed.
Based on the first thermodynamic law (cf. subsection 2.2), Skruch [76] defines a generalized building modeling framework considering a basis thermal model dispatching thermal power by conduction and ventilation, and gaining heat by radiators, the sun and internal sources. Optimization is not applied.
Underwood and Yik [80] show a detailed discussion for energy transfer within buildings. It is based on physical relations and considers all detailed side effects. Moreover,

details about assumptions, simplifications, linearization and implementation are provided.
The energy impact of solar radiation is stated with an equation to the power four (cf. subsection 2.2). Clemens [29] shows a linear approximation of its energy impact. It is embedded into a simulation of overheating of buildings where the temperature is modeled as one thermal zone which is affected only by solar radiation.
In conclusion, white-box models are generally based on the first thermodynamic law considering an equilibrium of energy balance within thermal zones (cf. e.g. [57, 62, 13, 61]).

Linear building optimization

Author	Linearization method
Picard et al. [68]	Taylor approach with Jacobian linearization and finite differences
Antunes et al. [15]	Finite differences
Pinzon et al. [70]	Linearization of individual polynomials by Taylor + finite differences + regression
Wu and Sun [85]	Simplified linear relation for radiation
Pajot et al. [67]	Taylor approach

Table 2: Summary table of linear building optimization.

When it comes to linearizing building models, Picard et al. [68] propose an approach based on first-order Taylor polynomials in combination with Jacobian linearization and finite differences. They obtain an error typically below $\pm$ 1K in the course of the building temperature. Additionally, in [69] the model is further analyzed with an error mostly smaller than $\pm$ 0.1K.
Antunes et al. [15] discuss models for mixed integer linear programming (MILP) to optimize the energy cost for thermostatically-controlled AC systems. Next to the basic room modeling, which is based on an energy balance with averaged conductive heat transfer and neglected internal loads, they use the approach of finite differences over time-steps Δt for linearization.
Also, quadratic programming is used for optimizing an HVAC-system with variable air volume (VAV), as indicated in [45]. Next to the fact that they could find only local optima, they use the trapezoidal discretization for approximating the time variation as piecewise time steps of zone temperatures.
A related approach with discrete time steps is suggested by Pinzon et al. [70]. However, the linearization is not performed globally for the whole equation. They investigate individual non-linear polynomials with three different approaches, Taylor, finite differences and regression for already gathered data.
Another estimate for linear optimization is proposed by Wu and Sun [85]. Their approximation considers only linear phenomena, such as steady state conduction (cf. section 2.2) in the energy balance, which leads to a linear system. Besides, they use a

simplified linear equation for the approximated impact of radiation
Even if the focus is set on white-box models, grey-box models must also be linearized when it comes to linear optimization. Yokoyama et al. [87] approximate the used rc-network by linear lower and upper boundaries, which are explained in the paper. Pajot et al. [67] similarly proceed who explained the approximation of solar radiation, on the one hand by a fixed value and on the other hand by a linear depending value based on a tailer development for the surface temperature.
Also, the results of Ostadijafari and Dubey [66] show that a feedback-based linearization performs as well as a non-linear one in the context of a closed-loop model-predictive controller of HVAC-systems reducing energy costs. The reason for this is the nature of the linearization method, which is also called the exact linearization, and does not produce any approximation errors (cf. [12]). However, it is essential to highlight that the other optimizations of buildings are based on open-loop control to predict a control strategy which is also the focus of this thesis.

All in all, this section shows that there is no consistent approach from a structured starting point of modeling a generalized building until efficiently optimizing its energy costs.

1.3. Research question

To conclude, the goal of this thesis consists of setting up a structured approach to optimize the energy costs of a building. This includes a generalized white-box model for buildings so that it is applicable as a modular framework in representing static properties of buildings and, secondly, their thermal dynamics. In the next step, the mathematical part of that model must be linearized suitably. Afterwards, the model is optimized via a linear program.
Within the scope of the thesis, the following research question (RQ) is answered:

RQ: How can the energy costs of an HVAC-building be optimized in terms of linear programming?

Besides, the subsequent subquestions are used to indicate the workflow:

RQ1: How can constructional characteristics of a building be described in a logical representation?

RQ2: How can dynamic heat transfers within a building be modeled?

RQ3: How can a linear program be used for optimizing that building model?

Moreover, the following subquestions are answered when the derived approach is validated with a case study:

a. Which effects have interpolation in the case of linearization?

b. Which effects have the time difference, Δt, when approximating the next state of the building?

c. Which effects have energy prices on the optimization?

d. Which effects have weather on the model?

e. Which effects have building configurations on the optimization?

1.4. Outline

The thesis is structured as follows. First, section 2 focuses on building modeling. Thereby, a generic white-box model is derived from physical relations based on investigating different building components, such as walls, and heating devices, such as radiators. In section 3, the approach of optimization is explained. This includes the adaptation of the building's model to be used as a valid input for optimization. Afterwards, the implementation of general problems is thematized. Then, a case study is performed to evaluate the whole concluded approach. In the end, a conclusion is drawn, and aspects for future work are pointed out.

2. Thermodynamics and building modeling

To discuss the optimization of heat costs in buildings in the following chapters, it is necessary to have a copy of reality first, on which the optimization acts. For this purpose, a generally valid thermal model has to be derived, which illustrates a building's heat dynamics.
Thus, the chapter is structured as follows. In the beginning, the applied methodology is presented. The next section states the basic principles of thermodynamics required for modeling (see subsection 2.2). Subsequently, the first submodel, a static model for buildings' structural properties, is explained in subsection 2.3. Then, the second submodel based on physics is given to show the heat transfers within buildings without heating or cooling elements (see section 2.4). Afterwards, different components of an HVAC-system are investigated, and their thermal effects are added to the model (see subsection 2.5). In the end, the complete model is given in subsection 2.6.

2.1. Methodology

The process of deriving a generally valid model is inspired by Hoffmann [40] and is based on model theory. Thus, in this section, an explanation model is derived, which indicates the heat transfer within a building. It is deduced from two submodels. Thereby, the submodels have a purely descriptive function and represent empirical observations, whereas the explanation model combines correlations, regularities, and causes from the submodels to improve them, predict future behavior or explain a behavior (cf. [40]).
In fact, the searched explanation model (III.), representing the dynamic heat behavior of buildings, is based on two submodels (I. + II.; see Figure 1).

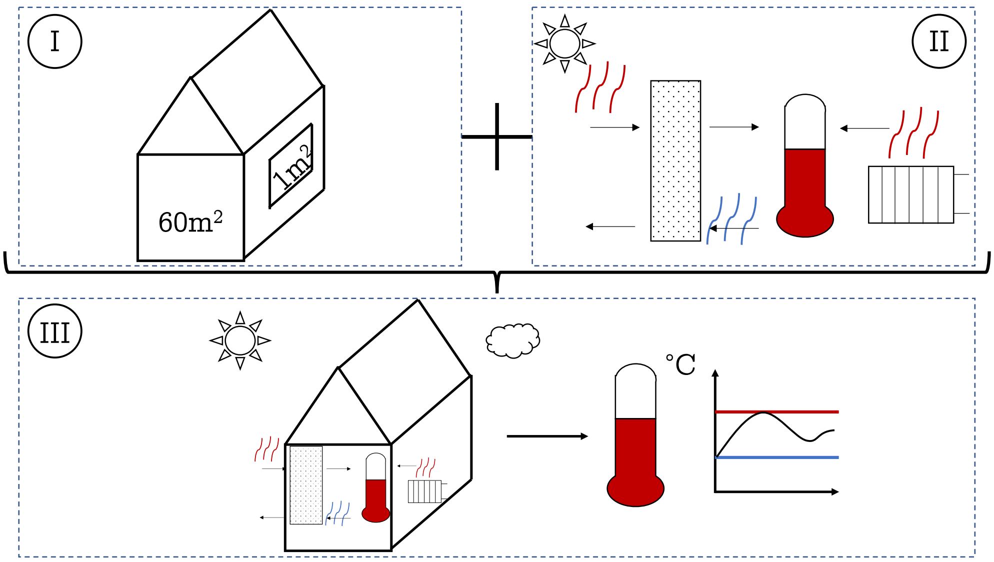

Figure 1: The explanation of heat transfer within a building is based on two individual submodels.

In heat transfer background, a building is defined by its constructions since these imply further heat movements. So, the first submodel (I.) is completely uncoupled of dynamic thermal processes and shows the constructional properties of buildings, e.g. room sizes, wall thicknesses, and used materials. In other words, it formalizes a static and logical representation of a building.
The second submodel (II.) concludes the thermodynamic processes of heat transfer within buildings in general, i.e. per generic square meter. It shows the broad impact of heat on building elements, such as walls, windows, or HVAC-components.
In conclusion, the explanatory model, the combination of the two descriptive models above, clarifies how heat acts in a building.

2.2. Thermodynamics foundations

Cengel [27] introduces thermodynamics as the science describing the amount of heat transfer, which a system performs when changing from one equilibrium state to another. Moreover, it does not indicate the needed time. The rate of heat transfer is the exciting part.
The necessary basics of thermodynamics needed for the main goal, especially about heat transfer, are given in this section. Thereby, the physical rules and explanations are based on El Hefni and Bouskela [33], Cengel [27] and Bergman [23].

2.2.1. Types of systems

In general, in thermodynamics, three types of systems can be identified depending on their mass and energy exchange capability beyond systems boundaries (cf. Figure 2).

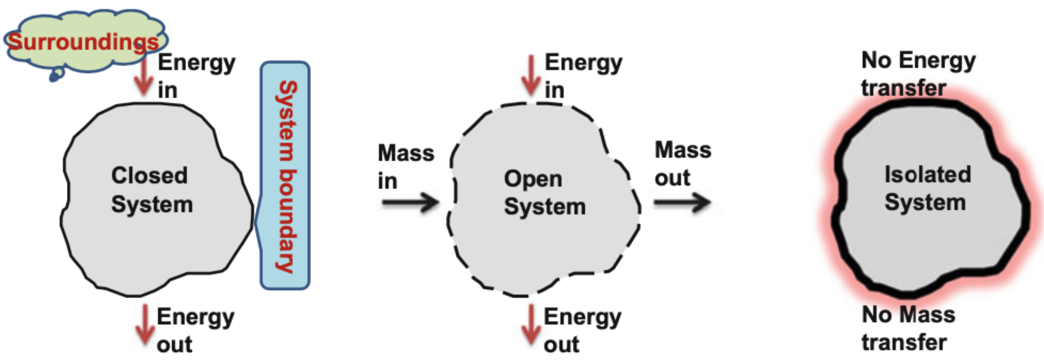

Figure 2: Three types of thermodynamic systems (see [33]).

Isolated systems are the simplest ones. As the name indicates, they are entirely isolated from the environment. Therefore, they exchange neither energy nor mass across their boundaries. These systems are an idealization of reality.

Closed systems have a fixed amount of mass. This means that no mass can cross the system's boundary. In contrast, energy can be exchanged with the system's surroundings.

Open systems usually involve mass flow. So, they allow energy and mass exchange across their boundaries. They are also known as control volume.

2.2.2. State conditions

When systems change their states from one equilibrium to another, this is called a process. Thereby, processes can be performed under different conditions that imply specific behaviours.

Steady means that the process proceeds all the time in equilibrium. This means that state parameters do not change with time. Thus, the system is independent of time. However, properties may change in position.

Non-steady/ transient is the opposite of steady, and properties are dependent on time. The velocity of a ball freely falling started by zero, for example.

Quasi-steady shows an often applied simplification. If the system keeps infinitesimally close to equilibrium during a process all the time, then it is quasi-steady. This means that sufficiently slow transient processes can be treated with steady state conditions to facilitate more straightforward calculations.

2.2.3. Notion of heat and thermal energy

In day for day use, the terms of heat and thermal energy are often used equivalent. However, heat transfer describes thermal energy, which is transferred from one system to another due to temperature differences, i.e. thermal energy in transit. In thermodynamics, heat transfer and heat are often treated equivalent.
The heat Q is measured in the unit Joule ($[J]$). On a rate basis, the heat transferred per unit of time $\dot{Q}$ is given in Watt ($[W = \frac{J}{s}]$). Also, heat transfer processes are often generalized by the heat flux q, which reduces the heat on a rate basis supplementary to the flow per unit of area with unit $[\frac{W}{m^2}]$. It is given by:

$$q = \frac{Q}{A \cdot \Delta t} = \frac{\dot{Q}}{A} \tag{1}$$

2.2.4. Laws of Thermodynamics

The two laws of thermodynamics describe the relations between the characteristics of surfaces.

First law The first law states the conservation of energy within a system. This means that the only way to change the amount of energy in a system (E_{st}) consists of crossing the system's boundaries. Due to the fact that energy is always converted during a process to another form, the balance holds because energy cannot only 'appear' or 'disappear' (cf. Figure 3). In fact, the law addresses the amount of total energy.

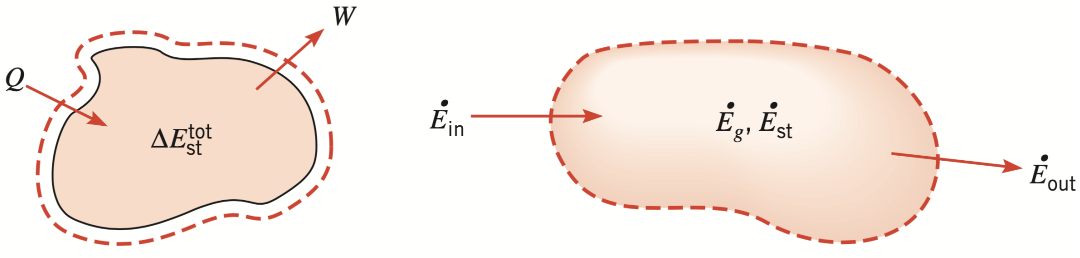

Figure 3: Conservation of energy in a closed system and for a control volume (see [23]).

For closed systems, it holds that

$$\Delta E_{st}^{tot} = Q - W \tag{2}$$

where ΔE_{st}^{tot} is the change in stored total energy. Q is the heat energy moved to the system and W the work done by the system.
Thereby, E describes the sum of all forms of energy. Concluded in an energy balance for a control volume, it means that:

$$\Delta E_{st} = E_{in} - E_{out} + E_g \tag{3}$$

where
E_{st} stored energy in the system,
E_{in} energy entering the system,
E_{out} energy leaving the system,
E_g energy generated in the system.

Second law There are many ways to express the second law. In order to provide only a general insight into the subject, one of the most important findings of the second law is given here:

Heat energy spontaneously flows from a hot body to a cold body.

In other words, that means that if there is heat transfer Q from one body to another, the direction is given per definition. In fact, if the heat flow from body B_1 with temperature T_1 happens to body B_2 with temperature T_2, then it holds that $T_1 > T_2$.

2.2.5. Types of thermal heat transfer

Heat transfer can be reduced to three main types. If there is a fluid flowing between two bodies, then the heat is transferred by convection. If the fluid does not flow, i.e. it is at rest, then the process of conduction is completed. The third case does not need contact between or presence of the bodies, e.g. vacuum, and is called radiation. Of course, any combination of transfer is possible.

Conduction requires contact between (parts) of bodies. The physical relation is based on *Fourier's law* from 1822:

$$\dot{Q} = -k\nabla T = -k(\mathbf{i}\frac{\partial T}{\partial x} + \mathbf{j}\frac{\partial T}{\partial y} + \mathbf{k}\frac{\partial T}{\partial z}) \tag{4}$$

where $\dot{Q}$ is the rate of heat flow $[W]$ and k the thermal conductivity of the material, which has got the unit $[\frac{W}{mk}]$.
For cartesian coordinates with a one-dimensional heat transfer, the equation can be reduced to:

$$\dot{Q} = -k\frac{\partial T}{\partial x} \tag{5}$$

Moreover, when taking constraints into account of steady state conditions, the equation can be concluded as follows:

$$\dot{Q} = k * A * \frac{T_1 - T_2}{L} \tag{6}$$

with
A area of heat exchange surface $[m^2]$,
ΔT temperature difference between the two surfaces,
L thickness of the material in $[m]$.

Convection happens when fluid is in contact with two bodies at a different temperature so that the fluid can transfer the heat from the warmer to the colder zone. In detail, there are two distinctions of convection. On the one hand, there is the natural convection where the fluid's movement is caused only by the temperature differences. On the other hand, forced convection is obtained using a pump or a fan to move the fluid.
Newton has expressed the heat transfer by convection in steady state conditions with the following equation:

$$\dot{Q} = h * A * (T_1 - T_2) \tag{7}$$

with h convection heat transfer coefficient expressed with the unit $[\frac{W}{m^2k}]$.

Radiation is based on the exchange of thermal energy by matter through space. The law given by *Stefan Boltzmann* describes the heat transfer in the case of radiation:

$$\dot{Q} = \varepsilon * A * \sigma * T^4 \tag{8}$$

where
ε is emissivity of surface $(0 < \varepsilon < 1)$,
A area of surface $[m^2]$,
σ Stefan-Boltzmann constant with $5.67 \cdot 10^{-8}$ $[\frac{W}{m^2 K^4}]$,
T surface temperature.

2.3. Model for structural building properties

By starting with a top-down approach for the whole building modeling, the outside perspective is taken where the building is one extensive system. The first step is to derive a static image of the investigating building without thermal dynamics. That includes all its structural properties, e.g. room sizes, wall thicknesses, and used materials, since these characteristics are essential when dealing with heat transfer. In other words, all constructional parameters influencing the temperature have to be identified. Therefore, an abstract model must be developed, which can be applied to individual buildings to formalize the constructional information logically.
So, the goal is a model formalizing all the structural properties of a building. Thus, this model fulfills two subgoals. First, it divides a building into rooms and shows their connections to each other. And second, it defines these rooms by their thermal character, which is needed for further heat calculations. In other words, this model maps a building to an energy system with all its crucial parameters.

2.3.1. Approach

If a building is viewed from outside, the building shapes a local energy system influenced by its surrounding environment. According to the first law of thermodynamics, this system has to be balanced. Under the assumption of a fixed amount of mass inside the building, it is seen as a closed system, i.e. there is no mass exchange with the environment, but an exchange in inflowing and outflowing energy (see Figure 4).

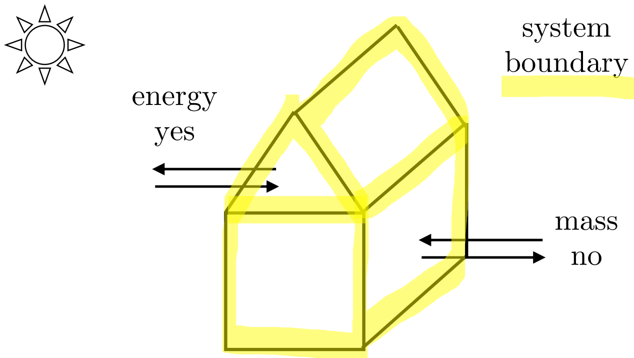

Figure 4: Closed energy system of a building.

According to the computer science principle 'divide and conquer', this system, i.e. the building, can be divided into less complex parts that have to be balanced. In the context of heat exchange, these parts are called thermal zones. They are used to divide a building into multiple smaller zones to enable an easier formulation of complex thermal relations (cf. [9]). Generally, these zones equal to enclosed rooms of the building or to a set of rooms which should maintain the same temperature (cf. [29]).
To keep the system balanced, not only the indoor zones have to be considered. Also, the outside environment (as indicated by the exemplary sun in Figure 4) has to be modeled to ensure the correct balances. In fact, the outside surrounding of the building can be split further into ground ($zone_{ground}$), on which the building is built, and the enveloping atmosphere ($zone_{outside}$).
Based on these thermal zones of a building and the modeling idea of Skruch [76], a graph-based model is proposed to define the static thermal characteristics of a building. Moreover, a four-step procedure is included to illustrate how to get the final representation.

2.3.2. Model

With the extension of Skruch [76], a building can be mapped to an undirected graph $G = (V, E)$ to obtain a logical formalization of its construction plan. Thereby, thermal zones are represented by nodes and thermal relations from zone to zone by edges, e.g. separated by a wall. The graph G is defined as follows:

$$V = \{zone_1, ..., zone_n, zone_{outside}, zone_{ground}\}$$

$$E = \{(x, y) | x, y \in V \text{ and } x \text{ and } y \text{ have got a thermal connection}\}$$

where n = number of thermal zones in the building.
So, this graph gives a floor plan of a building (cf. Figure 5) when considering a two-dimensional representation of the graph on paper. This means that thermal relations to other floors, e.g. an upper floor, are not shown graphically but considered in the adjacency matrix. Moreover, the outside zone Z_o is shown for a graphical reason only by four nodes. Formally it is one.

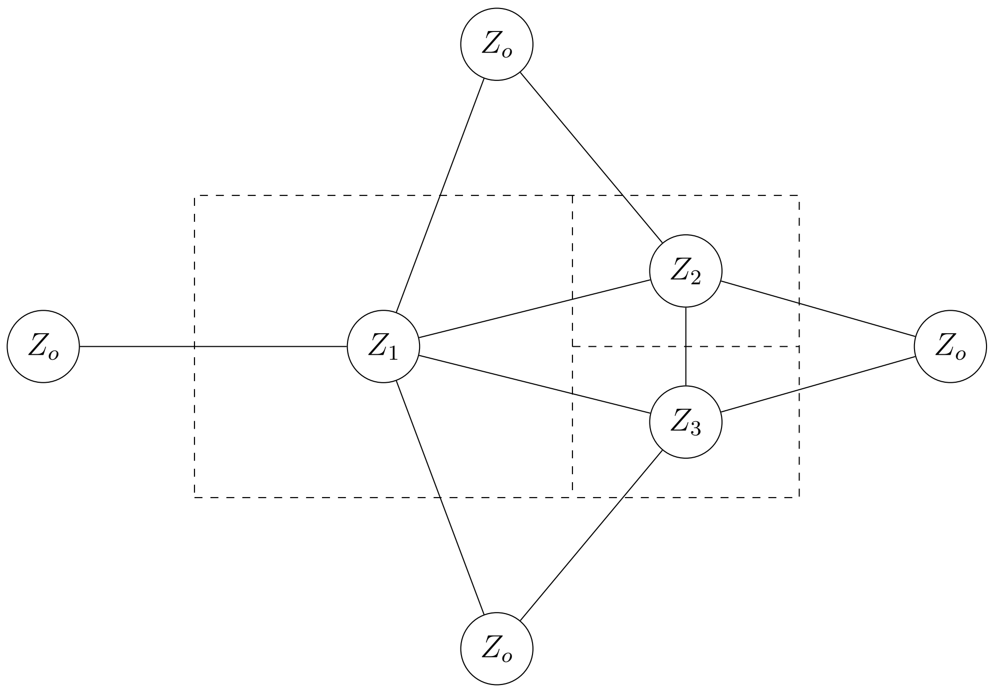

Figure 5: Exemplary floor modeled as graph with three interior thermal zones.

Nevertheless, having a "thermal connection", i.e. an edge, is not sufficient to describe building properties. In the context of heat transfer, the characteristics of a zone are more sophisticated. When considering a zone, it is evident that the zone temperature depends on the zone volume and its boundaries to the exterior since these boundaries control the energy exchanges. For example, a small room is heated faster than a bigger one, or the material of walls, concrete vs light plasterboard, affects the zone's isolation. As a result, the edge relations have to be specified further than just stating in a binary way that it exists or not.
So, if there is an edge between two nodes, it indicates a thermal relation between $zone_i$ and $zone_j$ with additional properties/parameters that concretize the system boundaries. For example, this means that there is a physical separator between two zones, a wall. Therefore, the area of the surface $A_{i,j}$, which connects the two systems $zone_i$ and $zone_j$, is essential. Furthermore, not only the area but also the thickness of the wall is decisive. Moreover, the material of the wall plays an essential role and implies with the depending thermal conductivity the speed of temperature deviations within the zone. In contrast, if the wall includes a window, the heat transfer is obviously affected.

The following parameters, belonging either to a node or an edge, are crucial when it comes to heat transfer in buildings.

Object	Relevant information
zone (node)	air volume
	heating & cooling device properties
	temperature profile
zone boundary (edge)	conductivity
	heat capacity
	thickness
	emissivity
	transmissivity
	absorptivity
	surface area
	tilting angle
	orientation to the sun
	density

All these parameters are used and explained throughout this thesis. However, for a suitable model, this information is necessary.
Depending on their object of purpose, zone properties, such as zone size, are assigned to a node, and properties of zone boundaries, such as wall thickness, are added to edges. They can be listed by adding other tables to the nodes or edges. An example is given in the case study in subsection 5.2.
The following four steps will illustrate the presented approach in a more summarized form. They have to be executed to obtain the final static model for a building:

1. Identify number of levels of the building and initialize one graph per level.
2. Identify the zones per level and initialize the corresponding nodes.
3. Identify thermal connections of zones and connect the nodes via edges.
4. Identify specific zone parameters and add them via tables to the corresponding graph component (node or edge).

In conclusion, this section builds up the first descriptive model to formalize the structural properties of buildings.

2.4. Thermodynamics model for buildings physics

After modeling the whole static building as a big picture (subsection 2.3), the point of view is restricted to one thermal zone. Thus, the generic exterior and interior heat transfers of a zone are explained in a white-box, physics, model.
Therefore, the deviation of temperature in one zone is derived from the foundations of

Bergman [23]. As described in the previous section, the starting point for physical relations is an energy balance within that zone. Due to the first law of thermodynamics, the conservation of energy within one zone is described as follows, since energy can not disappear:

$$\dot{E}_{in} + \dot{E}_g - \dot{E}_{out} - \frac{dE_{st}}{dt} = 0 \tag{9}$$

$$\frac{dE_{st}}{dt} = \dot{E}_{in} + \dot{E}_g - \dot{E}_{out} \tag{10}$$

In other words, this means that the stored energy E_{st}, the total introduced energy E_{in}, and the generated energy inside the zone E_g are equal to the total energy leaving the zone E_{out}. In the context discussed here, the energy is described by heat Q only. Mechanical work does not occur.
Additionally, the stored energy, respectively the stored heat, is defined as:

$$\dot{E}_{st} = \dot{Q}_{st} = \frac{d}{dt}(c\rho VT) \tag{11}$$

where $c\rho V$ represents the overall heat capacity of the zone volume V with density ρ and c specific heat capacity as well as its air temperature T.
Combining equations 10 and 11, the relations lead to:

$$\dot{Q}_{st} = \frac{d}{dt}(c\rho VT) = \dot{Q}_{in} + \dot{Q}_g - \dot{Q}_{out} \tag{12}$$

In fact, a thermal zone has got a fixed air volume with assumed constant air density and consequently constant specific heat capacity of air. When assuming that the indoor air is well mixed, then the following equation can be concluded:

$$C\frac{dT}{dt} = \dot{Q}_{in} + \dot{Q}_g - \dot{Q}_{out} \tag{13}$$

with $C = c\rho V$.
So, it reports the change of temperature within a zone with constant overall heat capacity depending on the ingoing and outgoing thermal heat transfer (cf. e.g. [80, 29, 76]). As a building has multiple zones in general, the equation above is indexed to indicate

the affiliation to zone Z_i.

$$C_{Z_i} \frac{dT_{Z_i}}{dt} = \dot{Q}_{Z_i}^{in} + \dot{Q}_{Z_i}^{g} - \dot{Q}_{Z_i}^{out} \tag{14}$$

Thus, equation 14 states the general energy balance for one zone. This allows evaluating internal and external gains and heat losses to obtain the zone temperature (cf. [9]). Moreover, the dependence on the in- and outgoing thermal heat flow enables the regulation of the temperature. In addition, the equation can be rewritten as follows when considering the direction of the flows that all ingoing heat flows are positive and outgoing flows negative:

$$C_{Z_i} \frac{dT_{Z_i}}{dt} = \sum \dot{Q}_{Z_i} \tag{15}$$

for all occurring heat flows $\dot{Q}$ in a thermal zone Z_i.

Now, the potential heat flows for zones are missing. Therefore, in the following, individual components of buildings, which add or remove heat energy, have to be investigated. First of all, based on Underwood and Yik [80] static building components, such as walls and windows, are analyzed. Then, HVAC-components are considered in subsection 2.5.

2.4.1. Wall, roof, ceiling and floor

The heat transfers occurring at walls, roofs, ceilings and floors are all based on the same approach (cf. [80]). Therefore, in this subsection, a one-layered wall is used as an explanation object, and the impacts on the zone temperature are derived from interior to exterior.
The following heat flow $\dot{Q}_{W_i}$ is needed because this flow influences the zone energy balance.

$$\dot{Q}_{W_i} = A_{W_i} \cdot q_{W_i,conv,in} \tag{16}$$

The heat flow is characterized by the surface area of the wall A_{W_i} (captured in the first static submodel) and the convective heat flux $q_{W_i,conv,in}$. This heat flux is caused by wall W_i with thickness L (cf. Figure 6) and is given by convection of the wall's interior surface ($W_{i,in}$) and the zone's air:

$$q_{W_i,conv,in} = h_{W_i,conv,in} \left(T_{W_i,in} - T_i\right) \tag{17}$$

where
$h_{W_i,conv,in}$ convective heat transfer coefficient at interior wall surface i,

T_i indoor temperature,
$T_{W_i,in}$ interior surface temperature of wall i.

For the convective heat transfer coefficient, there are formulas for calculation which are discussed in the following energy balances. However, for the calculation of the zone temperature, the interior wall surface temperature is missing. This is why the following analysis is needed.
By relating the results of two energy balances at the following points (cf. Figure 6), the wall temperature can be determined:

1. Energy balance at the interior wall surface described as $W_{i,in}$ at position ($x = L$)
2. Energy balance at the exterior wall surface described as $W_{i,ex}$ at position ($x = 0$)

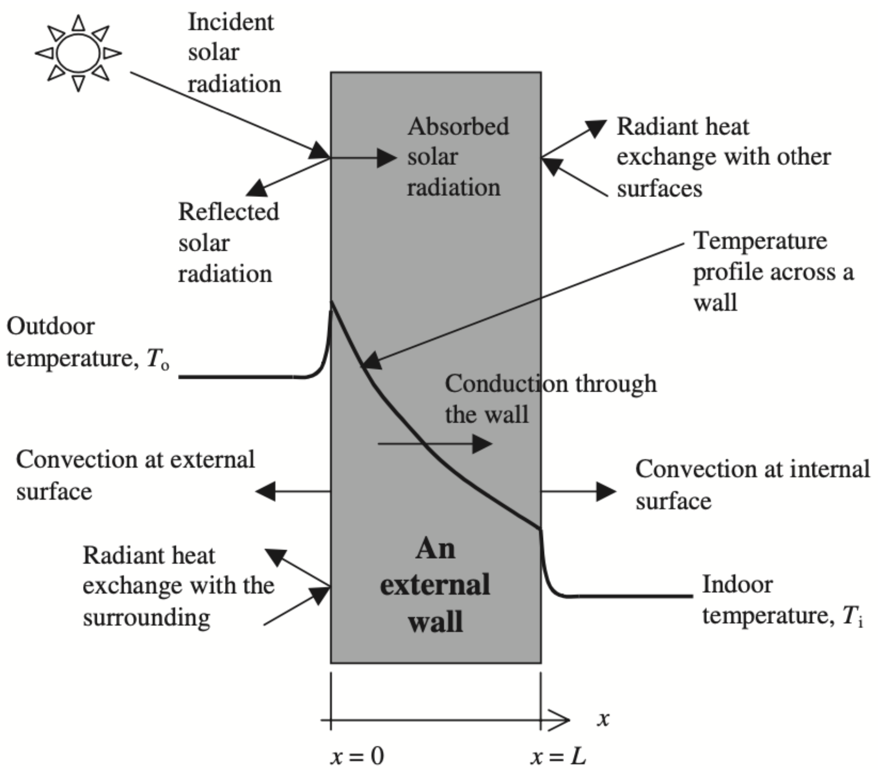

Figure 6: Effective heat flows at an exterior wall with higher outside temperature than inside temperature (see [80]).

These two energy balances are explained in the following.

Energy balance at the interior wall surface $(x = L)$**:** According to the graphical representation in Figure 6, the balance is composed of all types of heat transfer methods. In fact, these are conduction (*cond*), convection (*conv*), short wave solar radiation (*sol*), long wave radiation from other surfaces (*radS*), and long wave radiation from internal sources (*radInt*):

$$q_{W_i,cond} = q_{W_i,conv,in} - q_{W_i,sol,in} - q_{W_i,radS,in} - q_{W_i,radInt,in} \tag{18}$$

Every heat flux is individually explained in the following:

$\underline{q_{W_i,cond}}$ - Conduction through the wall i:
Due to the slow heat movements in buildings, the conduction is treated as quasi-static.

$$q_{W_i,cond} = k \cdot \frac{T_{W_i,ex} - T_{W_i,in}}{L} \tag{19}$$

with
k thermal conductivity of the wall,
L thickness of the wall,
$T_{W_i,ex}$ temperature at exterior wall surface $(x = 0)$,
$T_{W_i,in}$ temperature at interior wall surface $(x = L)$.

$\underline{q_{W_i,conv,in}}$ - Convection at the interior surface of wall i:

$$q_{W_i,conv,in} = h_{W_i,conv,in} \left(T_{W_i,in} - T_i\right) \tag{20}$$

where
T_i indoor temperature,
$T_{W_i,in}$ interior surface temperature of wall i.

However, the estimation of the convective heat transfer coefficient for internal surfaces depends on various side effects, as forced or natural convection and the direction of the flow. Due to the non-trivial estimation of these, ASHRAE [18] proposes simplified calculations for horizontal and vertical surfaces exchanging heat with air:

$$h_{W_i,conv,in,vertical} = 1.42 \left(\frac{|\Delta T|}{H}\right)^{0.25} \tag{21}$$

$$h_{W_i,conv,in,horizontal} = 0.59 \left(\frac{|\Delta T|}{H}\right)^{0.25} \tag{22}$$

with
ΔT temperature difference of air and wall,

H characteristic length of the wall (e.g. height in case of a vertical wall).

Thereby the absolute value of the temperature difference is needed. Otherwise, the direction of the heat flux could change, although it is not the case.
Since the general coefficient can vary by a factor of 5 to 6, in the literature can be found more methods for calculation (cf. eg. [46, 11, 21, 20]).

$\underline{q_{W_i,sol,in}}$ - Solar radiation at the interior surface of wall i:
The solar heat gain calculation at interior parts of the room is complicated due to the determination of the following parameters:

- The interior surfaces which are directly affected by solar radiation. They are not constant, vary by time and weather, and their exact determination is not practicable.
- The concatenated sum of energy caused by reflected and absorbed radiation across surfaces until the solar radiation is totally used, caused by the high number of different 'things' in the room.

Caused by these reasons, the interior heat gain from solar radiation is further simplified in the entire zone in general. It is assumed that the two components of solar radiation, direct and diffuse radiation, are uniformly distributed over the floor (direct and diffuse radiation) and to all surfaces inside the room (diffuse radiation). Therefore, the differentiation, which object absorbs the radiation, is essential because direct and diffuse radiation are differently considered for the following objects. Since the general explanation is based on walls, but they can be analogously applied to the other objects:

- If the object is a wall, window, or a ceiling, then only the diffuse radiation from window WG_j contributes to the heat gain of the object:

$$q_{W_i,sol,in} = \frac{\sum_j A_{\mathrm{WG},j} \tau_{\mathrm{d},j} I_{j,\ \mathrm{d}}}{A_{\mathrm{tot}}} \tag{23}$$

- If the object is a floor, then also the direct radiation is added in addition to the diffuse radiation:

$$q_{W_i,sol,in} = \frac{\sum_j A_{\mathrm{WG},j} \tau_{\mathrm{d},j} I_{j,\ \mathrm{d}}}{A_{\mathrm{tot}}} + \frac{\sum_j SLF_j \cdot A_{\mathrm{WG},j} \tau_{\mathrm{D},j} I_{j,\mathrm{D}}}{A_{\ \mathrm{floor}}} \tag{24}$$

with
A_{tot} sum of areas of all N enclosed surfaces within a zone (walls, windows, floor, ceiling),
$A_{\ \mathrm{floor}}$ area of the floor,
$A_{\mathrm{WG},j}$ area of window j,
$\tau_{\mathrm{d},j}$ diffuse solar radiation transmissivity of window j,

$\tau_{\mathrm{D},j}$ direct solar radiation transmissivity of window j,
$I_{j,\ \mathrm{d}}$ diffuse radiation intensity on a surface in the same direction as window j,
$I_{j,D}$ direct radiation intensity on a surface in the same direction as window j,
SLF_j fraction of area of window j with direct solar radiation contact.

Since transmissivity is a unique value for each glazing components and might be not known, DIN 4108 [3] gives generalized transmissivity values for different windows. More in detail, transmissivity (and absorptivity; important for window temperature in subsubsection 2.4.2) is calculated for specific beam angles by ASHRAE (cf. [18]). However, this is also related to a standard glass called DSA (double strength, heat absorbing).

$\underline{q_{W_i,radS,in}}$ - Long wave radiation heat exchange with other enclosing surfaces at wall i: A method to obtain that heat gain is a radiation heat transfer network analysis (for more information, see [80]). However, this method implies the concrete calculation of all shape factors within the zone.
Therefore, Underwood and Yik [80] propose using the MRT/Bal method, which acts as a reasonable tradeoff between simplicity and accuracy. Then, the heat flux can be determined as:

$$-q_{W_i,radS,in} = \sigma F_{\mathrm{MRT},i}\left(T_i^4 - T_{\mathrm{MRT},i}^4\right) - q_{\mathrm{Ba}} \tag{25}$$

This method introduces a fictitious surface for exchanging the long wave radiation of wall i with N other surfaces. Its shape factor[1] is constructed as:

$$F_{\mathrm{MRT},i} = \frac{1}{\frac{1-\varepsilon_i}{\varepsilon_i} + 1 + \frac{A_{W_i}\left(1-\varepsilon_{\mathrm{MRT},i}\right)}{A_{\mathrm{MRT},i}\varepsilon_{\mathrm{MRT},i}}} \tag{26}$$

Moreover, it has the surface temperature $T_{\mathrm{MRT},i}$:

$$T_{\mathrm{MRT},i} = \sum_{j=1}^{N} \frac{A_j \varepsilon_j T_j}{A_{\mathrm{MRT},i}\varepsilon_{\mathrm{MRT},i}} (\text{ for } j \neq i) \tag{27}$$

The area of the fictitious surface is stated as:

$$A_{\mathrm{MRT},i} = A_{\mathrm{tot}} - A_{W_i} = \sum_{j=1}^{N} A_j (\text{ for } j \neq i) \tag{28}$$

where A_{tot} sums up the area of all N enclosed surfaces within a zone (walls, windows, floor, ceiling).
Lastly, the emissivity is determined as:

[1]Shape factor $F_{i,j}$, also called view factor, describes the fraction of radiation leaving surface i and received by surface j.

$$\varepsilon_{\mathrm{MRT},i} = \sum_{j=1}^{N} \frac{A_j \varepsilon_j}{A_{\mathrm{MRT},i}} (\text{ for } j \neq i) \tag{29}$$

Additionally, the used simplifications in the shape factor and temperature of that method lead to imbalances in the total radiant energy. For correction, a balance term is introduced, which is valid for all surfaces:

$$q_{\mathrm{Bal}} = \frac{\sum_{i=1}^{N} \sigma A_i F_{\mathrm{MRT},i} \left(T_{\mathrm{MRT},i}^4 - T_{\mathrm{i}}^4 \right)}{A_{\mathrm{tot}}} \tag{30}$$

$\underline{q_{W_i,radInt,in}}$ - Long wave radiation by internal heat sources absorbed by wall i:
For the radiation of internal heat sources, e.g. radiators or internal loads by people, it is assumed that radiation is uniformly distributed to all enclosed surfaces, such as walls, floor, windows, and ceiling. So, the heat flux from the internal sources on each surface W_i is formalized as:

$$q_{W_i,radInt,in} = \frac{\sum_j \dot{Q}_{j,\mathrm{Rad}}}{A_{\mathrm{tot}}} \tag{31}$$

where
$\dot{Q}_{j,\mathrm{Rad}}$ rate of radiation from internal source j,
A_{tot} sum of areas of all N enclosed surfaces within a zone (walls, windows, floor, ceiling).

Energy balance at the exterior wall surface ($x = 0$)**:** The balance at the exterior side of wall i is influenced by the following heat fluxes (cf. Figure 6):

$$q_{W_i,conv,ex} + q_{W_i,sol,ex} + q_{W_i,rad,ex} = q_{W_i,cond} \tag{32}$$

Each heat flux is explained in the following paragraphs:

$\underline{q_{W_i,conv,ex}}$ - Convection at the exterior part of wall i:

$$q_{W_i,conv,ex} = h_{W_i,conv,ex}(T_o - T_{W_i,ex}) \tag{33}$$

where
$h_{W_i,conv,ex}$ convective heat transfer coefficient at external wall surface i,
T_o outside temperature,
$T_{W_i,ex}$ external surface temperate of wall i.

Due to the consideration of the thermal effect of wind, the convective heat transfer coefficient depends on wind speed and direction. Underwood and Yik suggest the use of the MoWiTT (Mobile Windows Thermal Test) model from Yazdanian and Klems [86] to determine the convective heat transfer coefficient as:

$$h_{W_i,conv,ex} = \sqrt{[C_t(T_o - T_{W_i,ex})^{1/3}]^2 + [av_0^b]^2} \tag{34}$$

where
C_t turbulent natural convection constant,
v_0 wind speed at standard conditions,
a, b constants.

The specific constants of that method are given below:

Wind direction	$C_t \left(\mathrm{Wm^{-2}\ K^{-4/3}}\right)$	$a \left(\mathrm{W\ m^{-2}\ K\ (\ m\ s^{-1})^{b}}\right)$	b (−)
Windward	0.84	2.38	0.89
Leeward	0.84	2.86	0.617

Figure 7: MoWiTT model constants (see [80]).

However, in the context of linear optimization, the MoWiTT model would lead to problems. Due to its complex non-linear structure regarding the exterior wall temperature $T_{W_i,ex}$, the linear approximation of this term would provoke errors. In this foresight, an alternative model is already presented. Mirsadeghi et al. [60] investigated the popularity and analyzed models for convective heat transfer coefficients. In general, it resulted in the use of only one model for all types of buildings in the context of building energy simulation (BES). The following model by McAdam is used as usual:

$$h_{W_i,conv,ex} = 5.678 \left(m + n \left(\frac{v_0}{0.3048}\right)^p\right) \tag{35}$$

Thereby, the following parameters m, n, p are used for the roughness of the surface and wind speed:

	$V_f < 4.88$ m/s (16 ft/s)			4.88 m/s (16 ft/s) $\leq V_f < 30.48$ m/s (100 ft/s)		
Surface type	m	n	p	m	n	p
Smooth	0.99	0.21	1	0	0.50	0.78
Rough	1.09	0.23	1	0	0.53	0.78

Figure 8: Constant parameters for the model by McAdam (see [60]).

$\underline{q_{W_i,sol,ex}}$ - Solar radiation at the exterior part of wall i:

$$q_{W_i,sol,ex} = \alpha_{W_i,ex} * I_{W_i,T,ex} \tag{36}$$

where
$\alpha_{W_i,ex}$ solar absorptivity of external wall surface i,
$I_{W_i,T,ex}$ total intensity of solar radiation at external wall surface i.

Due to its complexity, the explanation for the solar intensity calculation is given in subsubsection 2.4.3.

$\underline{q_{W_i,rad,ex}}$ - Long wave radiation at the exterior part of wall i:
Based on physical relations, the heat flux is given as:

$$q_{W_i,rad,ex} = \epsilon_{W_i,ex} * \sigma\{F_{W_i,\mathrm{A}}[T_o^4 - T_{W_i,ex}^4] + F_{W_i,\mathrm{G}}[T_G^4 - T_{W_i,ex}^4] + F_{W_i,\mathrm{S}}[T_S^4 - T_{W_i,ex}^4]\} \tag{37}$$

where
$\epsilon_{W_i,ex}$ long wave emissivity of external wall surface i,
σ Stefan-Boltzmann constant,
$F_{W_i,A}$ shape factor between external wall surface i and outdoor air,
$F_{W_i,G}$ shape factor between external wall surface i and ground,
$F_{W_i,S}$ shape factor between external wall surface i and sky,
T_S sky temperature,
T_G ground temperature.

However, to better handle that heat flux in terms of computational effort, it is possible to simplify exterior long wave radiation further as follows.
Since the radiation leaving an object can not be more than 100%, it is conserved. The summation rule (cf. [23]) of shape factors[2] defines that the sum has to equal one:

$$F_{W_i,A} + F_{W_i,G} + F_{W_i,S} = 1 \tag{38}$$

With this condition, the following manipulations can be executed to eliminate the shape factor between a wall and outside air:

$$\begin{aligned} q_{W_i,\mathrm{Rad},ex} =& \varepsilon_{W_i}\sigma\left\{\left[F_{W_i,\mathrm{A}}T_\mathrm{o}^4 + F_{W_i,\mathrm{G}}T_\mathrm{G}^4 + F_{W_i,\mathrm{S}}T_\mathrm{S}^4\right]\right. \\ &\left. - \left[F_{W_i,\ \mathrm{A}} + F_{W_i,\mathrm{G}} + F_{W_i,\mathrm{S}}\right]T_{W_i}^4\right\} \\ =& \varepsilon_{W_i}\sigma\left\{\left[F_{W_i,\mathrm{A}}T_\mathrm{o}^4 + F_{W_i,\mathrm{G}}T_\mathrm{G}^4 + F_{W_i,\mathrm{S}}T_\mathrm{S}^4\right.\right. \\ &\left.\left. - \left(F_{W_i,\ \mathrm{A}} + F_{W_i,\mathrm{G}} + F_{W_i,\mathrm{Sky}}\right)T_\mathrm{o}^4\right] + \left[T_\mathrm{o}^4 - T_{W_i}^4\right]\right\} \\ =& \varepsilon_{W_i}\sigma\left\{\left[F_{W_i,\mathrm{G}}\left(T_\mathrm{G}^4 - T_\mathrm{o}^4\right) + F_{W_i,\mathrm{S}}\left(T_\mathrm{S}^4 - T_\mathrm{o}^4\right)\ + \left(T_\mathrm{o}^4 - T_{W_i}^4\right)\right]\right\} \end{aligned} \tag{39}$$

[2]Shape factor $F_{i,j}$, also called view factor, describes the fraction of radiation leaving surface i and received by surface j.

So, a vertical wall indicates the shape factor to ground and sky by $F_{W,G} = F_{W,Sky} = 0.5$. For tilted surfaces with angle β to the horizontal, it holds that:

$$F_{W,G} = \frac{1 - \cos\beta}{2} \tag{40}$$

$$F_{W,S} = \frac{1 + \cos\beta}{2} \tag{41}$$

Furthermore, there are different approaches to approximate the needed sky and ground temperature.
For the sky temperature, the easiest method is to subtract 6K from the outside temperature. More sophisticated methods to predict the sky temperature under cloudy sky are shown for example by KIMURA [48], CLARKE [28] and RONOH AND RATH [72].
Secondly, the ground temperature can be assumed to equal the outside temperature (cf. [51]). A more accurate estimate with temperatures of sub-surfaces is presented by KUSUDA AND ACHENBACH [50].

Moreover, further summarizing manipulation can be performed by introducing a radiation heat transfer coefficients for the outdoor air:

$$h_{W_i,\mathrm{RadO},ex} = \frac{\varepsilon_{W_i,ex}\sigma\left(T_\mathrm{o}^4 - T_{W_i,ex}^4\right)}{T_\mathrm{o} - T_{W_i,ex}} \tag{42}$$

As well as for the ground:

$$h_{W_i,\mathrm{RadG},ex} = \frac{\varepsilon_{W_i,ex}\sigma F_{\mathrm{W_i,G}}\left(T_\mathrm{G}^4 - T_\mathrm{o}^4\right)}{T_\mathrm{G} - T_\mathrm{o}} \tag{43}$$

And for the sky:

$$h_{W_i,\mathrm{RadS},ex} = \frac{\varepsilon_{W_i,ex}\sigma F_{\mathrm{W_i,S}}\left(T_\mathrm{S}^4 - T_\mathrm{o}^4\right)}{T_\mathrm{S} - T_\mathrm{o}} \tag{44}$$

Then, the exterior radiation heat flux concludes to:

$$\begin{aligned} q_{W_i,Rad,ex} = & h_{W_i,\mathrm{RadO},ex}\left(T_\mathrm{o} - T_{\mathrm{W_i},ex}\right) \\ & + h_{W_i,\mathrm{RadG},ex}\left(T_\mathrm{G} - T_\mathrm{o}\right) + h_{W_i,\mathrm{RadS},ex}\left(T_\mathrm{S} - T_\mathrm{o}\right) \end{aligned} \tag{45}$$

Nonetheless, UNDERWOOD AND YIK [80] propose another simplification, which is advantageous for the upcoming linearization in the context of optimization.
By an approximation of each radiation heat transfer coefficient concerning the 4-th

power, the exponent can be decreased to the power of 3 with a reasonable accuracy. The coefficients are approximated by:

$$\frac{T_\mathrm{o}^4 - T_{\mathrm{W}_{i,ex}}^4}{T_\mathrm{o} - T_{\mathrm{W}_{i,ex}}} \approx 4 \cdot T_{\mathrm{Avg,o,W_i}}^3 = 4 \left(\frac{T_\mathrm{o} + T_{\mathrm{W_i,ex}}}{2} \right)^3 \tag{46}$$

$$\frac{T_\mathrm{G}^4 - T_\mathrm{o}^4}{T_\mathrm{G} - T_\mathrm{o}} \approx 4 \cdot T_{\mathrm{Avg,G,o}}^3 = 4 \left(\frac{T_\mathrm{G} + T_\mathrm{o}}{2} \right)^3 \tag{47}$$

$$\frac{T_\mathrm{S}^4 - T_\mathrm{o}^4}{T_\mathrm{S} - T_\mathrm{o}} \approx 4 \cdot T_{\mathrm{Avg,S,o}}^3 = 4 \left(\frac{T_\mathrm{S} + T_\mathrm{o}}{2} \right)^3 \tag{48}$$

Thus, the approximations can be directly substituted to obtain the following simplified radiant heat transfer coefficients:

$$h_{W_i,\mathrm{RadO},ex} = 4\varepsilon_{W_i,ex}\sigma T_{\mathrm{Avg,o,W_i}}^3 \tag{49}$$

$$h_{W_i,\mathrm{RadG},ex} = 4\varepsilon_{W_i,ex}\sigma F_{\mathrm{W_i,G}} T_{\mathrm{Avg,G,o}}^3 \tag{50}$$

$$h_{W_i,\mathrm{RadS},ex} = 4\varepsilon_{W_i,ex}\sigma F_{\mathrm{W_i,S}} T_{\mathrm{Avg,S,o}}^3 \tag{51}$$

So, as a result Equation 45 gives the radiation heat flux at the exterior wall surface with radiation heat transfer coefficient to the power of 4 or a simplified version to the power of 3.

2.4.2. Window

The heat transfer that happens on a window glazing component WG_i is comparable to the process at walls. Thus, the heat flow $\dot{Q}_{WG_i}$ which affects the zone temperature is given as:

$$\dot{Q}_{WG_i} = A_{WG_i} \cdot q_{WG_i,conv,in} = A_{WG_i} \cdot h_{WG_i,in}(T_\mathrm{WG} - T_\mathrm{i}) \tag{52}$$

Still, additionally, solar radiation can be transmitted through it (cf. Figure 9) and heats enclosing surfaces in the zones (see the paragraph about solar radiation at the interior surface of walls for the impact of that).

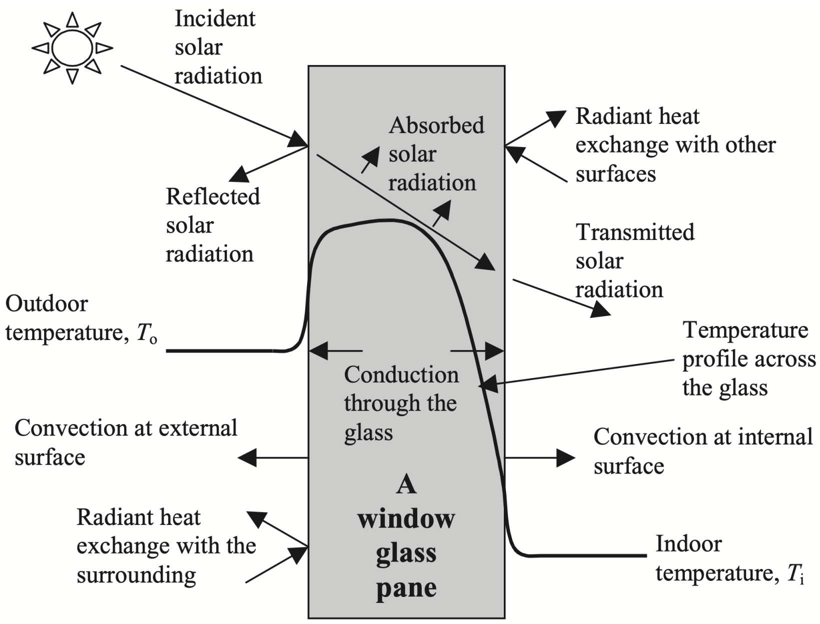

Figure 9: Effective heat flows at an exterior one-layered window with higher outside temperature than inside temperature (see [80]).

Even though the conduction heat transfer through the glazing is disregarded in the case of one-layered windows. Caused by the, in comparison to other objects, thin glass thickness, a uniform temperature for the interior and exterior surface can be assumed. Compared to walls, this means that $T_{W_i,ex} \neq T_{W_i,in}$ but $T_{WG,ex} = T_{WG,in} = T_{WG}$, i.e. the indoor and exterior temperature of the glazing are equal. So, the heat transfer via conduction is neglected.
However, analogously to multi-layered walls, in the case of multi-layered windows, the conduction process can be added as well for each layer of separating gas (see e.g. [18]). Additionally, it is also possible to add the conduction through the glazing component as well via the same approach. Nevertheless, the approach used here consists of the neglect of conduction.
Also, there are more significant differences, which are shown in the following energy balances for the interior and exterior surface of the window.

Energy balance at the interior window surface ($x = L$)**:** The heat flux at the interior side (described by q_{in}) of window i depends in fact on convection and radiation (cf. Figure 9), since the conduction is ignored due to the high conductivity of glass. For the rest, the balance is identical to walls.
On this basis, the heat flux consists of:

$$\begin{aligned} q_{WG_i,in} &= q_{WG_i,conv,in} - q_{WG_i,sol,in} - q_{WG_i,radS,in} - q_{WG_i,radInt,in} \\ &= q_{W_i,conv,in} - q_{W_i,sol,in} - q_{W_i,radS,in} - q_{W_i,radInt,in} \end{aligned} \tag{53}$$

Generalized heat transfer coefficients for convection depending on the number of windows layers can be found in 30.6 ASHRAE [18].

Energy balance at the exterior window surface $(x = 0)$ The heat flux at the exterior side (described by q_{ex}) of window i is influenced nearly by the same factors as already described in the case of walls (see subsubsection 2.4.1):

$$\begin{aligned} q_{WG_i,ex} &= q_{WG_i,conv,ex} + q_{WG_i,sol,ex} + q_{WG_i,rad,ex} \\ &= q_{W_i,conv,ex} + \alpha_\theta I_\mathrm{D} + \alpha_\mathrm{d} I_\mathrm{d} + q_{W_i,rad,ex} \end{aligned} \tag{54}$$

A window does not absorb the radiation completely. It also transmits part of it to the other side of the window. In other words, this means that solar radiation has to be considered differentiated in the case of windows (second and third summand in the equation above). Therefore, the diffuse and direct radiation is treated separately. The explanation of how to get this separation is given in the next subsubsection 2.4.3.
Furthermore, ASHRAE [18] propose generalized values for the absorptivity for the standard DSA glass.

2.4.3. Solar intensity calculation

The estimation of the total irradiance on a surface is not trivial since buildings are affected by two solar radiation components: Direct and diffuse solar radiation. The problem states in the provided information by meteorological station because they give only the global measurement on the horizontal plane, which has to be decomposed to the two components to calculate the total intensity for a wall. Due to the sun's relatively slow movements, a non-continuous consideration of the irradiance is sufficient for building modeling, e.g. every 15min.
In general, these approximations are based on the correlation of the total horizontal radiation $I_{T,h}$ and the clearness index k_C:

$$k_\mathrm{C} = \frac{I_\mathrm{T,h}}{I_\mathrm{E}} \tag{55}$$

where I_E relates to the extraterrestrial radiation, representing the total solar radiation on a horizontal surface without atmospherical constraints, i.e. a clear sky without particles. It is given by Duffie and Beckman [32] as:

$$I_\mathrm{E} = I_0 \left[1 + 0.033 \cos\left(360 n_\mathrm{day}/365\right)\right] \cos\left(\theta_\mathrm{h}\right) \tag{56}$$

with
$I_0 = 1367 \frac{W}{m^2}$ solar constant,
n_{day} the numerical representation of the day of the year $(1 \leq n_{day} \leq 365)$,
θ_h the solar beam angle to the horizontal plane.

For the decomposition of the global irradiance on the horizontal plane, Underwood and Yik shows the model of Skartveit and Olseth [75]. However, this is suitable

for high northern latitudes only. A comparison of models for other global sites is given by DUFFIE AND BECKMAN [32].
Since CLEMENS [29] discusses a general building model about overheating by solar radiation with the model of LIU AND JORDAN [55], that one is used in the following to split the global into diffuse radiation I_d:

$$\frac{\mathrm{I_d}}{\mathrm{I_{T,h}}} = 1,0045 + 0,04349 \cdot \mathrm{k_C} - 3,5227 \cdot \mathrm{k_C^2} + 2,6313 \cdot \mathrm{k_C^3} \tag{57}$$

After the computation of the diffuse component, the direct part of the radiation can be calculated with the following equation:

$$I_{D,h} = I_{T,h} - I_d \tag{58}$$

LIU AND JORDAN [56] propose the following calculation for a tilted surface with angle β that is beamed with angle θ to get the total irradiance that influences it:

$$I_{W_i,T,ex} = I_{\mathrm{D,h}} \cos\theta + I_{\mathrm{d}} \left(\frac{1+\cos\beta}{2}\right) + \rho_{\mathrm{g}} \left(I_{\mathrm{D,h}} + I_{\mathrm{d}}\right) \left(\frac{1-\cos\beta}{2}\right) \tag{59}$$

where
β tilting angle of the surface to the horizontal,
ρ_g ground reflectance (usually around 0.2 for normal conditions),
θ solar beam angle.

The angle between the direction of the sunbeams and the surface's normal of an arbitrarily inclined plane, the solar beam angle θ, is treated from DUFFIE AND BECKMAN [32] as:

$$\begin{aligned} \cos\theta = & \sin(d)\sin(l)\cos(\beta) \\ & - \sin(d)\cos(l)\sin(\beta)\cos(\gamma) \\ & + \cos(d)\cos(l)\cos(\beta)\cos(\omega) \\ & + \cos(d)\sin(l)\sin(\beta)\cos(\gamma)\cos(\omega) \\ & + \cos(d)\sin(\beta)\sin(\gamma)\sin(\omega) \end{aligned} \tag{60}$$

where
d declination angle,
l latitude angle with positive values for northern position,
β tilting angle of the surface to the horizontal,
γ surface azimuth angle,
ω hour angle.

A graphical representation of the used angles is shown in Figure 10 and explained afterwards.

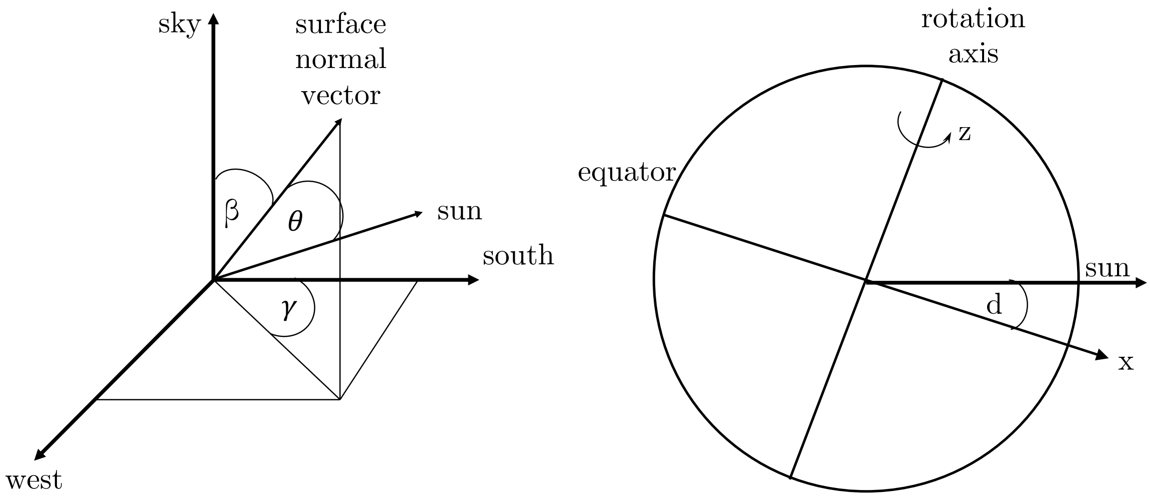

Figure 10: Graphical representation of angles used in the context of solar radiation (own figure based on [29]).

d The declination angle shows the angle between the sun and the plane of the equator when the sun is at its highest point (local meridian), i.e. the solar noon. It counts positive for northern positions and can take values between $-23.45° \leq d \leq 23.45°$ and is approximated for each day of the year by:

$$d = 23.45 \sin\left(360\left(284 + n_{\text{day}}\right)/365\right) \tag{61}$$

with $1 \leq n_{day} \leq 356$ day of the year.

γ The azimuth angle describes the orientation of the surface normal projected on the horizontal plane and the south. Thereby, south is indicated by 0° and is counted positive for value in the west and negative for east ($-180 \leq \gamma \leq 180$).

ω The hour angle is the displacement in degrees of the sun to the local meridian. As the name indicates, it is based on the local time. Each hour counts 15°, where the afternoon is counted positive and starts at 12 o'clock with 0°. Since the local time t_{clock} does not consider the geographical position, the solar time t_{sol} is used for the calculation which takes into account the time difference of local and solar time. In addition, the inclination of the earth axis has to be respected. That is why another correction term e is necessary.

$$t_{\text{Sol}} = t_{\text{Clock}} + 4\left(L_0 - L_{\text{loc}}\right) + e \tag{62}$$

where
t_{clock} local time,

L_0 longitude of standard meridian (west positive),
L_{loc} longitude of investigated location (west positive).

$$\begin{aligned} e =& 9.87 \sin\left[\frac{720\,(n_{\text{day}} - 81)}{364}\right] - 7.53 \cos\left[\frac{360\,(n_{\text{day}} - 81)}{364}\right] \\ & - 1.5 \sin\left[\frac{360\,(n_{\text{day}} - 81)}{364}\right] \end{aligned} \tag{63}$$

2.5. Thermodynamics model for HVAC components

After modeling the environmental impacts on buildings, this section deals with HVAC components that power is used to heat or cool the zone.

2.5.1. Hydronic radiator

A hydronic radiator (see Figure 11) is a typical heating device in buildings. By flowing hot water through it, it produces heat.

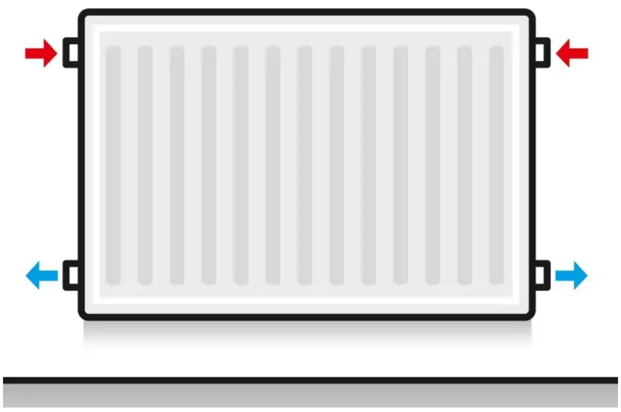

Figure 11: Exemplary radiator (see [6]).

Its working principle is based on the control of the mass flow of water through it and the control of inlet water temperature. The slower the water flows through, the more time the water has to transfer its heat to the radiator. This fact concludes with a lower outlet temperature of the water because the radiator can absorb more thermal energy during this time. Vise versa holds for a higher mass flow. This regularity is also reflected in the formula for describing heat output of an ideal radiator (cf. eg. [10][43][22][59]):

$$\dot{Q}_{\text{Radiator}} = \dot{m} c_W (T_{in} - T_{out}) \tag{64}$$

where
c_{W} specific heat capacity of water 1.163,
$\dot{m}$ mass flow of water $[\frac{kg}{s}]$,

T inlet respectively outlet temperature of the water.

However, the outlet temperature of a radiator depends on the environmental conditions. This is why the outlet temperature is not known. According to GUSTAFSSON ET AL. [36] and TESKEREDZIC AND BLAZEVIC [79] radiators are treated as heat exchangers to estimate the outlet temperature. Thereby, the outlet temperature is described by the difference of the heat capacitance of the introduced water with the heat loss by convection of the inside water flow:

$$m_W c_W \frac{dT_{out}}{dt} = \dot{m} c_W (T_{in} - T_{out}) - h_W A_{Rad,in} (T_{Water} - T_{body}) \tag{65}$$

where
h_W convective coefficient with water,
$A_{Rad,in}$ interior area of the radiator surface which interacts with the water,
T_{body} averaged body temperature of the radiator.

The water temperature inside the radiator is assumed to be the average between the inlet and outlet water temperature:

$$T_{Water} = \frac{T_{in} + T_{out}}{2} \tag{66}$$

The topic of forced convective heat transfer coefficients is a broad subject area. Therefore, a lot of models exists for different flow criteria (e.g. turbulent, laminar) with diverse characteristic numbers (e.g. Reynolds and Nusselt number) (cf. eg. [49, 77]). Due to the complex structure of the estimation of the coefficient, ASHRAE [18] clustered models for the coefficient and proposes a simplified model by MCADAMS for water flow inside of tubes with a temperature between 4 to 93°C. Thus, the convective heat transfer coefficient can be got by:

$$h_W = \frac{1057(1.352 + 0.0198 T_W) v^{0.8}}{D^{0.2}} \tag{67}$$

where
V the velocity of the water in $[\frac{m}{s}]$,
D the diameter of the tube in $[m]$.

The velocity of water is obtainable from the mass flow. Thereby, the definition of mass flow is used:

$$\dot{m} = \rho \cdot v \cdot A = \rho \dot{V} \tag{68}$$

with
ρ density of the fluid,
v velocity of the fluid,
A the cross-sectional area of the tube.

As a next step, the averaged body temperature of the radiator has to be estimated for the convection between the water and the radiator body. The stored heat in the radiator body is influenced on the interior side by the convection with water and, additionally, on the exterior side by convection with the room air (cf. [24]). This leads to:

$$m_{\text{body}}\, c_{\text{body}} \frac{dT_{\text{body}}}{dt} = h_{\text{A}} A_{\text{Rad,ex}} \left(T_{\text{body}} - T_{z_i}\right) - h_{\text{W}} A_{\text{Rad,in}} \left(\frac{T_{\text{in}} + T_{\text{out}}}{2} - T_{\text{body}}\right) \tag{69}$$

where
h_{A} convective coefficient with air,
$A_{\text{Rad,ex}}$ exterior area of the radiator surface which interacts with the air.

The natural convective heat transfer coefficient can be approximated with the simplified approach of ASHRAE [18] for vertical surfaces:

$$h_{\text{A}} = 1.42 \left(\frac{|\Delta T|}{H}\right)^{0.25} \tag{70}$$

with
ΔT temperature difference of air and surface,
H characteristic length of the radiator, i.e. height.

2.5.2. Electric floor heating

When it comes to floor heating, different systems can be used. In this thesis, electric floor heating is analyzed to compare other heating approaches. It is also called ohmic, or resistance or Joule heating (cf. [23]).
In general, electric floor heatings are based on long wave radiation since it produces heat by a wire's resistance. Thus, electric floor heat is built into the floor (see example in Figure 12).

[3] $R_{\text{el}} = \frac{V_{\text{el}}}{I_{\text{el}}}$

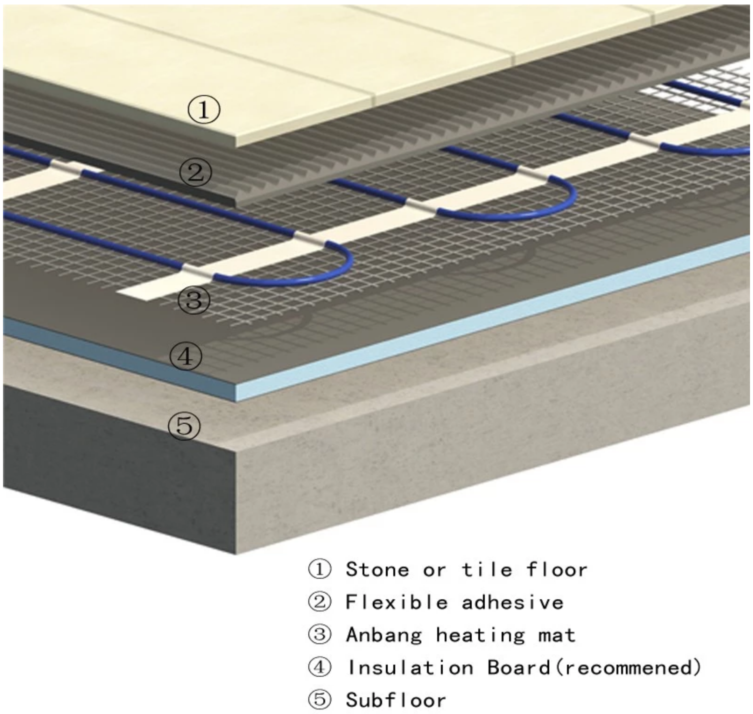

Figure 12: Exemplary build of electric floor heating into the floor(see [5]).

Thereby, the correlations for heating with electricity are based on Joule's law as follows (cf. [23]):

$$P = I_{\text{el}}^2 R_{\text{el}} \tag{71}$$

where
P electrical power in watt $[W]$,
I_{el} electrical current in ampere $[A]$,
R_{el} electrical resistance in ohm $[\Omega]$.

However, by construction, electric heat elements are designed for a specific heat output (e.g. $100W$ or 15 $\frac{W}{m^2}$). In reverse, this means that the resistance is fixed by the physical assembling of the device and not known. In contrast, the voltage of operating is known. Involving Ohm's law [3], the electrical power can be rearranged to:

$$P = I_{\text{el}}^2 R_{\text{el}} = I_{\text{el}}^2 \frac{V_{\text{el}}}{I_{\text{el}}} = I_{\text{el}} \cdot V_{\text{el}} \tag{72}$$

A benefit of electric heating is reflected in its efficiency. 100% of the electric energy is transformed into heat (cf. [63]). Therefore, the heat gain obtained by electric floor heating is described by the introduced electrical power volt-ampere:

[3] $R_{\text{el}} = \frac{V_{\text{el}}}{I_{\text{el}}}$

$$\dot{Q}_{\text{Floor}} = I_{\text{el}} \cdot V_{\text{el}} = \dot{E}_g = P \tag{73}$$

If the heat output of the electric heating device is given based on the area, e.g. 15 $\frac{W}{m^2}$, then the calculated heat gain from the equation above has to be multiplied further with the investigated area of interest.

2.6. Explanation model - state space model

The derived submodels now can be combined to get the temperature deviation inside a building.

Zone The following differential equation has to be solved for a zone Z_i with all necessary parameters given in the already shown models to get its temperature deviation:

$$\begin{aligned} c_{\text{A}}\rho_{\text{A}}V_{Z_i}\frac{dT_{Z_i}(t)}{dt} &= \sum_j \dot{Q}_j(t) = \sum_k \dot{Q}_{W_k}(t) + \sum_l \dot{Q}_{WG_l}(t) \\ &= \sum_k A_{W_k} \cdot q_{W_k,conv,in}(t) + \sum_l A_{WG_l} \cdot q_{WG_l,conv,in}(t) \end{aligned} \tag{74}$$

This includes the sum of all heat flows $\dot{Q}_j$ influencing the zone, i.e. all wall components W_k (including roofs, floors, ceilings) and window glazing components WG_l, have to be considered.
Note: Since radiators and floor heatings operate via radiation, they are not explicitly mentioned in the equation above. Their energy impact is already considered in the temperatures of walls and windows. The same holds for internal loads in the zone.

Walls The surface temperatures of walls can not be directly calculated because they are related to each other and given implicitly. Therefore, the heat transfer via conduction is computed with the state space method of the conduction transfer method portfolio (cf. e.g. [53, 42]). This includes the deviation of surface temperatures in a state space model. Additionally, this adds the energy storage functionality to the wall's mass.
In other words, this means that two more differential equations are needed to describe the temperature deviations at the surface. However, the approach is the same as for the temperature deviation in a zone. Furthermore, the required basis for this is already derived in the energy balances for walls.
So, each wall's surface temperature is influenced by the occurring heat fluxes at the surface (cf. energy balances for each surface).
With Equation 18, the interior wall surface temperature is given as:

$$
\begin{aligned}
c_{W_k}\rho_{W_k}\frac{V_{W_k}}{2}\frac{T_{W_k,in}(t)}{dt} =& A_{W_k}(q_{W_k,cond}(t) - q_{W_k,conv,in}(t) \\
&+ q_{W_k,sol,in}(t) + q_{W_k,radS,in}(t) + q_{W_k,radInt,in}(t))
\end{aligned}
\tag{75}
$$

And with Equation 32, the exterior wall surface temperature is concluded to:

$$
\begin{aligned}
c_{W_k}\rho_{W_k}\frac{V_{W_k}}{2}\frac{T_{W_k,ex}(t)}{dt} =& A_{W_k}(q_{W_k,conv,ex}(t) + q_{W_k,sol,ex}(t) \\
&+ q_{W_k,rad,ex}(t) - q_{W_k,cond}(t))
\end{aligned}
\tag{76}
$$

Since the conduction is treated in quasi-steady state conditions (cf. subsubsection 2.4.1), the temperature deviation within the wall is considered linearly. Therefore, the simplification can be made that the wall's volume is separated into two equal parts, whereas the temperature of each part equals to its surface temperature (cf. [36].
This holds for a wall constructed without inner layers. In the case of inner layers, e.g. isolation, differential equations per layer must be analogously added as shown above to capture the temperature at that point. These relations lead to x ODEs needed for each wall, where x is given by:

$$
\#\text{innerLayers} > 0 ? x = 2 \cdot \#\text{innerLayers} + 4 : x = 2 \tag{77}
$$

In the case that the wall is not an exterior wall, combinations with Equation 75 are made. This means that both surface temperatures for an interior wall are described by Equation 75 on each side (holds for ceilings too). If the wall is the ground floor, then only conduction at the exterior surface in Equation 76 has to be considered.

Windows The same approach from walls is used for windows. Nevertheless, one-layered windows need only one differential equation since the windows glazing component WG_l has a uniform temperature.
By considering Equation 53 (interior surface's heat flux) and Equation 54 (exterior surface's heat flux), the window glazing temperature is evaluated as:

$$
\begin{aligned}
c_{WG_l}\rho_{WG_l}V_{WG_l}\frac{T_{WG_l}(t)}{dt} &= A_{WG_l}(q_{WG_l,ex}(t) - q_{WG_l,in}(t)) \\
&= A_{WG_l}[q_{WG_l,conv,ex}(t) + q_{WG_l,sol,ex}(t) + q_{WG_l,rad,ex}(t) \\
&\quad - (q_{WG_l,conv,in}(t) - q_{WG_l,sol,in}(t) \\
&\qquad - q_{WG_l,radS,in}(t) - q_{WG_l,radInt,in}(t))]
\end{aligned}
\tag{78}
$$

If windows are multi-layered, the approach shown in the context of walls holds analogously, and the conduction process can be calculated for each layer of separating gas by adding a new temperature point to each side described by one ODE.

2.6.1. State space model

To give a better overview, all relations are concluded in a state space model. Due to its complexity and subsequent readability problems, the following state space model shows only one zone with one wall heated by one radiator and one floor heating. Analogously, it can be extended by the already explained relations.
So, in conclusion, the exemplary state space model is summarized as:

$$\begin{aligned} \dot{\mathbf{x}} &= \mathbf{f}(\mathbf{x}) + \mathbf{g}(\mathbf{x},\mathbf{u}) \\ \mathbf{y} &= \mathbf{h}(\mathbf{x}) \end{aligned} \tag{79}$$

where
$\mathbf{x}$ state vector,
$\mathbf{y}$ output vector,
$\mathbf{u}$ control vector.

$$
\dot{\mathbf{x}} = \begin{bmatrix} \dot{T}_{Z_i} \\ \dot{T}_{W_k,in} \\ \dot{T}_{W_k,ex} \\ \dot{T}_{Radiator_r,out} \\ \dot{T}_{Radiator_r,body} \end{bmatrix} = \begin{bmatrix} \frac{1}{c_{\mathrm{A}}\rho_{\mathrm{A}} V_{Z_i}} \\ \frac{2}{c_{W_k}\rho_{W_k} V_{W_k}} \\ \frac{2}{c_{W_k}\rho_{W_k} V_{W_k}} \\ \frac{1}{m_{\mathrm{W}} c_{\mathrm{W}}} \\ \frac{1}{m_{\mathrm{body}} c_{\mathrm{body}}} \end{bmatrix} \Bigg\{
$$

$$
\begin{bmatrix}
A_{W_k} 1.42 \left(\frac{|T_{Z_i} - T_{W_k,in}|}{H_{W_k}} \right)^{0.25} \left(T_{W_k,in} - T_{Z_i} \right) \\
\hline
A_{W_k} \left(k \cdot \frac{T_{W_k,ex} - T_{W_k,in}}{L} - 1.42 \left(\frac{|T_{z_i} - T_{W_k,in}|}{H_{W_k}} \right)^{0.25} \left(T_{W_k,in} - T_{Z_i} \right) + \frac{\sum_j A_{\mathrm{W},j} \tau_{\mathrm{L},j} I_{j,\ \mathrm{d}}}{A_{\mathrm{tot}}} \right) \\
\hline
\begin{aligned}
& A_{W_k} \left(5.678 \left(m + n \left(\frac{v_0}{0.3048} \right)^p \right) \left(T_{\mathrm{o}} - T_{W_k,ex} \right) - k \cdot \frac{T_{W_k,ex} - T_{W_k,in}}{L} \right) \\
& + A_{W_k} \varepsilon_{W_k,ex} \cdot 4\sigma \left[\left(\frac{1 - \cos\gamma}{2} \right) \left(\frac{T_{\mathrm{G}} + T_{\mathrm{o}}}{2} \right)^3 \left(T_{\mathrm{G}} - T_{\mathrm{o}} \right) + \left(\frac{1 + \cos\gamma}{2} \right) \left(\frac{T_{\mathrm{S}} + T_{\mathrm{o}}}{2} \right)^3 \left(T_{\mathrm{S}} - T_{\mathrm{o}} \right) \right] \\
& + A_{W_k} \cdot 4 \cdot \varepsilon_{W_k,ex} \cdot \sigma \left(\frac{T_{\mathrm{o}} + T_{\mathrm{W_k,ex}}}{2} \right)^3 \left(T_{\mathrm{o}} - T_{W_k,ex} \right)
\end{aligned} \\
\hline
0 \\
\hline
-1.42 \left(\frac{|T_{\mathrm{body}} - T_{Z_i}|}{H_{Radiator_r}} \right)^{0.25} A_{\mathrm{Radiator_r,ex}} \left(T_{\mathrm{body}} - T_{Z_i} \right)
\end{bmatrix}
$$

$$
+ \begin{bmatrix}
0 \\
0 \\
\hline
\begin{aligned}
& A_{W_k} \alpha_{\mathrm{W}_k,ex} \left(I_{T,h} - \left(1{,}0045 + 0{,}04349 \cdot \mathrm{k_C} - 3{,}5227 \cdot \mathrm{k_C^2} + 2{,}6313 \cdot \mathrm{k_C^3} \right) \cdot \mathrm{I_{T,h}} \right) \cos\theta \\
& + A_{W_k} \alpha_{\mathrm{W}_k,ex} \left[\left(1{,}0045 + 0{,}04349 \cdot \mathrm{k_C} - 3{,}5227 \cdot \mathrm{k_C^2} + 2{,}6313 \cdot \mathrm{k_C^3} \right) \cdot \mathrm{I_{T,h}} \left(\frac{1 + \cos\beta}{2} \right) + \rho_{\mathrm{g}} I_{T,h} \left(\frac{1 - \cos\beta}{2} \right) \right]
\end{aligned} \\
\hline
0 \\
0
\end{bmatrix}
$$

$$
+ \begin{bmatrix}
0 \\
\hline
A_{W_k} \cdot \frac{\dot{m} c_W \left(T_{in} - T_{out} \right)}{A_{\mathrm{tot}}} + A_{W_k} \cdot \frac{I_{\mathrm{el}} \cdot V_{\mathrm{el}}}{A_{\mathrm{tot}}} \\
\hline
0 \\
\hline
\dot{m} c_{\mathrm{W}} \left(T_{\mathrm{in}} - T_{\mathrm{out}} \right) - \left(\frac{1057 \left(1.352 + 0.0198 \frac{T_{\mathrm{in}} + T_{\mathrm{out}}}{2} \right) \left(\frac{\dot{m}}{\rho_{\mathrm{W}} \pi \frac{D}{2}} \right)^{0.8}}{D^{0.2}} \right) A_{\mathrm{Radiator_r,in}} \left(\frac{T_{\mathrm{in}} + T_{\mathrm{out}}}{2} - T_{\mathrm{body}} \right) \\
\hline
\left(\frac{1057 \left(1.352 + 0.0198 \frac{T_{\mathrm{in}} + T_{\mathrm{out}}}{2} \right) \left(\frac{\dot{m}}{\rho_{\mathrm{W}} \pi \frac{D}{2}} \right)^{0.8}}{D^{0.2}} \right) A_{\mathrm{Radiator_r,in}} \left(\frac{T_{\mathrm{in}} + T_{\mathrm{out}}}{2} - T_{\mathrm{body}} \right)
\end{bmatrix} \Bigg\}
$$

where

$$
\cos\theta = \sin(d)\sin(l)\cos(\beta) - \sin(d)\cos(l)\sin(\beta)\cos(\gamma) + \cos(d)\cos(l)\cos(\beta)\cos(\omega)
$$

$$
+ \cos(d)\sin(l)\sin(\beta)\cos(\gamma)\cos(\omega) + \cos(d)\sin(\beta)\sin(\gamma)\sin(\omega)
$$

$$
d = 23.45 \sin\left(360 \left(284 + n_{\mathrm{day}} \right) / 365 \right)
$$

$$
\omega = 15 \cdot \left(t_{\mathrm{Clock}} + 4 \left(L_0 - L_{\mathrm{loc}} \right) + 9.87 \sin\left[\frac{720 \left(n_{\mathrm{day}} - 81 \right)}{364} \right] - 7.53 \cos\left[\frac{360 \left(n_{\mathrm{day}} - 81 \right)}{364} \right] - 1.5 \sin\left[\frac{360 \left(n_{\mathrm{day}} - 81 \right)}{364} \right] - 12 \right)
$$

and

$$
y = T_{Z_i} = \begin{bmatrix} 1 & 0 & 0 & 0 & 0 \end{bmatrix} \cdot \begin{bmatrix} T_{Z_i} \\ T_{W_k,in} \\ T_{W_k,ex} \\ T_{Radiator_r,out} \\ T_{Radiator_r,body} \end{bmatrix} \tag{80}
$$

Thereby, the parameters used are listed below to allow a summarized overview. They are given in three tables. The first one lists all parameters which are constant during the whole optimization. The second one specifies parameters that are expected to be continually entered during optimization since they are time-dependent. The last one indicates the control variables used.

Constant parameter	Unit	Description	Property of
ρ_{A}	$kg \cdot m^{-3}$	Density of air	
c_{A}	$\frac{J}{kg \cdot K}$	Heat capacity of air	Zone
V_{Z_i}	m^3	Volume of zone Z_i	
A_{tot}	m^2	Area of all surfaces inside a zone (wall, windows, ceiling, floor)	
A_{W_k}	m^2	Area of wall W_k	
ρ_{W_k}	$kg \cdot m^{-3}$	Density of wall	
c_{W_k}	$\frac{J}{kg \cdot K}$	Heat capacity of wall	Wall
V_{W_k}	m^3	Volume of wall W_k	
$\alpha_{W_k,ex}$	-	Absorptivity of exterior wall surface W_k	
β	$\circ$	Tilting angle of surface to the horizontal	
l	$\circ$	Latitude angle of building	
γ	$\circ$	Surface azimuth angle	Solar radiation
L_{loc}	$\circ$	Longitude angle of building	
L_0	$\circ$	Longitude angle of standard meridian	
σ	$\frac{W}{m^2 K^4}$	Stefan-Boltzmann constant	
$\tau_{\mathrm{d},j}$	-	Diffuse solar transmissivity of window j	
$\tau_{\mathrm{D},j}$	-	Direct solar transmissivity of window j	
$\varepsilon_{W_k,ex}$	-	Emissivity of exterior wall surface W_k	
ρ_g	-	Outside ground reflectance	Long wave radiation
$\varepsilon_{W_k,in}$	-	Emissivity of interior wall surface W_k	
H_{W_k}	m	Characteristical length of wall W_k	
C_t	$\frac{W}{m^2 K^{4/3}}$	Turbulent natural convection constant	Convection

Constant parameter	Unit	Description	Property of
V_{W_k}	m^3	Volume of wall W_k	
L	m	Thickness of wall W_k	
k	$\frac{W}{mK}$	Thermal conductivity	Conduction
ρ_{W}	$kg \cdot m^{-3}$	Density of water	
c_{W}	$\frac{J}{kg \cdot K}$	Heat capacity of water	
c_{body}	$\frac{J}{kg \cdot K}$	Heat capacity of radiator's material	
m_{W}	kg	Mass of water inside the radiator	
m_{body}	kg	Mass radiator body	
D	m	Diameter of radiator tubes	
$A_{\mathrm{Radiator_r,in}}$	m^2	Inside (waterside) heat exchange surface of radiator	Radiator
$A_{\mathrm{Radiator_r,ex}}$	m^2	Exterior (airside/room) heat exchange surface of radiator	
$H_{Radiator_r}$	m	Characteristical length of radiator	
V_{el}	V	Voltage of the electric heating	Electric floor heating

External input parameter	Unit	Description
T_o	°C	Outside temperature
T_G	°C	Outside ground temperature
T_S	°C	Sky temperature
$I_{T,h}$	$\frac{W}{m^2}$	Solar intensity on horizontal plane
n_{day}	-	Day of the year
t_{clock}	-	Local time
SLF_j	-	Fraction of window being in direct solar radiation
v_0	$\frac{m}{s}$	Wind speed
k_c	-	Clearness index of the sky

Table 3: Description of external input parameters.

Control parameters	Unit	Description
T_{in}	°C	Inlet water temperature of radiator
$\dot{m}$	$\frac{kg}{s}$	Water mass flow of radiator
I_{el}	A	Electrical intensity of floor heating

Table 4: Description of Control parameters.

2.6.2. Summary of simplifications used

All in all, the derived explanation model uses the following simplifications:

- conduction under quasi-steady state conditions
- uniform window glazing temperature, i.e. neglecting of conduction through glazing components
- in long wave radiation an approximation is performed to reduce the exponent from power four to power three
- the water temperature inside the radiator results as the average between inlet and outlet water temperature
- the MRT method is used to estimate the internal radiation by enclosing surfaces
- direct short wave radiation is uniformly distributed to the floor, whereas diffuse short wave radiation is uniformly distributed to the floor and all other enclosing surfaces
- constant air density
- constant water density

3. Optimization

After modeling the generalized building and its thermal relations in an explanation model, this combined information can be used for optimization. Thereby, the goal consists of predicting the best control strategy regarding minimal operating costs. This problem leads to an optimal control problem, where under all admissible controls, the optimal control regarding an objective function has to be identified (cf. [58]). In fact, that problem corresponds to the problem of optimization.
For the goal of linear optimization, the non-linear differential equations must be made usable as a suitable input for the optimization by using appropriate methods. Therefore, the foundations of linearization and linear optimization are introduced (see subsection 3.1). Afterwards, the building's differential equations are linearized in subsection 3.2. Then, an economic model for quantifying the costs of energy is deduced (cf. subsection 3.3). In the end, the linear program is derived and listed (cf. subsection 3.4).

3.1. Foundations of linearization and linear programming

The following section describes the needed foundations to linearize a differential equation to make it suitable for linear optimization. Moreover, linear optimization itself is introduced in subsubsection 3.1.2.

3.1.1. Linearization of differential equations

Differential equations are a widespread tool in natural sciences. This discipline, however, often implies non-linear behaviour. Nevertheless, due to numerical calculations by computers, usually, complex systems are analyzed in a small environment around a specific operation point. In general, the linear system's theory is more advanced and non-linear systems are often linearized at an operation point to proceed on this basis. This means that the derivation at the given working point is of importance. Moreover, linear calculations require less computational effort.

Tailer's theorem Taylor gave in 1715 the definition that a n-time differentiable function can be approximated by the n-th order Taylor polynomial p_n around a working point x_o (cf. [16]):

$$p_n(x) = \sum_{k=0} \frac{f^{(k)}(x_0)}{k!} (x - x_0)^k \tag{81}$$

This series can be used for linearization by stopping after the second term, i.e. after the first-order Taylor polynomial.
Graphically spoken, the first-order Taylor polynomial creates a tangent at the working point x_0 (cf. Figure 13). In other words, only one point of the given function characterizes the linearization. For multi-dimensional problem, the approach is called Jacobian linearization (cf. [38]).

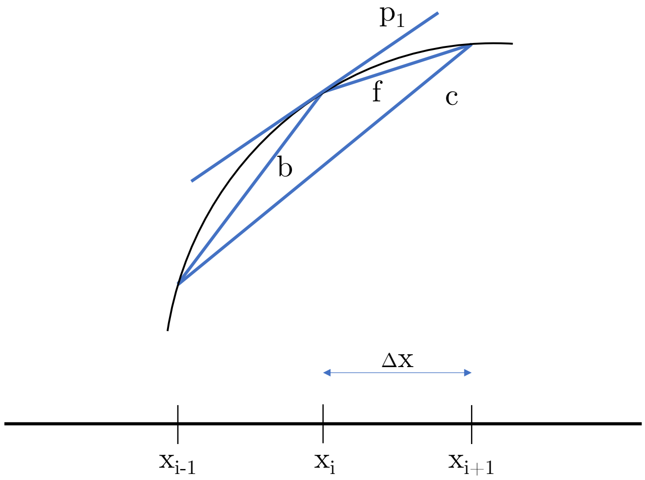

Figure 13: Illustration of first order Taylor polynomial p_1, forward f, backward b, and central difference c at working point x_i.

Finite difference method Based on Taylor's theorem, the finite difference method (FDM) goes a step further and relates two points of the function to each other. As the name already indicates, it is based on the difference quotient from mathematical analysis, which gives with limits of functions the foundations of differential calculus (cf. [34]).

Before the actual linearization, however, the method includes an important preliminary step of discretization. This is because FDM linearly approximates a derivate between two discrete points. Therefore, the continuous function is discretized onto a uniform grid with the width Δx between two points.

Based on Taylor's theorem, the FDM can be explained. The idea consists of the following. By using the approach of the first-order Taylor polynomial $p_1(x)$ at working point x_0, the next point of the grid $x_0 + \Delta x$ is approximated:

$$\begin{aligned} f(x + \Delta x) = p_1(x + \Delta x) &= f(x_0) + ((x_0 + \Delta x) - x_0)f'(x_0) \\ &= f(x_0) + \Delta x f'(x_0) \end{aligned} \tag{82}$$

This leads by algebraic manipulations to the approximation of the derivation:

$$f'(x_0) = \frac{f(x + \Delta x) - f(x_0)}{\Delta x} \tag{83}$$

This equation is called the forward difference of FDM and is used for linearization (cf. Figure 13). Analogously, the two other differences, backwards and central, can be derived. In general, they are given as (cf. [34]):

Forward difference:

$$f'(x_i) = \frac{f(x_{i+1}) - f(x_i)}{\Delta x}$$

Backward difference:

$$f'(x_i) = \frac{f(x_i) - f(x_{i-1})}{\Delta x} \tag{84}$$

Central difference:

$$f'(x_i) = \frac{f(x_{i+1}) - f(x_{i-1)}}{2\Delta x}$$

Feedback linearization However, linearization can not only be performed around a specific operation point. The method of feedback linearization acts contrary and offers the advantage that no approximation errors are made (cf. [38, 12]). By non-linear coordinate transformations and non-linear state feedback, the method creates a linear model (cf. [38]). There are two approaches of feedback linearization, i) *state-space* linearization and ii) *input-output* linearization.

i) In state-space linearization (cf. [12]) the idea consists of transforming a non-linear system

$$\begin{aligned} \dot{\mathbf{x}} &= \mathbf{f(x)} + \mathbf{g(x)u} \\ \mathbf{y} &= \mathbf{h(x)} \end{aligned} \tag{85}$$

into a linear system with a new control vector v

$$\dot{\mathbf{z}} = A\mathbf{z} + \mathbf{bv} \tag{86}$$

The goal (cf. [12]) is to linearize the impact of the transformed inputs on the states. Thereby, an artificial output z is used.
Nonetheless, this approach can fail because the relation of transformed input (v) and original output (y) is non-linear in general. This is why the second approach is preferred in most cases (cf. [38]).

ii) In contrast, input-output linearization (cf. [12]) tries to map the non-linear behaviour of a system (cf. Equation 85) from the Laplace-transformed control input v directly to the actual output y via the transfer function G:

$$y(s) = G(s)v(s) \tag{87}$$

Therefore, the original input is transformed by the static state feedback as:

$$u = \frac{v - L_f^r h(x)}{L_g L_f^{r-1} h(x)} + \frac{\sum_{k=1}^{r} \beta_{k-1} L_f^{k-1} h(x)}{L_g L_f^{r-1} h(x)} \tag{88}$$

where L is the Lie derivate.

Then, linear behavior can be expressed as:

$$G(s) = \frac{1}{\beta_r s^r + \beta_{r-1} s^{r-1} + \beta_1 s + \beta_0} \tag{89}$$

In addition, detailed mathematical explanations about both approaches are given in [47, 65].

3.1.2. Linear optimization

The field of linear optimization, which is also called linear programming (LP), was born in the year 1947 with a solution proposed by Danzig to optimize the planning problem of the US air force efficiently (cf. [74, 81]). The method introduced by Danzig is called simplex and is still a popular tool today. From then, linear programming has established as a discipline of applied mathematics, and further theory was explored and developed by mathematics and economics (cf. [52]).
The types of problems, which are solved by linear programming, consist of a linear *cost function* $f(x)$, also known as *objective function* (cf. [39]). That function has to be either minimized or maximized in boundaries of given *linear constraints* ($ax < b$ or $ax = b$). Therefore, the dependent variables of the cost functions and the constraints, the so called *decision variables* x, are used to find a feasible solution to satisfy all constraints. Formally spoken, that means with aim of vector notation:

$$\begin{array}{ll} \text{minimize} & f(x) = c^T x \\ \text{subject to} & Ax = b, \\ & x \geq 0, \end{array}$$

with vectors

$$x = \begin{bmatrix} x_1 \\ x_2 \\ \vdots \\ x_n \end{bmatrix}, \quad c = \begin{bmatrix} c_1 \\ c_2 \\ \vdots \\ c_n \end{bmatrix}, \quad b = \begin{bmatrix} b_1 \\ b_2 \\ \vdots \\ b_m \end{bmatrix}$$

and

$$A = \begin{bmatrix} a_{11} & a_{12} & \dots & a_{1n} \\ \vdots & \vdots & & \vdots \\ a_{m1} & a_{m2} & \dots & a_{mn} \end{bmatrix}$$

where x decision variables and rest given parameters. Besides, the non-negativity constraint is added in the last line.
That shown representation is already a linear program that can be solved. Moreover, this is even the standard form. Equalities in the constraints characterize it. There are

cases where the constraints are formalized by inequalities. Then, by introducing slack variables the standard form can be achieved to get a valid input format for the simplex method (cf. eg. [78, 52, 74, 14]).
With the accompanying possibilities of optimization and the resulting popularity, many state-of-the-art algorithms and especially implementations for solving linear as well as non-linear problems have been established. These are often freely available and easy to use. As an example, the interpretation of simplex is given.

Simplex method a prevalent method is simplex when it comes to solving linear programs. To illustrate that method's idea, a graphical explanation is given (cf. [39]). By combining the linear constraints in a vector-space, they form a polyhedron (cf. Figure 14).

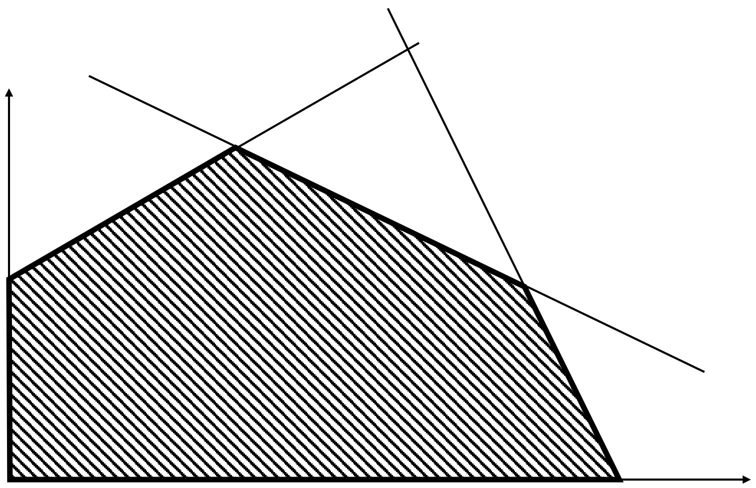

Figure 14: Exemplary 2D solution space of linear constraints.

Then, simplex is searching for corners of that polyhedral. When the polyhedron is intersected with the objective function, then there is one optimal corner (cf. eg. [39, 81]).

3.2. Linearization of building's differential equations

A finite difference approach is used to transform the non-linear building's ODEs into a valid linear input for linear optimization. This method is applied because its tradeoff between accuracy and simplicity is reasonable for that use case since Picard et al. [68] and [69] showed a temperature error smaller than $\pm$ 0.1K by the approach of Taylor. In contrast, conceptualizing feedback linearization raises the complexity of the problem and demands high effort, as indicated in [12]. The needed precision of a feedback linearized flight control system of a quadrocopter (cf. [25]), for example, is not in proportion with the required level of detail of the investigated use case in this thesis. However, the error rate of ± 0.1K from PICARD ET AL. is reasonable for heat analysis in buildings.

In general, ODEs can not be used out of the box as a valid input for linear programming because ODEs are a particular class of equations. That is why the following intermediate steps have to be performed for converting it to a suitable input.
If the building's ODEs (cf. subsubsection 2.6.1) are solved for a concrete but arbitrary control configuration of the system, this would mean that this configuration would be constant over that period of time. In reality, however, this is not the case for long periods, e.g. on a daily base. A radiator, for example, does not operate in a constant setting all day. It is more or less constantly readjusted. For this reason, it is necessary to discretize the continuous target range of prediction time P of the ODEs into uniform and smaller time intervals of size Δt, i.e. from time point t_i until t_{i+1}, in which new configurations can be applied.

$$P = \Delta t \cdot n \tag{90}$$

Thereby, n shows the number of time frames.
Then, individual temperature changes can be identified for each time period with its specific system configuration, e.g. radiator setting. Nonetheless, for this evaluation, an initial start point is necessary. Decoupled from a specific zone, the temperature curve from initial point t_0 until t_2 is given as:

$$T_{t_2} = T_{t_0} + \int_{t_0}^{t_1} \dot{T} dt + \int_{t_1}^{t_2} \dot{T} dt \tag{91}$$

with T_{t_i} temperature at time point t_i.
However, this would imply solving one ODE per time frame Δt. This is computationally expensive. Moreover, this is not compatible with linear programming because the building's ODEs are non-linear.
Nevertheless, due to the low-speed processes in the heat context, it is sufficient to approximate the temperature change during the periods in a linear manner without solving the ODEs explicitly and permanently. Therefore, the linearization at the given time point (operation point) is needed. As already described, the system configuration is not static over the day, but at smaller intervals such as 15 minutes, it can be assumed to be fixed because the effects of the changes in the configuration must first evolve. In addition, it is not possible in reality to change the inlet water temperature of a radiator from 40°C to 80°C in 1 second, for example. Overall, this also results in a reduced calculation effort.
So, the ODEs are discretized on a grid of fixed size Δt. Since for each calculation, the next time point t_{i+1} is of interest, i.e. the resulting temperature at this point for a given control input, the approach is extended by the forward finite difference to relate two discrete points together. However, this does not lead to an approximation of the rate of change of the temperature because $T_{t_{i+1}}$ is not known and depends on the tem-

perature of the previous time step T_{t_i}. In other words, this approach gives a recursive approach for temperature estimation. Thus, it can be integrated into the optimization as follows:
The building's ODEs at time point t_i are given as (cf. Equation 74):

$$\frac{dT_{t_i}}{dt} = f'(S) \tag{92}$$

where S are the state space variables.
Since the considered problem of temperature change is evolving in positive time, the forward difference (cf. subsubsection 3.1.1) is used to relate the actual time point to the next time point. As a result, the rate of change between two discrete points can be approximated as:

$$\frac{dT_{t_i}}{dt} \approx \frac{T_{t_{i+1}} - T_{t_i}}{\Delta t} \tag{93}$$

Thus, by combining Equation 92 and Equation 93, it holds that:

$$\frac{T_{t_{i+1}} - T_{t_i}}{\Delta t} \approx f'(S) \tag{94}$$

With algebraic manipulation, it finally leads to:

$$T_{t_{i+1}} \approx T_{t_i} + \Delta t \cdot f'(S) = T_{t_i} + \Delta t \cdot \frac{dT_{t_i}}{dt} \tag{95}$$

Since the control strategy's primary goal is to maintain the comfort requirements, i.e. control the indoor temperature within some given temperature boundaries for comfort temperature, every temperature point T_{t_i} is needed as a state variable for the optimization. Thus, the recursive and linear Equation 95 for every period t_i can be used as a valid constraint for the linear optimization.
However, the case study has shown that a $\Delta t = 15\text{min}$ leads to infeasible models because the temperature changes are over-approximated. Nonetheless, the control inputs should still not be applied much more often than every 15min due to the reason mentioned above, but in contrast, the temperature values have to be calculated more often than every 15min. This is why a further scaling factor s is introduced:

$$\Delta t = \frac{t_{\text{control}}}{s} \tag{96}$$

This leads to the possibility to specify the time interval for control data in t_{control} and via the scaling factor s the frequency of temperature changes calculations, Δt, can be adjusted.

Nevertheless, the derivate $f'(S)$ is non-linear (compare to the state space model given in subsubsection 2.6.1).
At first, it appears that Taylor linearization can be used here. Generally, that is true because $f'(S)$ describes the derivate at a specific state S. However, in the context of an

interdependent state space model in combination with linear optimization, Taylor can not be used because the state at time point t_{i+1} depends on the previous time point t_i. For example, an exemplary state is characterized by an equation to the power of four. Thus, the first-order Taylor polynomial is still given by an equation to the power of three. When considering only one operation point, this does not lead to problems (as the definition states) since this state is constant. However, for the optimization, all operation points in the investigated time period have to be considered in time steps Δt. And since these depend on the previous states, this leads again to non-linearities in the Taylor polynomial because the investigated state is variable. In other words, this means that a linear derivate $f'(S)$ is required for linear optimization with a recursive equation.

3.2.1. Interpolation

To obtain a linear derivate, the local linearization at a given state by Taylor's approach is replaced by a global linearization for the whole differential equation. This means, in other words, that a linear state space model is needed. When looking at the non-linear state space model, it is noticeable that not all occurring polynomials are non-linear. The majority is already linear. There are only a few mathematical terms that are non-linear.

Moreover, they are isolated and not embedded into complex non-linear relations, e.g. the wall temperature to the power of three. Motivated by this fact, a linear interpolation is performed for each individual non-linear term. Therefore, the minimum and maximum values of these terms are estimated and used for the interpolation.

However, this means that the following intermediate steps have to be executed before to eliminate non-linearities within the state variables. These are all temperature variables that are not given by e.g. measurements and have to be calculated. These include the indoor temperature T_{Z_i} of a zone i, the interior wall temperature $T_{W_i,in}$ of a wall i and the exterior wall temperature $T_{W_i,ex}$ of wall i. Thereby, the terms $T^4_{Z_i}, T^4_{\mathrm{W_i,in}}, T^3_{\mathrm{W_i,ex}}$ and $T^4_{\mathrm{W_i,ex}}$ appear within the differential equations and have to be linearized therefore. This is done by linear interpolation between the highest and lowest possible occurring temperatures for each individual component to obtain the best results in linearization. These points are roughly estimated from literature research or weather influence. Since no further coefficients occur in each term and due to the high slope of the terms, this method leads to a reasonable approximation.

Zone temperature $T^4_{Z_i}$ The ideal room temperature varies between about 16°C and 24°C. Therefore, the interpolation is performed as:

$$
\begin{aligned}
y(16) &= 16^4 = 65536 \\
y(24) &= 24^4 = 331776 \\
y &= mx + b \text{ (straight line equation)} \\
m &= \frac{\Delta y}{\Delta x} = \frac{331776 - 65536}{24 - 16} = 33280 \\
b &= y - mx = 65536 - 33280 \cdot 16 = -466944
\end{aligned}
\tag{97}
$$

Thus, $T^4_{Z_i}$ is approximated by:

$$T_i^4 \approx 33280 \cdot T_{Z_i} - 466944 \tag{98}$$

Interior wall temperature $T^4_{\mathrm{W_i,in}}$ The interior wall surface temperature is assumed to be limited downwards by 10°and upwards by 30°C since it is affected by solar radiation on the one hand, but on the other hand, it is however limited due to the solar transmissivity of windows.

$$
\begin{aligned}
y(10) &= 10^4 = 10000 \\
y(30) &= 30^4 = 810000 \\
y &= mx + b \text{ (straight line equation)} \\
m &= \frac{\Delta y}{\Delta x} = \frac{810000 - 10000}{30 - 10} = 4000 \\
b &= y - mx = 10000 - 4000 \cdot 10 = 6000
\end{aligned}
\tag{99}
$$

Thus, $T^4_{\mathrm{W_i,in}}$ is approximated by:

$$T^4_{\mathrm{W_i,in}} \approx 4000 \cdot T_{\mathrm{W_i,in}} + 6000 \tag{100}$$

Exterior wall temperature $T^3_{\mathrm{W_i,ex}}$ Depending on the location, the temperatures on the exterior wall surface turn out differently. Taking into account the heating by the sun, occurring temperatures can be assumed between -10 and 40 degrees.

$$
\begin{aligned}
y(-10) &= -10^3 = -1000 \\
y(40) &= 40^3 = 64000 \\
y &= mx + b \text{ (straight line equation)} \\
m &= \frac{\Delta y}{\Delta x} = \frac{64000 - -1000}{40 - -10} = 1300 \\
b &= y - mx = 64000 - 1300 \cdot 40 = 12000
\end{aligned}
\tag{101}
$$

Thus, $T^3_{\mathrm{W_i,ex}}$ is approximated by:

$$T^3_{\mathrm{W_i,ex}} \approx 1300 \cdot T_{\mathrm{W_i,ex}} + 12000 \tag{102}$$

Exterior wall temperature $T^4_{\mathrm{W_i,ex}}$ Analogously, the exterior wall temperature to the power of four is treated as:

$$\begin{aligned} y(-10) &= -10^4 = 10000 \\ y(40) &= 40^4 = 2560000 \\ y &= mx + b \text{ (straight line equation)} \\ m &= \frac{\Delta y}{\Delta x} = \frac{2560000 - 10000}{40 - -10} = 51000 \\ b &= y - mx = 10000 + 51000 \cdot 10 = 520000 \end{aligned} \tag{103}$$

Thus, $T^4_{\mathrm{W_i,ex}}$ is approximated by:

$$T^4_{\mathrm{W_i,ex}} \approx 51000 \cdot T_{\mathrm{W_i,ex}} + 520000 \tag{104}$$

Convection of air and water Another non-linear term is caused by the interior convection. This type of heat transfer occurs on walls and at the radiator:

$$q_{W_i,conv,in} = 1.42 \left(\frac{|\Delta T|}{H}\right)^{0.25} (T_{W_i,in} - T_i) \tag{105}$$

Thereby, the state variables are treated non-linearly, especially the absolute value and the fourth square root.
Since all seven models given by ASHRAE [18] are based on the temperature difference of the state variables, which are multiplied again with the state variables, another approach has to be used to get a linear approximation of convection.
Picard et al. [68] proposes to use an averaged convective coefficient, $\bar{h}$, over one year. If this value is not known, an exemplary static coefficient from a test case by ASHRAE [19] can be used for example:

Surface Type	Interior Convective Surface Coefficient ($h_{conv,in}$) W/ (m$^2 \cdot$ K)
Walls	2.2
Ceiling	1.8
Raised Floor	2.2
Windows	2.4

Figure 15: Exemplary convective heat transfer coefficients for interior surfaces (see [19]).

Control variables At the same time, the non-linear state space model does not only include non-linearities caused by the n-th power of one variable. In the state space model, nevertheless, the multiplication of two different control or state variables leads to non-linearities, which have to be linearized. Williams [84] gives a procedure to split a product of continuous variables into a separable function, i.e. into a sum. This procedure is performed exemplary for the multiplication of a radiator's mass flow and inlet water temperature in the following.

Mass flow and inlet water temperature $\dot{m}{\cdot}T_{in}$ The separation is done by introducing two new relations as follows:

$$\begin{aligned} u_1 &= \frac{1}{2}(\dot{m} + T_{in}) \\ u_2 &= \frac{1}{2}(\dot{m} - T_{in}) \end{aligned} \tag{106}$$

Additionally, the product $\dot{m} \cdot T_{in}$ equals to the following equation, which can be easily proven by algebraic manipulations, and is therefore replaced:

$$u_1^2 - u_2^2$$

Nevertheless, the resulting difference is still not linear. That is why a linear interpolation for the minimum and maximum values of $\dot{m}$ respectively T_{in} is applied to obtain a linear approximation of the values.

The mass flow is limited by the maximum volume flow of around $8\frac{m^3}{h}$ for standard circulation pumps in houses:

$$0 \leq \dot{m} \leq 8000\frac{kg}{h} \tag{107}$$

Whereas the inlet temperature has got the following bounds according to manufacturers of heating systems (cf. [7, 4]):

$$40 \leq T_{in} \leq 90°C \tag{108}$$

Thus, it holds:

$$\begin{aligned} u_1^2(min) &= (\frac{1}{2}(0 + 40))^2 = 400 \\ u_1^2(max) &= (\frac{1}{2}(8000 + 90))^2 = 16362025 \end{aligned} \tag{109}$$

$$\begin{aligned} u_2^2(min) &= (\frac{1}{2}(0 - 40))^2 = 400 \\ u_2^2(max) &= (\frac{1}{2}(8000 - 40))^2 = 15840400 \end{aligned} \tag{110}$$

This results by the help of the straight line equation $y = mx + b$ to:

$$\begin{aligned} m_1 = \frac{\Delta u_1^2}{\Delta x} &= \frac{16362025 - 400}{(8000 + 90) - (0 + 40)} = 2032.5 \\ b_1 &= y - mx = 400 - 2032.5 \cdot 40 = -80900 \\ \rightarrow u_1^2 &\approx 2032.5 \cdot u_1 - 80900 \end{aligned} \tag{111}$$

$$\begin{aligned} m_2 &= \frac{\Delta u_2^2}{\Delta x} = \frac{15840400 - 400}{(8000-40)-(0-40)} = 1980 \\ b_2 &= y - mx = 400 - 1980 \cdot 40 = -78800 \\ \rightarrow u_2^2 &\approx 1980 \cdot u_2 - 78800 \end{aligned} \tag{112}$$

$$\Rightarrow \dot{m} \cdot T_{in} \approx 2032.5 \cdot \frac{1}{2}(\dot{m} + T_{in}) - 80900 - (1980 \cdot \frac{1}{2}(\dot{m} - T_{in}) - 78800) \tag{113}$$

Furthermore, all occurring products of $\dot{m} \cdot T_{in}$ have to be substituted in the state space model. This method has to be performed for every occurring multiplication of state and control variables. That shown in the following.

Mass flow and outlet water temperature $\dot{m} \cdot T_{out}$

$$\begin{aligned} u_1 &= \frac{1}{2}(\dot{m} + T_{out}) \\ u_2 &= \frac{1}{2}(\dot{m} - T_{out}) \end{aligned} \tag{114}$$

$$u_1^2 - u_2^2$$

$$50 \leq T_{out} \leq 70°C \tag{115}$$

$$\begin{aligned} u_1^2(min) &= (\frac{1}{2}(0 + 50))^2 = 625 \\ u_1^2(max) &= (\frac{1}{2}(8000 + 70))^2 = 16281225 \end{aligned} \tag{116}$$

$$\begin{aligned} u_2^2(min) &= (\frac{1}{2}(0 - 50))^2 = 625 \\ u_2^2(max) &= (\frac{1}{2}(8000 - 50))^2 = 15800625 \end{aligned} \tag{117}$$

$$\begin{aligned} m_1 &= \frac{\Delta u_1^2}{\Delta x} = \frac{16281225 - 625}{(8000+70)-(0+50)} = 2030 \\ b_1 &= y - mx = 625 - 2030 \cdot 50 = -100875 \\ \rightarrow u_1^2 &\approx 2030 \cdot u_1 - 100875 \end{aligned} \tag{118}$$

$$\begin{aligned} m_2 &= \frac{\Delta u_2^2}{\Delta x} = \frac{15800625 - 625}{(8000-50)-(0-50)} = 1975 \\ b_2 &= y - mx = 625 - 1975 \cdot 50 = -98125 \\ \rightarrow u_2^2 &\approx 1975 \cdot u_2 - 98125 \end{aligned} \tag{119}$$

$$\Rightarrow \dot{m} \cdot T_{out} \approx 2030 \cdot \frac{1}{2}(\dot{m} + T_{out}) - 100875 - (1975 \cdot \frac{1}{2}(\dot{m} - T_{out}) - 98125) \tag{120}$$

Inlet water temperature and radiator body temperature $T_{in} \cdot T_{body}$

$$u_1 = \frac{1}{2}(T_{in} + T_{body})$$
$$u_2 = \frac{1}{2}(T_{in} - T_{body}) \tag{121}$$

$$u_1^2 - u_2^2$$

$$45 \leq T_{body} \leq 80°C \tag{122}$$

$$u_1^2(min) = (\frac{1}{2}(40+45))^2 = 1806.25$$
$$u_1^2(max) = (\frac{1}{2}(90+80))^2 = 7225 \tag{123}$$

$$u_2^2(min) = (\frac{1}{2}(40-45))^2 = 6.25$$
$$u_2^2(max) = (\frac{1}{2}(90-45))^2 = 506.25 \tag{124}$$

$$m_1 = \frac{\Delta u_1^2}{\Delta x} = \frac{7225 - 1806.25}{(90+80) - (40+45)} = 63.75$$
$$b_1 = y - mx = 1806.25 - 63.75 \cdot (40+45) = -3612.5 \tag{125}$$
$$\rightarrow u_1^2 \approx 63.75 \cdot u_1 - 3612.5$$

$$m_2 = \frac{\Delta u_2^2}{\Delta x} = \frac{506.25 - 6.25}{(90-45) - (40-45)} = 10$$
$$b_2 = y - mx = 6.25 - 10 \cdot (40-45) = 56.25 \tag{126}$$
$$\rightarrow u_2^2 \approx 10 \cdot u_2 + 56.25$$

$$\Rightarrow T_{in} \cdot T_{body} \approx 63.75 \cdot \frac{1}{2}(T_{in} + T_{body}) - 3612.5 - (10 \cdot \frac{1}{2}(T_{in} - T_{body}) + 56.25) \tag{127}$$

Outlet water temperature and radiator body temperature $T_{out} \cdot T_{body}$

$$u_1 = \frac{1}{2}(T_{out} + T_{body})$$
$$u_2 = \frac{1}{2}(T_{out} - T_{body}) \tag{128}$$

$$u_1^2 - u_2^2$$

$$u_1^2(min) = (\frac{1}{2}(50+45))^2 = 2256.25$$
$$u_1^2(max) = (\frac{1}{2}(70+80))^2 = 5625 \tag{129}$$

$$
\begin{aligned}
u_2^2(min) &= (\frac{1}{2}(50-45))^2 = 6.25 \\
u_2^2(max) &= (\frac{1}{2}(70-45))^2 = 156.25
\end{aligned} \tag{130}
$$

$$
\begin{aligned}
m_1 &= \frac{\Delta u_1^2}{\Delta x} = \frac{5625 - 2256.25}{(70+80)-(50+45)} = 61.25 \\
b_1 &= y - mx = 2256.25 - 61.25 \cdot (50+45) = -3562.5 \\
&\to u_1^2 \approx 61.25 \cdot u_1 - 3562.5
\end{aligned} \tag{131}
$$

$$
\begin{aligned}
m_2 &= \frac{\Delta u_2^2}{\Delta x} = \frac{156.25 - 6.25}{(70-45)-(50-45)} = 7.5 \\
b_2 &= y - mx = 6.25 - 7.5 \cdot (50-45) = -31.25 \\
&\to u_2^2 \approx 7.5 \cdot u_2 - 31.25
\end{aligned} \tag{132}
$$

$$
\Rightarrow T_{out} \cdot T_{body} \approx 61.25 \cdot \frac{1}{2}(T_{out} + T_{body}) - 3562.5 - (7.5 \cdot \frac{1}{2}(T_{out} - T_{body}) - 31.25) \tag{133}
$$

Inlet water temperature and outlet water temperature $T_{in} \cdot T_{out}$

$$
\begin{aligned}
u_1 &= \frac{1}{2}(T_{in} + T_{out}) \\
u_2 &= \frac{1}{2}(T_{in} - T_{out})
\end{aligned} \tag{134}
$$

$$
u_1^2 - u_2^2
$$

$$
\begin{aligned}
u_1^2(min) &= (\frac{1}{2}(40+50))^2 = 2025 \\
u_1^2(max) &= (\frac{1}{2}(90+70))^2 = 6400
\end{aligned} \tag{135}
$$

$$
\begin{aligned}
u_2^2(min) &= (\frac{1}{2}(40-50))^2 = 25 \\
u_2^2(max) &= (\frac{1}{2}(90-50))^2 = 400
\end{aligned} \tag{136}
$$

$$
\begin{aligned}
m_1 &= \frac{\Delta u_1^2}{\Delta x} = \frac{6400 - 2025}{(90+70)-(40+50)} = 62.5 \\
b_1 &= y - mx = 2025 - 62.5 \cdot (40+50) = -3600 \\
&\to u_1^2 \approx 62.5 \cdot u_1 - 3600
\end{aligned} \tag{137}
$$

$$
\begin{aligned}
m_2 &= \frac{\Delta u_2^2}{\Delta x} = \frac{400 - 25}{(90-50)-(40-50)} = 7.5 \\
b_2 &= y - mx = 25 - 7.5 \cdot (40-50) = 100 \\
&\to u_2^2 \approx 7.5 \cdot u_2 + 100
\end{aligned} \tag{138}
$$

$$\Rightarrow T_{in} \cdot T_{out} \approx 62.5 \cdot \frac{1}{2}(T_{in} + T_{out}) - 3600 - (7.5 \cdot \frac{1}{2}(T_{in} - T_{out}) + 100) \tag{139}$$

Mass flow and radiator body temperature $\dot{m} \cdot T_{body}$

$$\begin{aligned} u_1 &= \frac{1}{2}(\dot{m} + T_{body}) \\ u_2 &= \frac{1}{2}(\dot{m} - T_{body}) \end{aligned} \tag{140}$$

$$u_1^2 - u_2^2$$

$$\begin{aligned} u_1^2(min) &= (\frac{1}{2}(0 + 45))^2 = 506.25 \\ u_1^2(max) &= (\frac{1}{2}(8000 + 80))^2 = 16321600 \end{aligned} \tag{141}$$

$$\begin{aligned} u_2^2(min) &= (\frac{1}{2}(0 - 45))^2 = 506.25 \\ u_2^2(max) &= (\frac{1}{2}(8000 - 45))^2 = 15820506.25 \end{aligned} \tag{142}$$

$$\begin{aligned} m_1 &= \frac{\Delta u_1^2}{\Delta x} = \frac{16321600 - 506.25}{(8000 + 80) - (0 + 45)} = 2031.25 \\ b_1 &= y - mx = 506.25 - 2031.25 \cdot 45 = -90900 \\ \rightarrow u_1^2 &\approx 2031.25 \cdot u_1 - 90900 \end{aligned} \tag{143}$$

$$\begin{aligned} m_2 &= \frac{\Delta u_2^2}{\Delta x} = \frac{15820506.25 - 506.25}{(8000 - 45) - (0 - 45)} = 1977.5 \\ b_2 &= y - mx = 506.25 - 1977.5 \cdot 45 = -88481.25 \\ \rightarrow u_2^2 &\approx 1977.5 \cdot u_2 - 88481.25 \end{aligned} \tag{144}$$

$$\Rightarrow \dot{m} \cdot T_{body} \approx 2031.25 \cdot \frac{1}{2}(\dot{m} + T_{body}) - 90900 - (1977.5 \cdot \frac{1}{2}(\dot{m} - T_{body}) - 88481.25) \tag{145}$$

Inlet water temperature T_{in}^2

$$\begin{aligned} y(40) &= 40^2 = 1600 \\ y(90) &= 90^2 = 8100 \\ y &= mx + b \text{ (straight line equation)} \\ m &= \frac{\Delta y}{\Delta x} = \frac{8100 - 1600}{90 - 40} = 130 \\ b &= y - mx = 1600 - 130 \cdot 40 = -3600 \end{aligned} \tag{146}$$

$$\Rightarrow T_{in}^2 \approx 130 \cdot T_{in} - 3600 \tag{147}$$

Outlet water temperature T_{out}^2

$$
\begin{aligned}
y(50) &= 50^2 = 2500 \\
y(70) &= 70^2 = 4900 \\
y &= mx + b \text{ (straight line equation)} \\
m &= \frac{\Delta y}{\Delta x} = \frac{4900 - 2500}{70 - 50} = 120 \\
b &= y - mx = 2500 - 120 \cdot 50 = -3500
\end{aligned}
\tag{148}
$$

$$
\Rightarrow T_{out}^2 \approx 120 \cdot T_{out} - 3500 \tag{149}
$$

Mass flow $\dot{m}^{0.8}$

$$
\begin{aligned}
y(0) &= 0^{0.8} = 0 \\
y(8000) &= 8000^{0.8} = 64000000 \\
y &= mx + b \text{ (straight line equation)} \\
m &= \frac{\Delta y}{\Delta x} = \frac{64000000 - 0}{8000 - 0} = 8000 \\
b &= y - mx = 0 - 120 \cdot 0 = 0
\end{aligned}
\tag{150}
$$

$$
\Rightarrow \dot{m}^{0.8} \approx 8000 \cdot \dot{m} \tag{151}
$$

3.2.2. Linear state space model

In summary, the non-linear state space model (see subsubsection 2.6.1) can be transformed linearly by substituting with the shown approximations.

$$
\begin{bmatrix}
\dot{T}_{Z_i} \\
\dot{T}_{W_k,in} \\
\dot{T}_{W_k,ex} \\
\dot{T}_{Radiator_r,out} \\
\dot{T}_{Radiator_r,body}
\end{bmatrix}
=
\begin{bmatrix}
\frac{1}{c_{\mathrm{A}}\rho_{\mathrm{A}}V_{Z_i}} \\
\frac{2}{c_{W_k}\rho_{W_k}V_{W_k}} \\
\frac{2}{c_{W_k}\rho_{W_k}V_{W_k}} \\
\frac{1}{m_{\mathrm{W}}c_{\mathrm{W}}} \\
\frac{1}{m_{\mathrm{body}}c_{\mathrm{body}}}
\end{bmatrix}
\Bigg\{
\begin{bmatrix}
A_{W_k}\cdot \bar{h}(T_{W_k,in}-T_{Z_i}) \\
\hline
A_{W_k}\cdot k\cdot \frac{T_{W_k,ex}}{L} - A_{W_k}\cdot k\cdot \frac{T_{W_k,in}}{L} - A_{W_k}\cdot \bar{h}\cdot T_{W_k,in} + A_{W_k}\cdot \bar{h}\cdot T_{Z_i} + A_{W_k}\cdot \frac{\sum_j A_{\mathrm{W},j}\tau_{\mathrm{L},j}I_{j,\ \mathrm{d}}}{A_{\mathrm{tot}}} \\
\hline
\begin{array}{l}
A_{W_k}\cdot 5.678\left(m+n\left(\frac{v_0}{0.3048}\right)^p\right)T_{\mathrm{o}} + A_{W_i}\cdot T_{\mathrm{o}}\cdot 4\varepsilon_{W_i,ex}\sigma\left(\frac{T_{\mathrm{o}}}{2}\right)^3 + A_{W_i}\cdot T_{\mathrm{o}}\cdot\varepsilon_{W_i,ex}\sigma 650\cdot T_{\mathrm{W_i,ex}} \\
+ A_{W_i}\cdot T_{\mathrm{o}}\cdot\varepsilon_{W_i,ex}\sigma 6000 \\
+ A_{W_k}\varepsilon_{W_k,ex}\cdot 4\sigma\left[\left(\frac{1-\cos\gamma}{2}\right)\left(\frac{T_{\mathrm{G}}+T_{\mathrm{o}}}{2}\right)^3(T_{\mathrm{G}}-T_{\mathrm{o}}) + \left(\frac{1+\cos\gamma}{2}\right)\left(\frac{T_{\mathrm{S}}+T_{\mathrm{o}}}{2}\right)^3(T_{\mathrm{S}}-T_{\mathrm{o}})\right] \\
- A_{W_k}\cdot k\cdot\frac{T_{W_k,ex}}{L} + A_{W_k}\cdot k\cdot\frac{T_{W_k,in}}{L} - A_{W_k}\cdot 5.678\left(m+n\left(\frac{v_0}{0.3048}\right)^p\right)T_{W_k,ex} \\
- A_{W_i}\cdot T_{W_i,ex}\cdot 4\varepsilon_{W_i,ex}\sigma\left(\frac{T_{\mathrm{o}}}{2}\right)^3 - A_{W_i}\cdot\varepsilon_{W_i,ex}\sigma 25500\cdot T_{W_i,ex} - A_{W_i}\cdot\varepsilon_{W_i,ex}\sigma 260000
\end{array} \\
\hline
0 \\
\hline
-\bar{h}\cdot A_{\mathrm{Radiator_r,ex}}\left(T_{\mathrm{body}} - T_{Z_i}\right)
\end{bmatrix}
$$
$$
+\begin{bmatrix}
0 \\
0 \\
\hline
\begin{array}{l}
A_{W_k}\alpha_{\mathrm{W_k},ex}\left(I_{T,h} - \left(1,0045+0,04349\cdot \mathrm{k_C} - 3,5227\cdot\mathrm{k_C^2} + 2,6313\cdot\mathrm{k_C^3}\right)\cdot\mathrm{I_{T,h}}\right)\cos\theta \\
+ A_{W_k}\alpha_{\mathrm{W_k},ex}\left[\left(1,0045+0,04349\cdot\mathrm{k_C} - 3,5227\cdot\mathrm{k_C^2} + 2,6313\cdot\mathrm{k_C^3}\right)\cdot\mathrm{I_{T,h}}\left(\frac{1+\cos\beta}{2}\right) + \rho_{\mathrm{g}}I_{T,h}\left(\frac{1-\cos\beta}{2}\right)\right]
\end{array} \\
\hline
0 \\
\hline
0
\end{bmatrix}
$$
$$
+\begin{bmatrix}
0 \\
\hline
\begin{array}{l}
A_{W_k}\cdot\frac{c_W\left(2032.5\cdot\frac{1}{2}(\dot{m}+T_{in}) - 80900 - (1980\cdot\frac{1}{2}(\dot{m}-T_{in}) - 78800)\right)}{A_{\mathrm{tot}}} \\
- A_{W_k}\cdot\frac{-c_W\left(2030\cdot\frac{1}{2}(\dot{m}+T_{out}) - 100875 - (1975\cdot\frac{1}{2}(\dot{m}-T_{out}) - 98125)\right)}{A_{\mathrm{tot}}} + A_{W_k}\cdot\frac{I_{\mathrm{el}}\cdot V_{\mathrm{el}}}{A_{\mathrm{tot}}}
\end{array} \\
\hline
0 \\
\hline
\begin{array}{l}
c_W\left(2032.5\cdot\frac{1}{2}(\dot{m}+T_{in}) - 80900 - (1980\cdot\frac{1}{2}(\dot{m}-T_{in}) - 78800)\right) \\
- c_W\left(2030\cdot\frac{1}{2}(\dot{m}+T_{out}) - 100875 - (1975\cdot\frac{1}{2}(\dot{m}-T_{out}) - 98125)\right) \\
- \left(\frac{1057A_{\mathrm{Radiator_r,in}}\left(\frac{(\dot{m})^{0.8}}{(\rho_{\mathrm{W}}\pi\frac{D}{2})^{0.8}}\right)}{D^{0.2}}\right)[\frac{T_{\mathrm{in}}+T_{\mathrm{out}}}{2}1.352 + 0.0198*\left((\frac{T_{\mathrm{in}}}{2})^2 + (\frac{2T_{\mathrm{in}}\,T_{\mathrm{out}}}{2}) + (\frac{T_{\mathrm{out}}}{2})^2\right)] \\
+ \left(\frac{1057A_{\mathrm{Radiator_r,in}}\left(\frac{(\dot{m})^{0.8}}{(\rho_{\mathrm{W}}\pi\frac{D}{2})^{0.8}}\right)}{D^{0.2}}\right)\left(1.352T_{\mathrm{body}} + 0.0198\left(\left(\frac{T_{\mathrm{in}}\,T_{\mathrm{body}}}{2}\right) + \left(\frac{T_{\mathrm{body}}\,T_{\mathrm{out}}}{2}\right)\right)\right)
\end{array} \\
\hline
\begin{array}{l}
\left(\frac{1057A_{\mathrm{Radiator_r,in}}\left(\frac{(\dot{m})^{0.8}}{(\rho_{\mathrm{W}}\pi\frac{D}{2})^{0.8}}\right)}{D^{0.2}}\right)[\frac{T_{\mathrm{in}}+T_{\mathrm{out}}}{2}1.352 + 0.0198*\left((\frac{T_{\mathrm{in}}}{2})^2 + (\frac{2T_{\mathrm{in}}\,T_{\mathrm{out}}}{2}) + (\frac{T_{\mathrm{out}}}{2})^2\right)] \\
- \left(\frac{1057A_{\mathrm{Radiator_r,in}}\left(\frac{(\dot{m})^{0.8}}{(\rho_{\mathrm{W}}\pi\frac{D}{2})^{0.8}}\right)}{D^{0.2}}\right)\left(1.352T_{\mathrm{body}} + 0.0198\left(\left(\frac{T_{\mathrm{in}}\,T_{\mathrm{body}}}{2}\right) + \left(\frac{T_{\mathrm{body}}\,T_{\mathrm{out}}}{2}\right)\right)\right)
\end{array}
\end{bmatrix}
\Bigg\}
\tag{152}
$$

This linear state space model can be used by executing the last step of substitution of the non-linear temperatures as given above.

At this point, the possibility arises to use the model in two ways. On the one hand, the still remaining non-linear temperatures have to be substituted with the given interpolations above. Then, a constant mass flow for radiators is assumed in the model, which means that the third control variable can be set only once at the beginning of the optimization.
However, on the other hand, a second step of interpolation can be performed to cancel out the resulting non-linearities by the multiplication of all temperature variables with the mass flow. Then, the mass flow gets fully controllable. Again, the given interpolations above can be used to substitute the multiplication.
An investigation of both approaches is performed in the case study (cf. section 5) to check if the second and additional interpolation step promotes further interpolation errors.

3.3. Economic cost model of heating

Summing up, the ODE (cf. Equation 74) describes the relationship between the input and output of heat in a zone to its provoking temperature changes. However, in the context of cost optimization, it makes a significant difference whether $1kW$ heat is produced by electric or hydronic heating[4]. To explain this, the notion of efficiency regarding heat generation is introduced. It describes the ratio between introduced work to a heating device and its produced thermal energy as output. Thus, each heating device has got its individual efficiency, also called the coefficient of performance (COP). It indicates how many units of thermal energy E_{th} can be converted from another type of energy E_{in}, as e.g. electrical, (cf. [73]). In fact, COP defers from device to device and from the heat generation method. Generally, COP is stated as:

$$COP = \frac{E_{th}}{E_{in}} \tag{153}$$

In the case of transforming electrical power to heat for example, the COP is defined as:

$$COP = \frac{Q_{out}}{P_{in}} \tag{154}$$

Under these aspects of energy transformation efficiency, the heat output of the investigated HVAC-components (cf. subsection 2.5) has to be mapped to an economic cost model to enable the calculation of their implying operation costs needed heat output. Besides, the discretization enables the treatment of flexible resource prices per daytime, as often occurring for electricity.

3.3.1. Electric resistance heating

As already indicated by electrical floor heating (cf. subsubsection 2.5.2), the COP of electric resistance heating equals one, since $1W$ electrical power is converted to $1W$

[4]Heating by warm water.

heat. This allows a simple calculation of the costs caused by this type of heating.

$$price(Q(\text{elFloorHeat})) = Q(\text{elFloorHeat}) * time * electricityPrice \tag{155}$$

where the heat output is obtained as illustrated in subsection 2.5.
For example, a heating device with $2000W$ heat output is considered. The operating costs can be exemplary calculated for a defined time and arbitrary electricity costs as follows:

$$0.4€ = 2kW \cdot 1h \cdot 0.2\frac{€}{kWh} \tag{156}$$

3.3.2. Hydronic heating

In the case of heating by warm water, the cost computation is not as light as before because the efficiency of heat pumps, which heat the water, is not constant and depends on their mode of operation. It is obvious that it needs more energy to heat a medium from 5° to 30° than from 10° to 30°. To make the efficiency comparable, DIN 14511 [1] gives nominal test conditions for heat humps. Nowadays, under nominal conditions, modern water and ground source heat pumps achieve a COP of around 3 to 5 (cf. [31]). Anyhow, that coefficient is a snapshot of a given operation point. It is impossible to test all operation points in advance to know their coefficients for a needed operating point.
That is why the seasonal COP (SCOP) is used for the cost estimation. It considers the averaged COP over the whole year.

$$SCOP = \frac{\bar{Q}_{out}}{\bar{P}_{in}} \tag{157}$$

Nonetheless, for each investigating case, the SCOP has to be calculated for the specific heat system configuration. Then, DIN 14825 [2] specifies a calculation guideline. Moreover, VDI-Fachbereich Energietechnik concludes the methods for electrical heat pumps [83] and for gas heat pumps [82]. Additionally, there is also an online calculation tool that already includes preimplemented different types of heat pumps (see [26]).
As a result, the operating costs of a radiator within a hydronic heating system are calculated as:

$$price(Q(\text{Radiator})) = \left(\frac{Q(\text{Radiator})}{SCOP}\right) * time * resourcePrice \tag{158}$$

where the resourcePrice indicates the price of the input resource for energy transformation, e.g. gas or electricity.
An example is given below:

$$0.2€ = \frac{3kW}{3} \cdot 1h \cdot 0.2\frac{€}{kWh} \tag{159}$$

3.4. Formulation of linear program

By concluding all the analyzed information, the linear program can be given. Based on the generalized zone ODE (cf. Equation 74), the goal is to optimize the building's overall running costs.
The formulation is based on the procedure suggested by PYAE [71] for setting up linear programs which consists of four steps:

Define decision variables All variables, which can be used to control the temperature, can be pointed out. These are the following parameters that can be modified externally and are not given by the atmospheric effects, e.g. outdoor temperature or system properties. In fact, an HVAC device D is meant. However, not every device offers each of the following parameters. It depends on its type. Nonetheless, these parameters can be used in general:

1. Mass flow of water $\dot{m}_{Radiator_r}$ (radiator)
2. Inlet water temperature $T_{Radiator_r,in}$ (radiator)
3. Electrical current I_{Floor_m} (electric floor heat)

Set objective function It is apparent that the overall control problem is a minimization problem of operating costs. This leads to an objective function which sums up all occurring operating costs of the HVAC-system during the optimization period P with discretization $P = \Delta t \cdot n$. The operating costs are calculated for the generated heat Q_{gen}. With consideration of the economic model of operation, the function to minimize is summarized as:

$$min \text{ overall operating costs} = \sum_{j=1}^{n} \sum_{devices} price(Q_{gen}) \tag{160}$$

Set constraints An HVAC-system's goal is to maintain the comfort temperature T within a given temperature profile (cf. Figure 16).

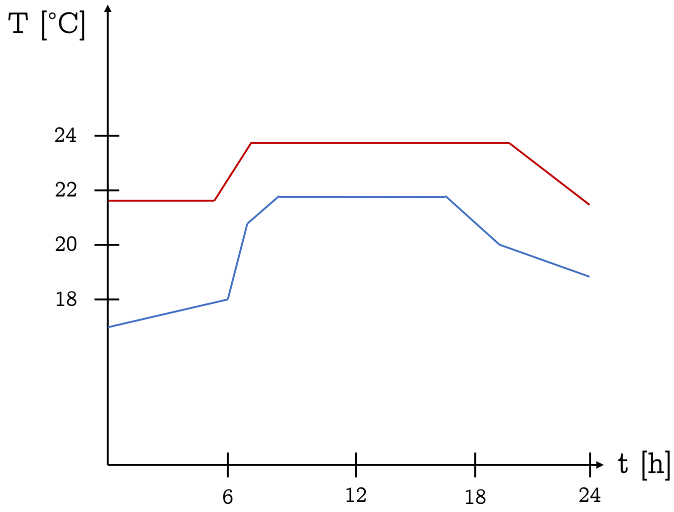

Figure 16: Exemplary temperature profile for one day for a zone.

This means that T has to be in its lower l and upper bound u. Applied on the time frames t_j ($j = 1..n$ due to $P = \Delta t \cdot n$) of the discretized ODE and different zone z_i, that leads to the following constraints:

$$l_{z_i,t_j} \leq T_{z_i,t_j} \tag{161}$$

$$T_{z_i,t_j} \leq u_{z_i,t_j} \tag{162}$$

The temperature relates to the zone temperature deviation (see Equation 95) as:

$$T_{z_i,t_{j+1}} = T_{z_i,t_j} + \Delta t \cdot \dot{T}_{z_i,t_j} \tag{163}$$

And the initial values for the zone temperature are given:

$$T_{z_i,t_0} = T_{z_i}(t = 0) \tag{164}$$

For the evaluation of the zone temperature, the wall temperatures are needed as well. The same principle is applied for the temperatures of all wall surfaces, although that temperatures do not have upper and lower limits:

$$T_{W_i,in,t_{j+1}} = T_{W_i,in,t_j} + \Delta t \cdot \dot{T}_{W_i,in,t_j} \tag{165}$$

$$T_{W_i,ex,t_{j+1}} = T_{W_i,ex,t_j} + \Delta t \cdot \dot{T}_{W_i,ex,t_j} \tag{166}$$

where the rate of changes is given by the ODEs evaluated at the specific time point t_j and depends on the decision variables.
In addition, initial values for all wall surfaces, interior and exterior, have to be considered:

$$T_{W_i,in,t_0} = T_{W_i,in}(t = 0) \tag{167}$$

$$T_{W_i,ex,t_0} = T_{W_i,ex}(t = 0) \tag{168}$$

Analogously, the window glazing temperature, outlet water temperate, and body temperature of a radiator have to be considered.

When looking at HVAC-devices D, they also have constraints in their mode of operation. Hydronic heating devices D_r^{h} have a limited inlet mass flow of water.
Radiator:

$$\dot{m}_{Radiator_r} \leq \dot{m}_{max}(D_r^{\mathrm{h}}) \tag{169}$$

Furthermore, all used electric devices D_m^{el} are designed from the manufacturer for a specific maximal power output P_{max}. In other words, their output is limited upwards with a maximal capacity.
Electric floor heat:

$$P(D_m^{\mathrm{el}}) \leq P_{max}(D_m^{\mathrm{el}}) \tag{170}$$

Non-negativity restriction As all devices D have got an upper limit, exactly the same holds downwards. They can not produce negative power.
Radiator:

$$0 \leq \dot{m}_{Radiator_r} \tag{171}$$

Electric floor heat:

$$0 \leq I_{Floor_m} \tag{172}$$

3.4.1. Linear program

In summary, the complete, but generalized linear program for an optimization period $P = \Delta t \cdot n$ with $j \in \{1..n\}$ results as for all zones z_i, walls W_k, hydronic radiators $Radiator_r$, and el. floor heatings $Floor_m$:

$$
\begin{aligned}
min \text{ operating costs} = \sum_{j=1}^{n} \sum_{devices} price(Q_{generated}) &= \sum_{j=1}^{n} \sum_{devices} price \cdot \Delta t \cdot \dot{Q}_{generated} \\
l_{z_i,t_j} &\leq T_{z_i,t_j} \\
T_{z_i,t_j} &\leq u_{z_i,t_j} \\
T_{z_i,t_{j+1}} &= T_{z_i,t_j} + \Delta t \cdot \dot{T}_{z_i,t_j} \\
T_{W_k,in,t_{j+1}} &= T_{W_k,in,t_j} + \Delta t \cdot \dot{T}_{W_k,in,t_j} \\
T_{W_k,ex,t_{j+1}} &= T_{W_k,ex,t_j} + \Delta t \cdot \dot{T}_{W_k,ex,t_j} \\
T_{WG_l,t_{j+1}} &= T_{WG_l,t_j} + \Delta t \cdot \dot{T}_{WG_l,t_j} \\
T_{Radiator_r,out,t_{j+1}} &= T_{Radiator_r,out,t_j} + \Delta t \cdot \dot{T}_{Radiator_r,out,t_j} \\
T_{Radiator_r,body,t_{j+1}} &= T_{Radiator_r,body,t_j} + \Delta t \cdot \dot{T}_{Radiator_r,body,t_j} \\
T_{z_i,t_0} &= T_{z_i}(t=0) \\
T_{W_k,in,t_0} &= T_{W_k,in}(t=0) \\
T_{W_k,ex,t_0} &= T_{W_k,ex}(t=0) \\
T_{WG_l,t_0} &= T_{WG_l}(t=0) \\
T_{Radiator_r,out,t_0} &= T_{Radiator_r,out}(t=0) \\
T_{Radiator_r,body,t_0} &= T_{Radiator_r,body}(t=0) \\
\dot{m}_{Radiator_r,t_j} &\leq \dot{m}_{max,Radiator_r} \\
P(D^{\text{el}}_{Floor_m,t_j}) &\leq P_{max}(D^{\text{el}}_{Floor_m}) \\
0 &\leq \dot{m}_{Radiator_r,t_j} \\
0 &\leq I_{Floor_m,t_j} \\
40^\circ C &\leq T_{Radiator,in,t_j} \\
T_{Radiator,in,t_j} &\leq 90^\circ C \\
& i \in \{1..|\text{zones}|\} \\
& k \in \{1..|\text{walls}|\} \\
& l \in \{1..|\text{windows}|\} \\
& r \in \{1..|\text{hydronic radiators}|\} \\
& m \in \{1..|\text{el. floor heatings}|\}
\end{aligned}
$$

4. Implementation

The derived approach of linear building control is implemented to enable the optimization for general buildings. The implementation is based on the procedure for deriving the explanation model for thermal movements (cf. subsection 2.1) and optimizes a building given as input according to the object-oriented structure (see Figure 18). The used approach is explained in this section.
In general, the program proceeds according to the following flow structure (cf. Figure 17) and consists of four main steps.

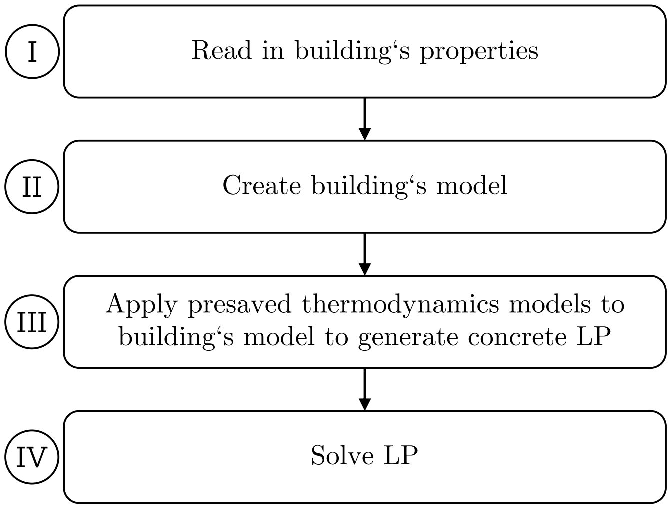

Figure 17: Flow chart of the general implementation of optimal building control.

First, it reads in all necessary building parameters, which can be concretely found in subsection 2.3. Therefore, a detached file is provided, in which, for example, the wall thickness can be adapted, or the weather and price data is imported from CSV-files.
In the next step, an internal building model is created. This is comparable to the first descriptive model. It describes the static building properties, e.g. zone air volume. It is inspired by the graph structure presented in subsection 2.3 and maps a building to an object-oriented approach. Thereby, the relations are characterized by the following class diagram:

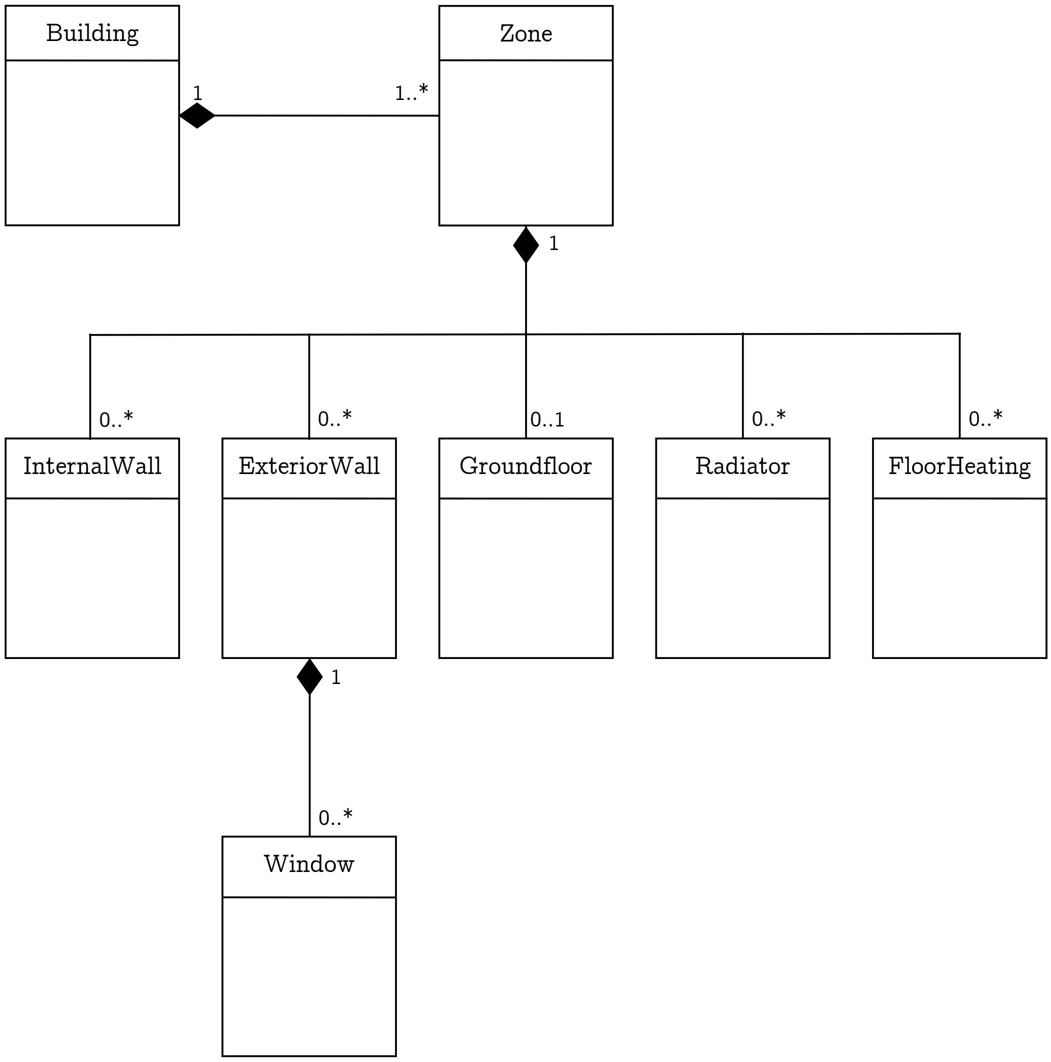

Figure 18: Object-oriented building structure used in the implementation.

Thereby, a roof is treated as an exterior wall and ceilings between two levels as an internal wall.

The third step includes the generation of the concrete linear program for the investigated building. Therefore, the derived thermodynamic models describing heat movements in buildings (see subsection 2.4) and HVAC components (see subsection 2.5) are presaved in a general form and applied according to the description model of the building built in step I and II. So, the linear program for the building of interest can be generated in *.mps* format, a standardized format for mathematical problems.
In the last step, a solver is used to solve the linear program. In this case *Gurobi* is used in combination with *Python V3.8* and extension *Gurobipy V9.1.1*. Nevertheless,

the generated linear program can be solved by any solver which is compatible to the *.mps* format.

5. Case Study and results

To validate the whole approach of the structured building optimization, a case study is performed.
First, the used approach is introduced. Then, the investigated building is given. Afterwards, the necessary information for optimization is transformed by the presented four-step approach to a logical graph. In the end, the case study results are analyzed in the context of the research questions.

5.1. Approach

With the help of the case study, the processes taking place in the derived models are to be verified and analyzed.
To make this possible, a rudimentary building is used for the case study in order to be able to verify the processes logically. For this purpose, all derived components from the explanation model are placed in the case study building (see subsection 5.2).
Therefore, the following characteristics are used during the case study:

- The investigated building is always optimized under the same external circumstances during a period of 24 hours to create comparable situations.
- The control data for heating devices is applied every 15min because the test data (weather and energy costs) have got the same interval.
- The costs for the heat gained by hydronic and electric heating are treated equally and are not distinguished further. The prices are fictitious and higher than in reality.

As a result, the following subquestions in the context of optimal control are answered by varying different parameters of the optimization:

- Does the second step of interpolation, when linearizing the multiplication of three state and control variables ($\dot{m} \cdot T_{in} \cdot T_{out}$) instead of only two ($T_{in} \cdot T_{out}$) in case of controlling a radiator, lead to other results since $\dot{m}$ and T_{in} are used as control variables instead of controlling only T_{in} and to assume the mass flow to be constant?
  → Comparison of both linear models (constant $\dot{m}$ (100 kg/h) vs. variable mass flow $\dot{m}$ (max. 100 kg/h)) with a uniform energy price of 1€/kWh.
- Which effects have the time difference, Δt, when approximating the next state of the building?
  → Investigation of different time differences of 10sec, 90sec, 3min, 5min and 7.5min with a uniform energy price of 1€/kWh.
- Which effects have energy prices on the optimization?
  → Application of two price models: One is dynamic, which means that every

15min another price is applied. The other one divides the optimization period of 24h into three intervals with different prices. Thereby, the last interval (18h-24h) contains negative prices for testing the modeling and optimization logic.

- Which effects have weather (solar radiation and outside temperature) on the building? → Analysis of their impacts on the zone temperature and caused heat gain.
- Which effects have building configurations on the optimization? → Comparison of standard and doubled thickness of exterior walls.

5.2. Investigated Building

The simplistic building results in an object with two zones and single-layer walls:

- Zone 1 is heated by electrical floor heating and has no windows.
- Zone 2 is heated by hydronic radiator and includes a one-layered window.
- All exterior walls have got the same thermal properties and are made of concrete.
- The weather data is taken for the location Aachen in Germany from the 11th January 2021. Thus, the building is located at 52°N latitude and 6°E longitude, where the standard meridian is given at 15°E.

To enable a two-dimensional representation that is not overloaded, the floor and the roof are neglected. Nevertheless, these two components are included in the validation by the model of walls.
In order to give an uniform representation of the building, it is already transformed below via the four-step procedure as a graph (cf. subsection 2.3):

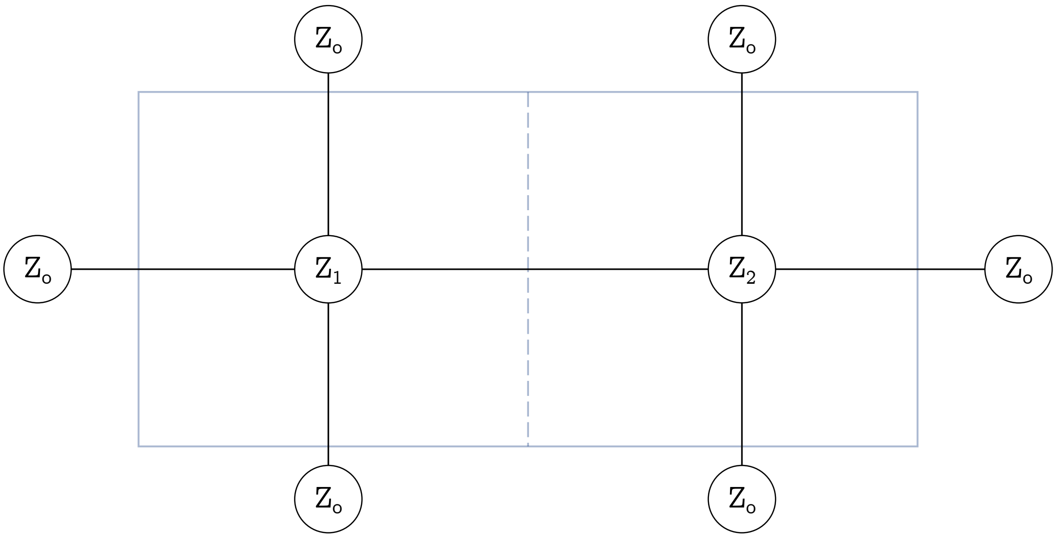

Figure 19: Graph representation of the exemplary building.

Afterwards, the specific zone properties have to be identified. For a summarized representation, these parameters are given for each zone (node) in Figure 20 and for each thermal connection (edge) in Figure 21 and Figure 22.

Zone 1:	Zone 2:
- volume: 3m*4m*2m = 24m^3	- volume: 3m*4m*2m = 24m^3
- el. floor heating	- hydronic radiator
V_{el} = 220V	massWater = 5kg
P = 100 W/m^2	massBody = 40kg
area = 3m*4m = 12m^2	capacityBody = 470 J/(kg*K) (steel)
	aIn = 1m^2
	aEx = 1m^2
	dTubes = 0.002m

Figure 20: Zone parameters of the exemplary building.

Zone 1 <-> Outside:	Zone 1 <-> Zone 2:
- wall1	- wall
width = 4m	width = 3m
γ = 180°	L = 0.2m
- wall2	c = 800 J/(kg*K)
width = 3m	
γ = 90°	
- wall3	
width = 4m	
γ = 0°	

Valid for all exterior walls:
height = 2m; β = 90°; k = 0.7; L = 0.4; ε = 0.94; c = 1000; ρ = 2000; α = 0.1

Figure 21: Thermal connection parameters of the first zone in the exemplary building.

Zone 2 <-> Outside:

- wall1
  - width = 4m
  - γ = -180°
  - window
    - width = 1m
    - τ = 0.3
    - ε = 0.2
    - α_D = 0.3
    - α_d = 0.2
- wall2
  - width = 3m
  - γ = -90°
- wall3
  - width = 4m
  - γ = 0°

Valid for all exterior walls:
height = 2m; β = 90°; k = 0.7; L = 0.4; ε = 0.94; c = 1000; ρ = 2000; α = 0.1

Figure 22: Thermal connection parameters of the second zone in the exemplary building.

5.3. Results

By the use of an 8 core processor (2.4 GHz) with 32gb RAM, the following results are calculated with default Gurobi settings, which also imply multithreading.
The results are presented in the order of the subquestions given at the beginning of the section. Thereby, the following plots always show data for one specific zone over the optimization period of 24h and compare two different data sets on the y-axis.

5.3.1. Test: Time and mass flow modeling

This section compares different time differences Δt (grid size in discretization) for calculation the new states of a building. Thereby, in parallel, the two approaches of constant and variable mass flow are distinguished. The energy price is simplified to 1€/kWh.
Further on, this section is divided into three paragraphs, where the different impacts on i) the entire optimization, ii) zone 1 and iii) zone 2 are shown.

Effects on the optimization The test shows the following impacts for the entire optimization (cf. Table 5):

- From a time of 7.5min, the optimization model has no more solution, i.e. it becomes infeasible because the calculations are more over-approximated, so that the next states are no longer within the specified temperature boundaries.
- With a more detailed computation of the ODEs, i.e. smaller Δt, the complexity of the problem increases, reflected in the number of iterations and the solving time. Both are increasing significantly, although the test building is kept simple.
- The complexity of the approach with the variable mass flow is higher than the approach with the constant mass flow. That is logical because the mass flow changes from a constant to an other control variable.
- The resulting energy costs are increasing with the complexity of the calculation since the it gets more detailed and not as over-approximated as in the other cases. This can be caused by a coincidentally good starting point of the optimization.
- Generally, the costs do not show significant differences. However, when the task consists only of the estimation of the overall energy costs, then the approach with constant mass flow can be used, because it has a lower complexity and no significant variance in price.

Table 5 shows a summary of the investigated values and results.

Δt	Iterations	Solving time	Costs	Mass flow radiator
7.5min	infeasible			
5min	3523	0.62sec	23.31€	
3min	513	0.62sec	23.36€	constant 100 kg/h
90sec	609	1.77sec	23.39€	
10sec	3354	42.35sec	23.41€	
7.5min	infeasible			
5min	5650	2.04sec	23.30€	
3min	6081	1.76sec	23.35€	variable max. 100kg/h
90sec	11716	5.26sec	23.38€	
10sec	97116	326.98sec	23.42€	

Table 5: Comparison of different Δt with constant and variable mass flow for controlling radiators.

Effects on zone 1 The are no significant effects on the first zone. This is due to the gain through electrical heating:

- The calculation of the heat gain is, compared to a radiator, simple. This causes no crucial changes with different time differences. Only around 7h, 13h, and 16h, a slightly higher heat gain is noticeable.
- Zone 1 is heated electrical. Therefore, the differentiation between constant and variable water mass flow of radiators does not affect it.

To underline the facts, the plots for $\Delta t = 5$min with constant mass flow and $\Delta t = 10$sec with variable mass flow are provided below.
The other combinations of time difference and mass flow modeling approach are shown in A.

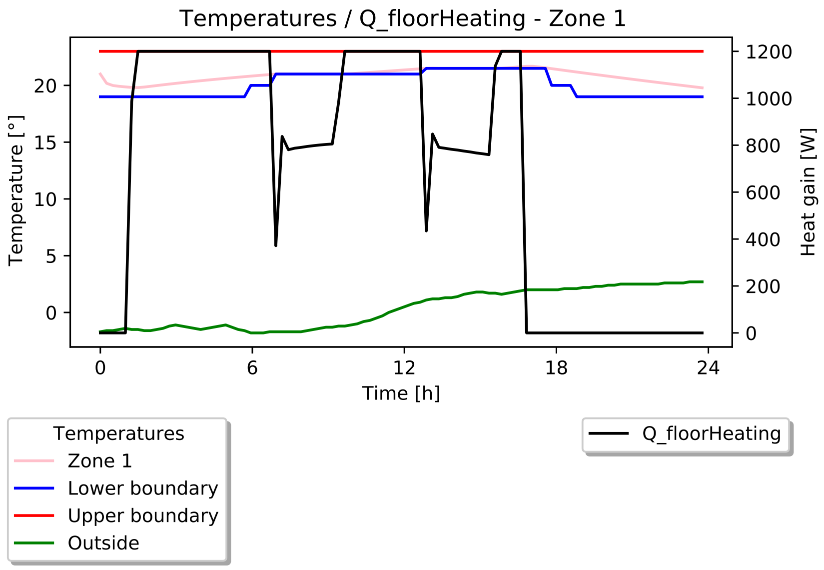

Figure 23: ΔTime 5min, constant mass flow 100kg/h

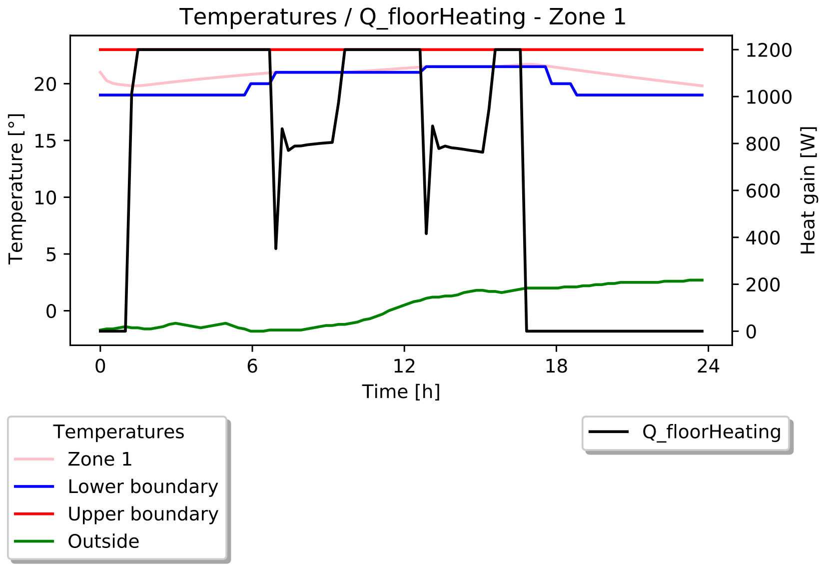

Figure 24: ΔTime 10sec, variable mass flow max. 100kg/h

Effects on zone 2 In zone 2, the expected changes in the heat gain from the radiator get identifiable in the following figures.
In general, several facts can be noticed (cf. A for the plots):

- All generated values of the two compared approaches differ. Only the plots for constant mass flow with $\Delta t = 90$sec and 10sec are comparable, which means that there is no further and significant improvement possible for this scenario.

- The emitted heat at variable mass flow moves in the same scale (approx. 95-120W) over all examined time intervals Δt. This is not the case for constant mass flow. There, the output varies significantly (approx. 0-800W). It can be concluded that the controllability of a radiator is better for the additional control variable $\dot{m}$, which is logical.

- Moreover, not only the general minimum and maximum values are different, but also the amplitude from one time step to another is much bigger in the case of constant mass flow. Since the given temperature profile is not complex, and the external conditions are not changing very much, the heat gain should be pretty smooth, which roughly holds for all cases with variable mass flow. However, in the case of variable mass flow with $\Delta t = 90$sec the difference of minimum and maximum values results in about 12W and in the case of variable mass flow with $\Delta t = 10$sec in about 2W.

As an interim result of this test, it can be concluded that the approach of variable mass flow with $\Delta t = 90$sec and 10sec perform best. Since the objective function for both time differences is comparable, for the subsequent investigations, the model with $\Delta t = 90$sec, and variable mass flow is used because it offers a reasonable tradeoff on complexity and accuracy.

5.3.2. Test: Price models

In this section, the logical plausibility of the modeled optimization approach is analyzed with the two different price models for energy as given in subsection 5.1. Thereby, the optimization model with the variable mass flow and $\Delta t = 90$sec is used.
As insight, both obtained results from the objective function are given below.

Price	Costs
Dynamic	124.05€
Interval with negative	-2416.68€

Table 6: Resulting costs caused by optimization with different price models.

Zone 1 with dynamic prices In the following temperature profile can be seen that around 6h, a higher temperature is needed. Therefore, the zone is preheated in advance because the price there is lower than at the moment when it is really needed (see Figure 26).

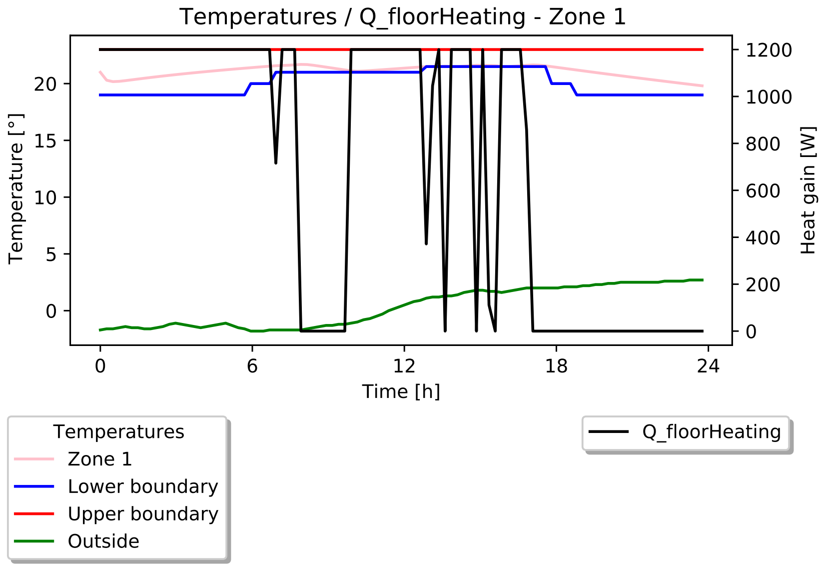

Figure 25: Dynamic price

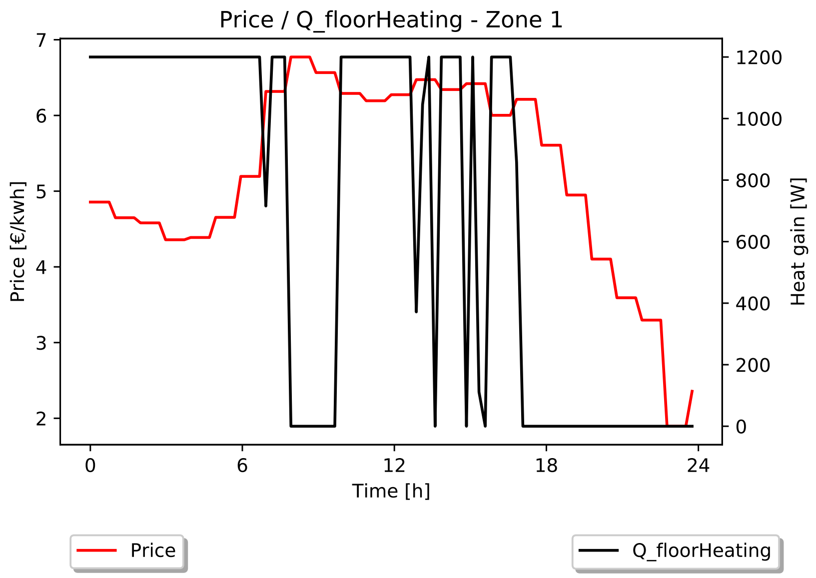

Figure 26: Dynamic price

Zone 2 with dynamic prices In zone 2, there is no change in the temperature profile. However, around 5h, it is cheaper to preheat the room for a moment than to keep the temperature permanently at the lower boundary. This is explained by the fact that the energy price increases in the daytime (cf. Figure 28).

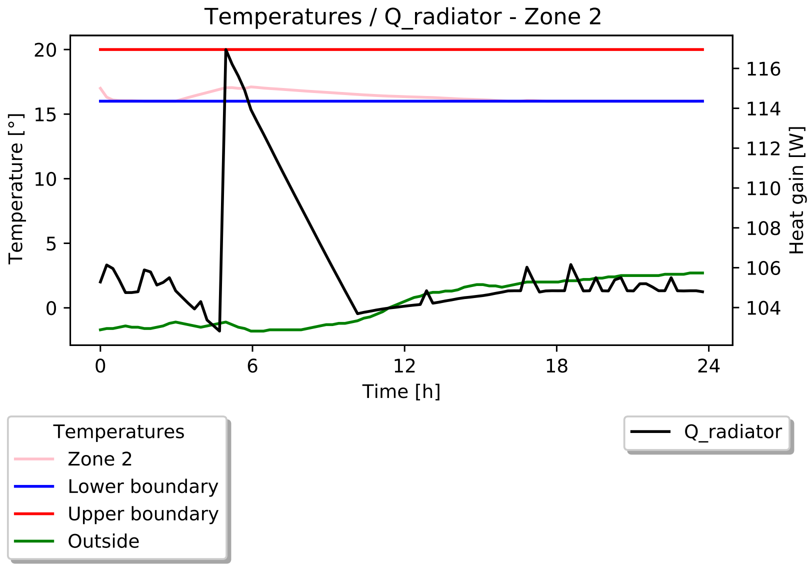

Figure 27: Dynamic price

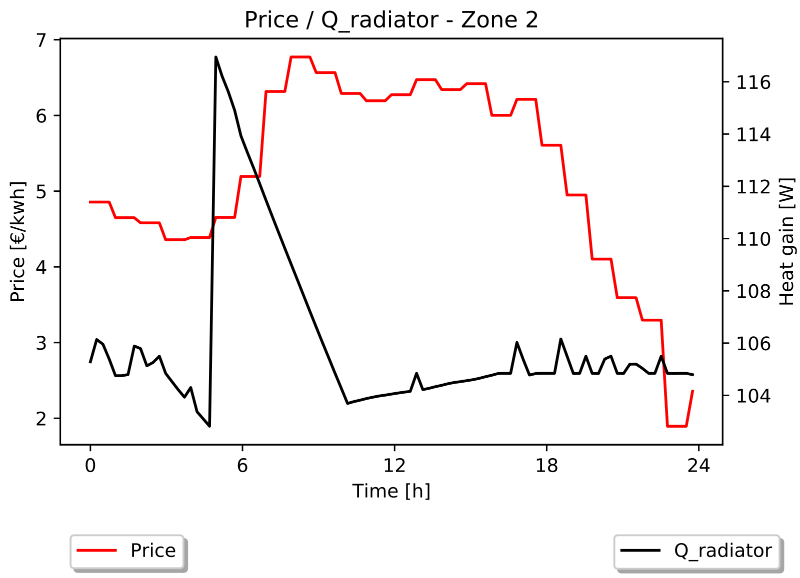

Figure 28: Dynamic price

Zone 1 with interval prices In the following two paragraphs, the interval prices are applied, where after 18h negative prices are used for testing.
It can be determined that the heat gain is reduced as much as possible in the expensive interval. Moreover, until 7h the zone is preheated to compensate the higher energy prices and raised temperature profile in the next interval. Additionally, there is a peak in heat gain to take advantage of the negative energy prices in the evening.

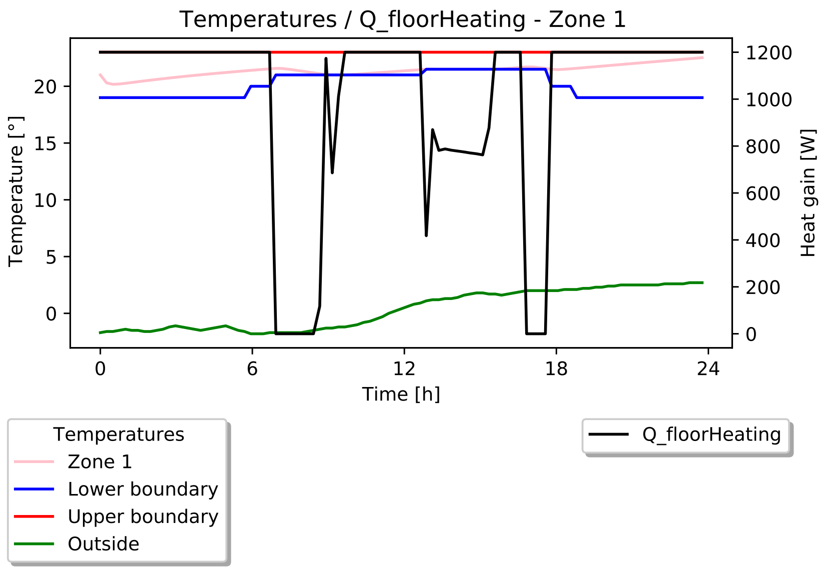

Figure 29: Interval price

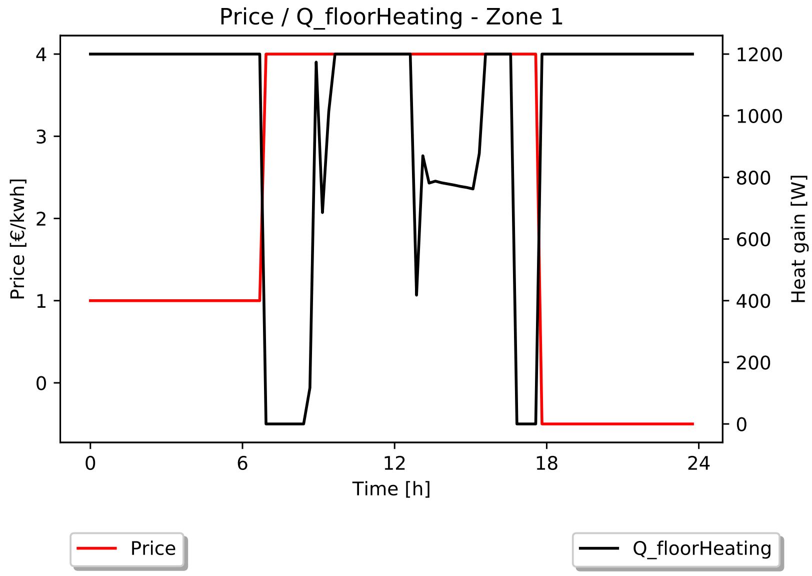

Figure 30: Interval price

Zone 2 with interval prices The same phenomena from zone 1 are repeating in zone 2, which indicates a reasonable model.
In the evening, around 18h, when the negative prices are activated, a peak in heating is visible. Also, this leads to a raised zone temperature.

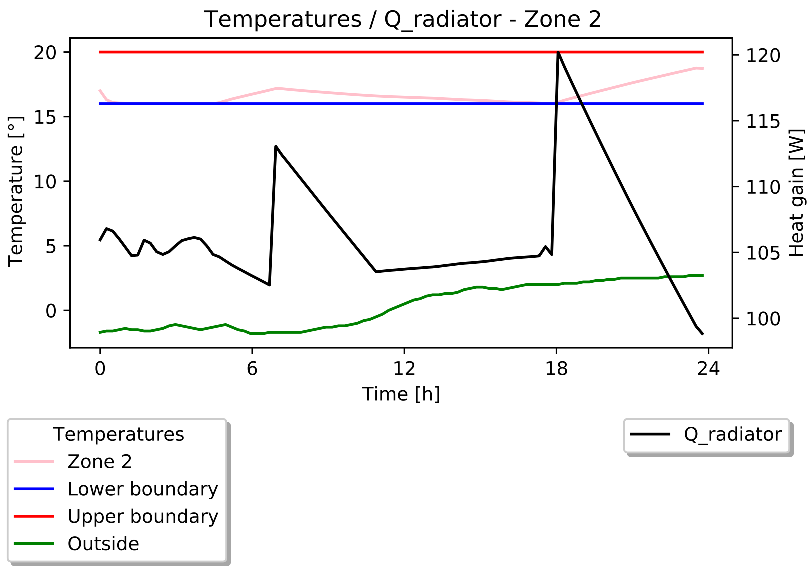

Figure 31: Interval price

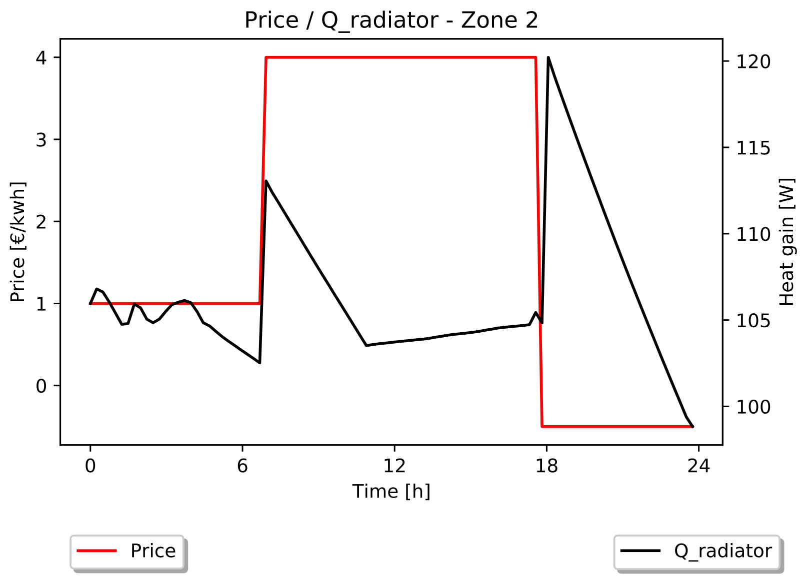

Figure 32: Interval price

5.3.3. Test: Weather impact

In this section, the impact of solar radiation and outside temperature to the zones is analyzed. Therefore, variable mass flow, $\Delta t = 90$sec and a price of 1€/kWh is used.

Effect on zone 1 Around 12h, the zone temperature advances, although the heat gain is reduced by about 30% for a larger interval (12-14h). The increased sun radiation and outdoor temperature cause this at this time. As a result, it can be concluded that the optimization considers the sun radiation in combination with outside temperature correctly and handles the heating right.

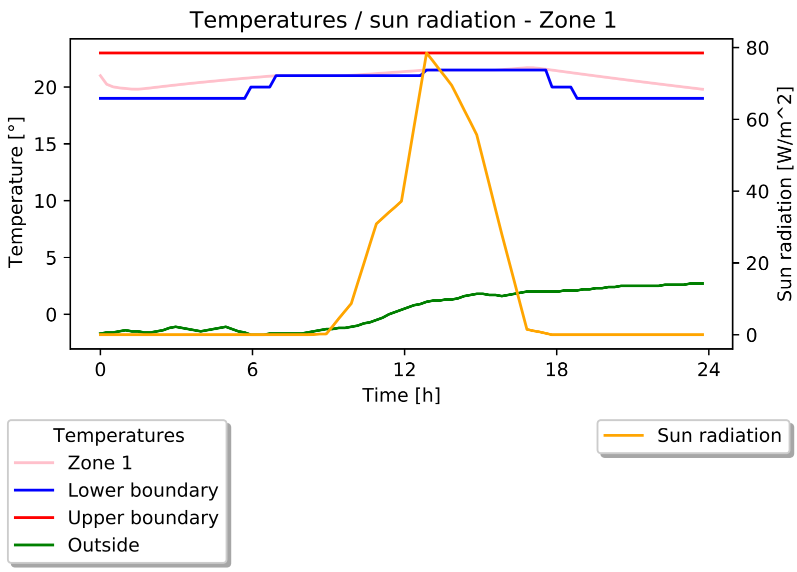

Figure 33

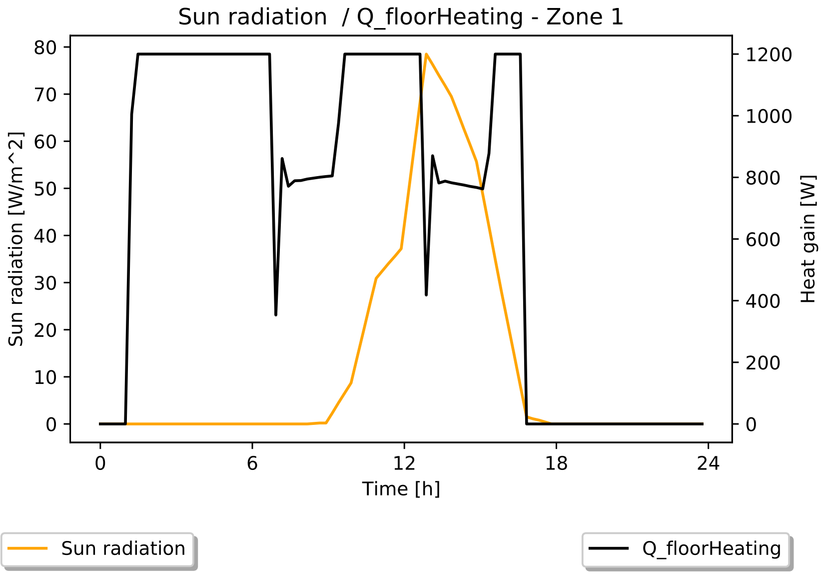

Figure 34

Effect on zone 2 Again, the sun radiation shows that the heat gain can be reduced in time of high sun radiation, although the zone temperature is around its lower bound. In other words, this means that the impact of sun radiation is treated correctly in the model.

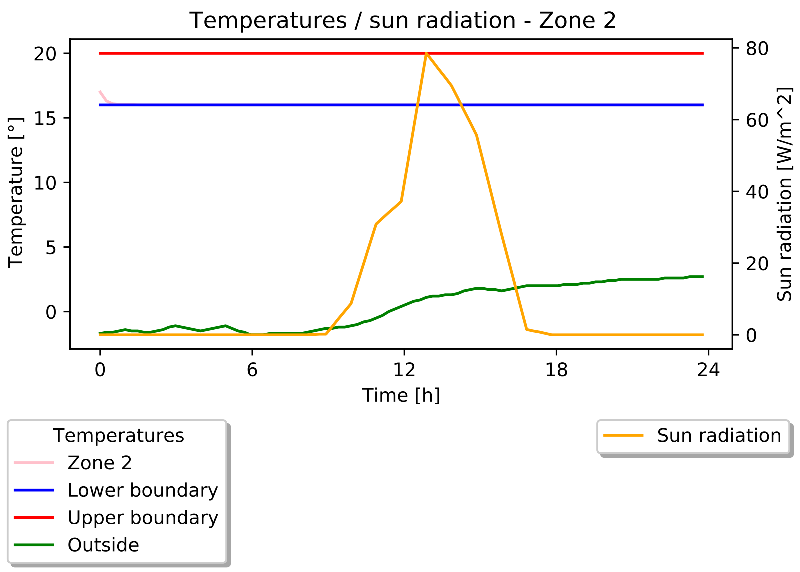

Figure 35

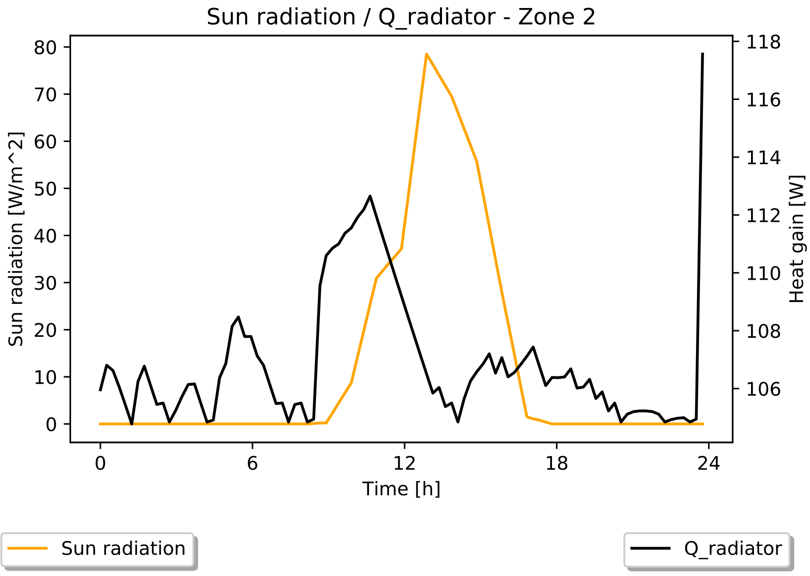

Figure 36

5.3.4. Test: Building model

With the parameters of 1€/kWh, $\Delta t = 90$sec, and variable mass flow, a change in the building configuration is studied. Therefore, the exterior wall thickness is doubled.

Effect on zone 1 It is noticeable that the energy storage functionality of walls shows up here since, for the temperature changes in the lower boundary at 7h and 13h, less energy is needed to perform these changes in the case of thicker walls. Moreover, the zone temperature is higher after 18h without heating.

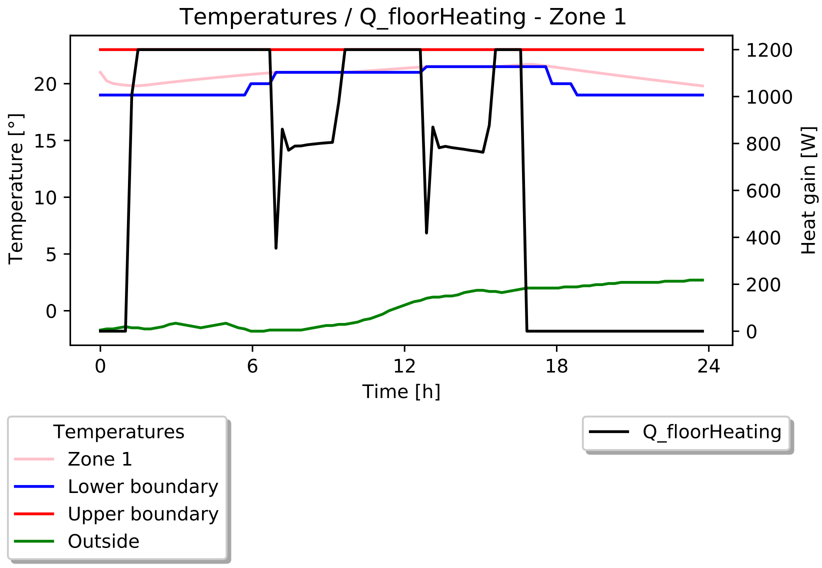

Figure 37: Thickness 0.4m; 23.38€

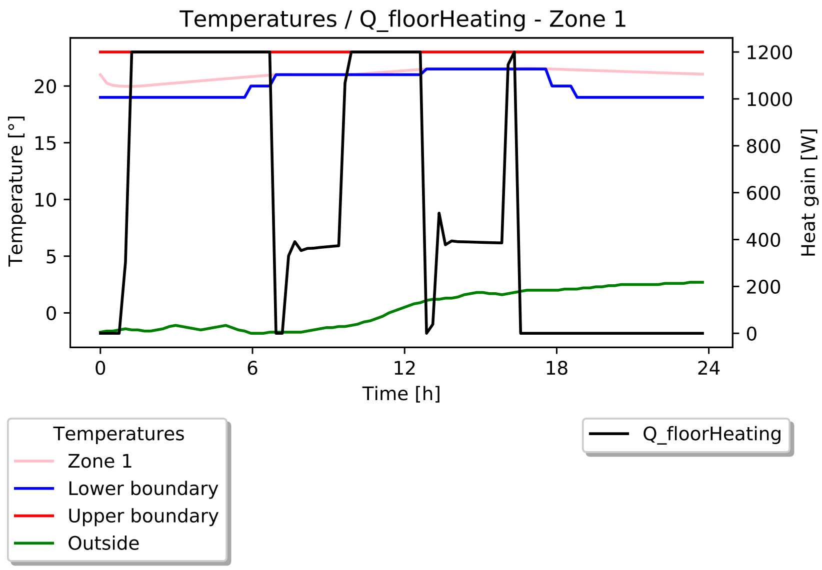

Figure 38: Thickness 0.8m; 15.85€

Effect on zone 2 Also, in zone 2 the walls' storage effect comes to use as the thicker walls are warmed more in the beginning in comparison to the thinner walls. This leads by the approx. equal value of 104-108W heat gain during the day in both cases to a minimal higher zone temperature after 12h in the situation with thicker walls.

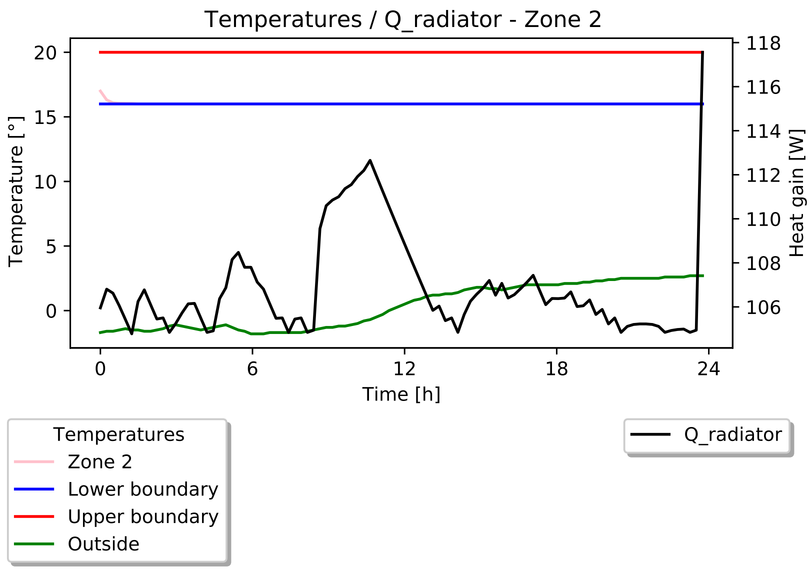

Figure 39: Thickness 0.4m; 23.38€

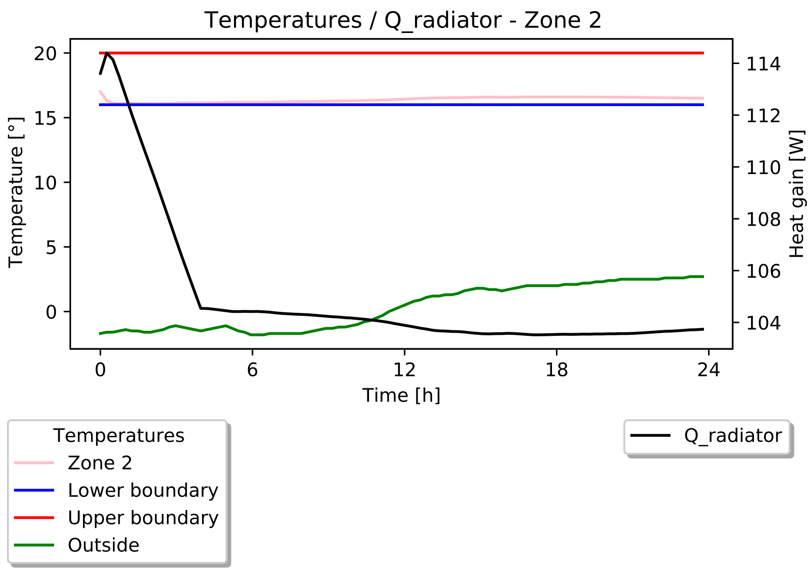

Figure 40: Thickness 0.8m; 15.85€

The results in terms of costs of the entire building are summarized below.

Exterior wall thickness	Costs
0.4m	23.38€
0.8m	15.85€

Table 7: Resulting costs caused by optimization with different wall thicknesses.

In conclusion, doubled walls lead to a saving of approximately 30% in energy. Since the impact of the thickness of a wall is treated linearly in the conduction process, the relationship is well reflected concerning other heat losses and interpolation errors. This leads to a saving of approx. 30% in the energy costs.

5.3.5. Conclusion

In summary, all planned tests are successfully passed. The derived linear model is logically optimized and allows the variation of parameters.
Thereby, the impact of different time steps of state approximations, price models, weather effects, and building configurations is investigated.
However, it is crucial to consider possible numerical errors by floating-point arithmetics when further extending the model.

Limitations Since the implementation is generalized, also multi-layered windows were tested for the simple building during the case study.
However, due to the high range of occurring numeric values, which are caused by the terms to the power of 3 and 4, and the thin gas layer in multi-layered windows in the tens of millimeters range (cf. e.g. [8]), which is converted to meters, the Gurobi solver gets into numeric errors while solving. In other words, this means that variables randomly change their sign and values, and the performed floating-point arithmetics are incorrect, although Gurobi's settings were adjusted to quad-precision or numerical focus.
This is why only a one-layered window is used for the case study, where the glazing thickness can be neglected due to the uniform glazing temperature (cf. subsection 2.4).

6. Conclusion

In summary, the thesis shows a structured and computational light approach for the linear optimization of a generalized physics (white-box) building model. Thereby, the control of HVAC-components in the context of energy costs is optimized. The result can be applied to any building in order to optimize it.
Therefore, a generalized explanation model is derived which relates a static and logical graph representation of the investigated building, formalizing its structural properties (RQ1; subsection 2.3), to a physics model, describing the general heat movements in buildings (RQ2; subsection 2.4 and subsubsection 2.6.1).
However, since physics relations are generally non-linear, this system is linearized by interpolation to obtain a linear state space model. Additionally, by the use of a finite differences approach, state space values are discretized on a uniform grid so that the ODEs are transformed to recursive equations to become a valid input for linear optimization (RQ3; subsection 3.2 and subsection 3.4).
For application, the whole approach is implemented. Thereby, the logical representation of the investigated building is built via an input of the relevant information of the building.

6.1. Future work

Nonetheless, the interpolation in this thesis is roughly estimated for all locations. This procedure can be dynamically performed to adapt the interpolation to the investigated building's location to reduce the error. Since the exterior influences of weather differ from, e.g. northern to southern location, this would change the interpolated values, e.g. for the exterior wall temperatures, that are possible.
Although the linearization performed leads to reduced complexity, an more complex approach, such as feedback linearization, could be investigated to exclude linearization errors.
Due to the modular design of the entire approach, further HVAC-components can be easily added to extend the variety in heating and cooling devices. This would enable the model to cool the building also.
Moreover, the resulting linear program itself can be optimized further by advanced methods to reduce the high range of minimum and maximum values to enable the treatment of multi-layered windows without numerical issues. Therefore, different solving algorithms, which are numerical stable, can be investigated. An example could be to use iterative refinement while solving to enable better precision in floating-point arithmetics (cf. e.g. [35]).

Appendices

A. Test: Time and mass flow modeling

Effect on zone 1

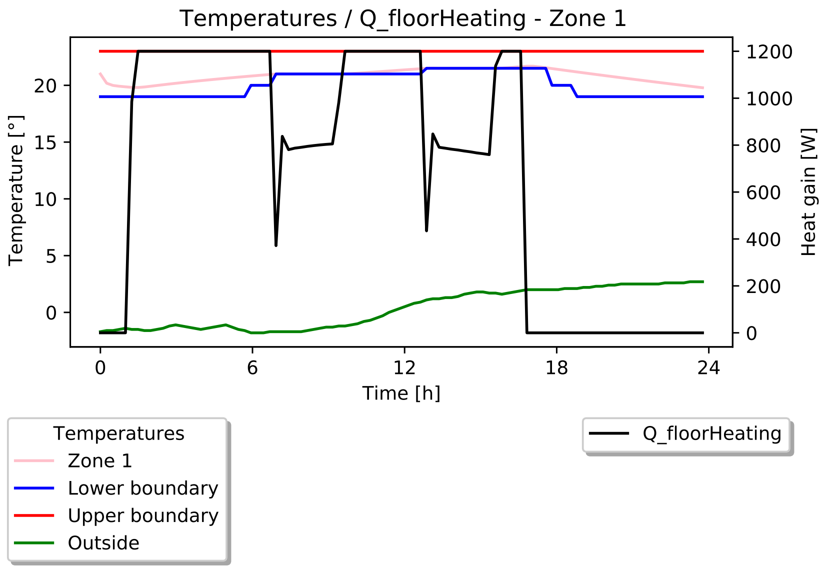

Figure 41: ΔTime 5min, constant mass flow

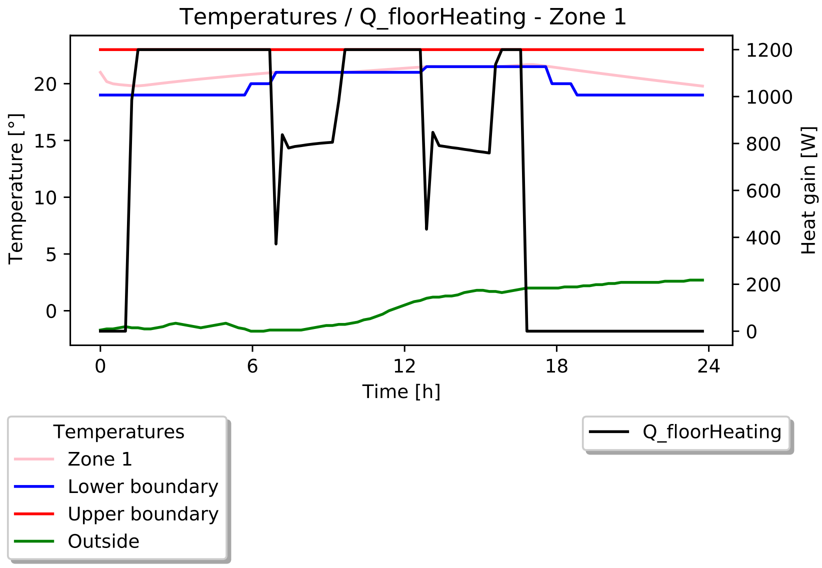

Figure 42: ΔTime 5min, variable mass flow

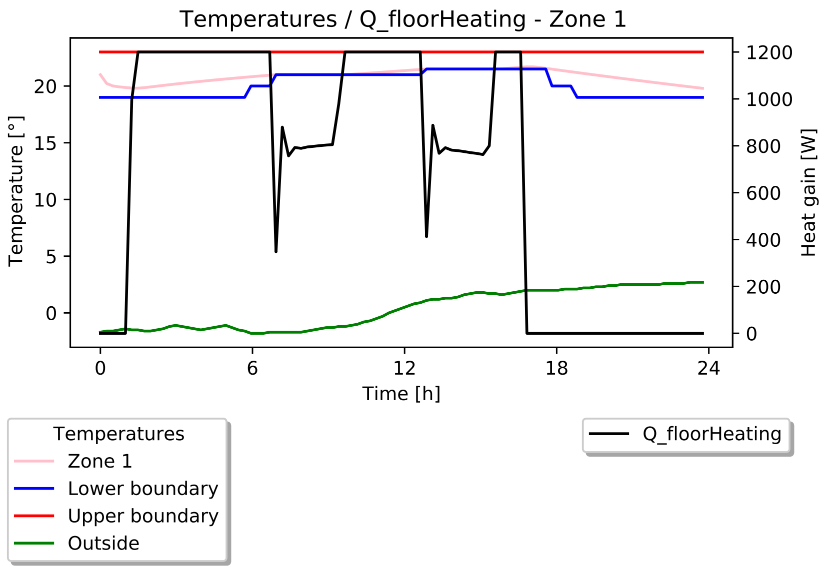

Figure 43: ΔTime 3min, constant mass flow

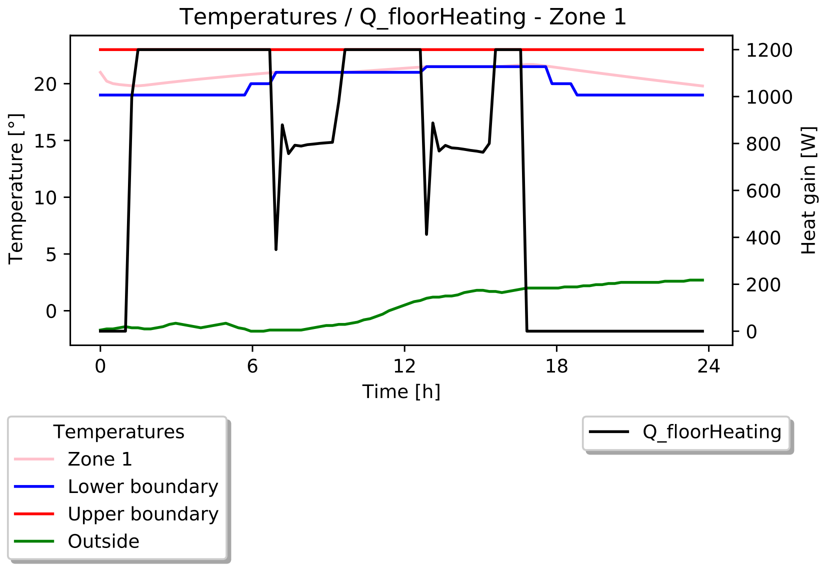

Figure 44: ΔTime 3min, variable mass flow

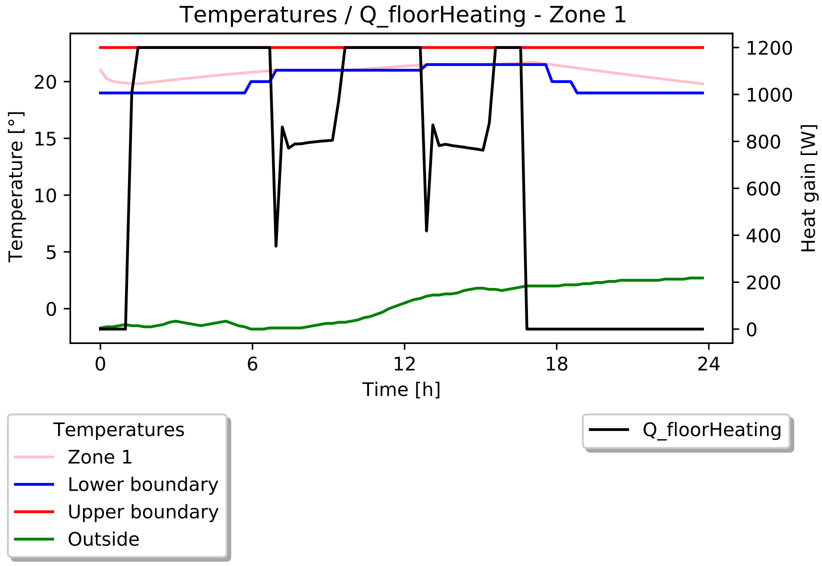

Figure 45: ΔTime 90sec, constant mass flow

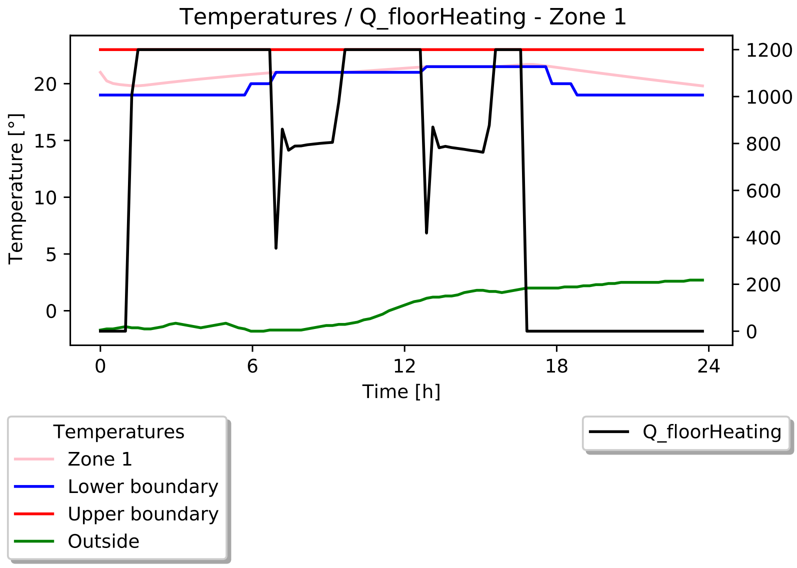

Figure 46: ΔTime 90sec, variable mass flow

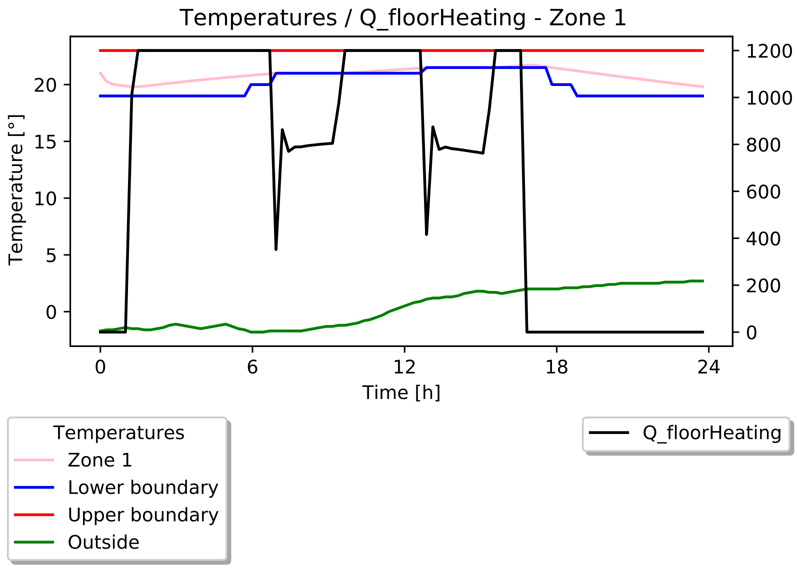

Figure 47: ΔTime 10sec, constant mass flow

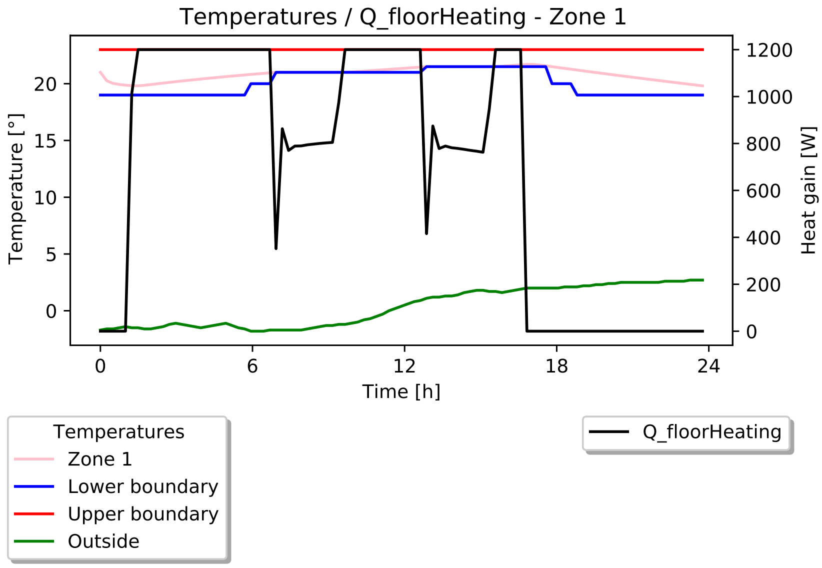

Figure 48: ΔTime 10sec, variable mass flow

Effect on zone 2

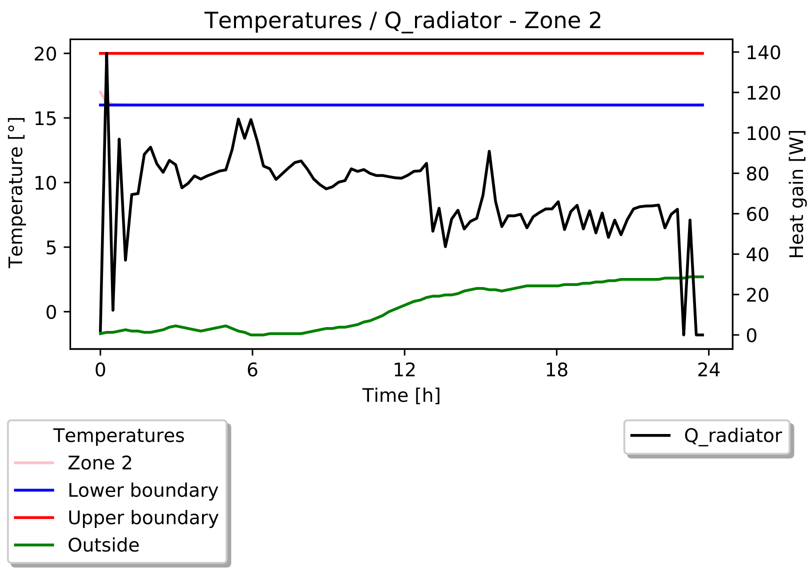

Figure 49: ΔTime 5min, constant mass flow

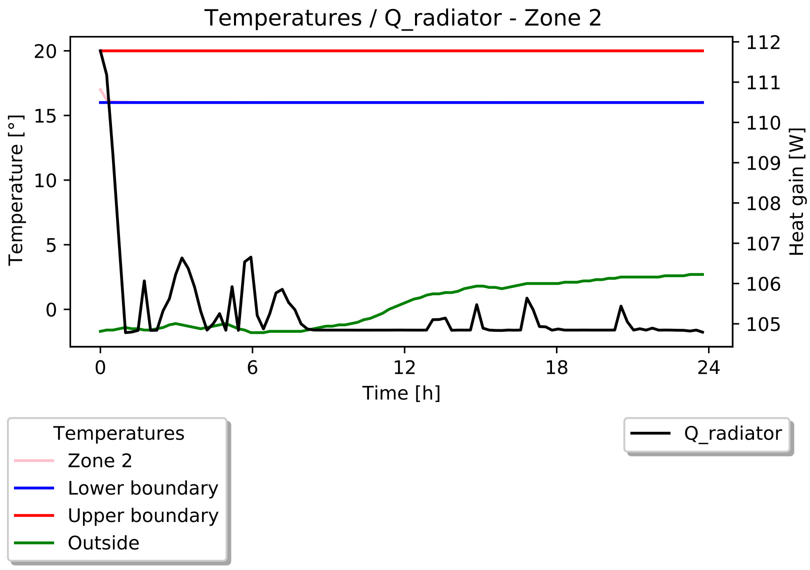

Figure 50: ΔTime 5min, variable mass flow

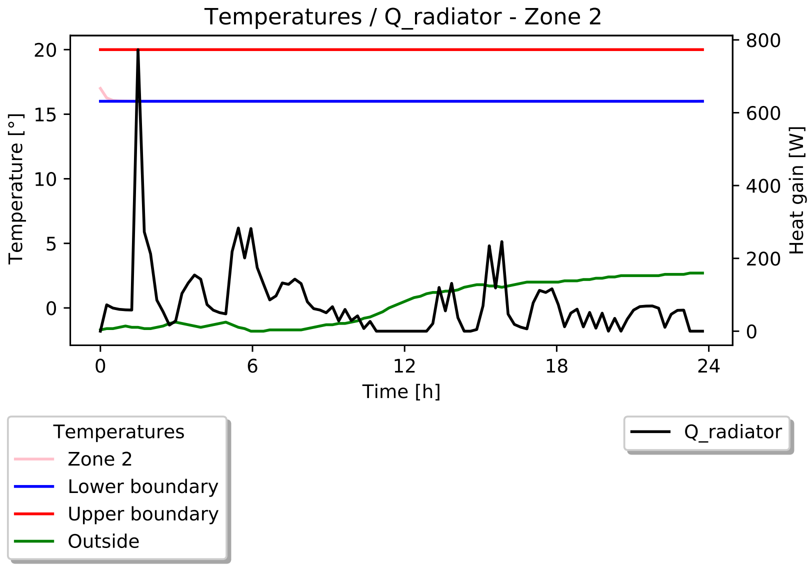

Figure 51: ΔTime 3min, constant mass flow

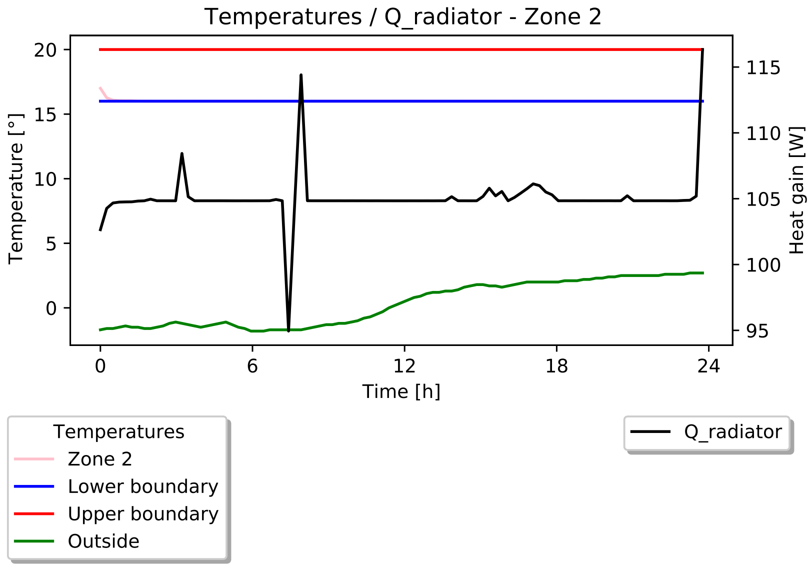

Figure 52: ΔTime 3min, variable mass flow

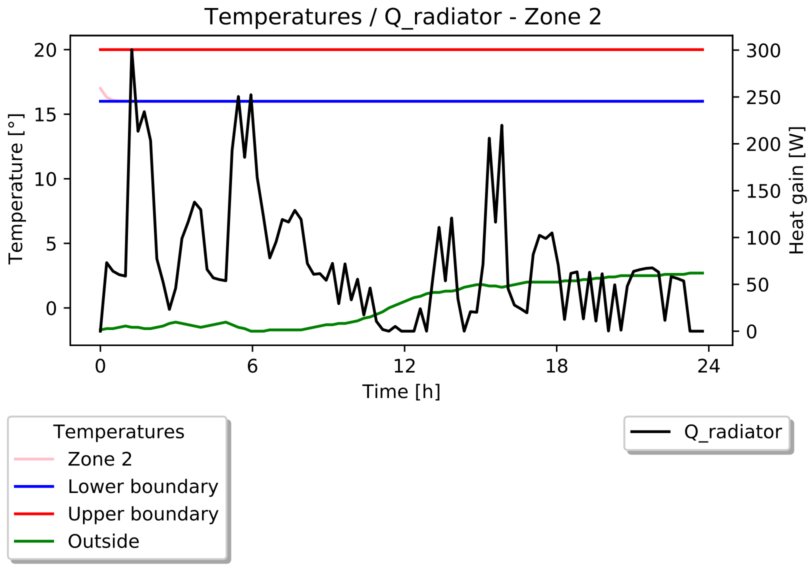

Figure 53: ΔTime 90sec, constant mass flow

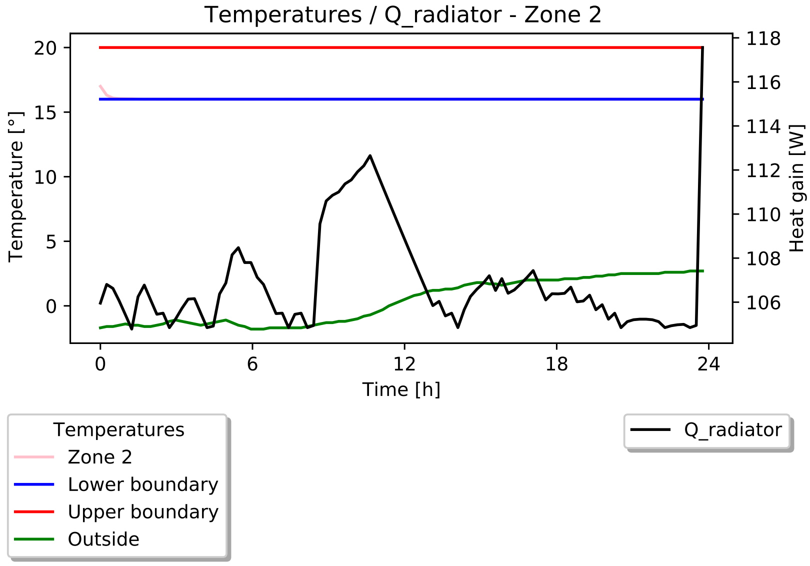

Figure 54: ΔTime 90sec, variable mass flow

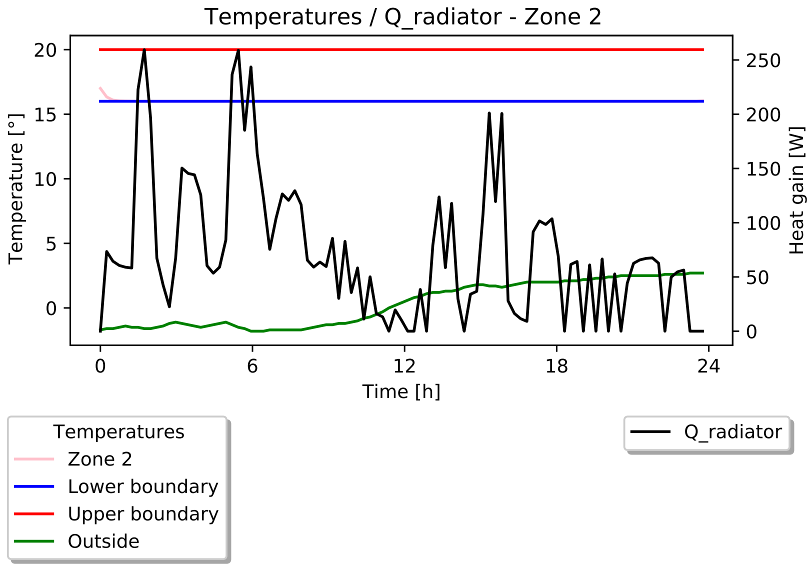

Figure 55: ΔTime 10sec, constant mass flow

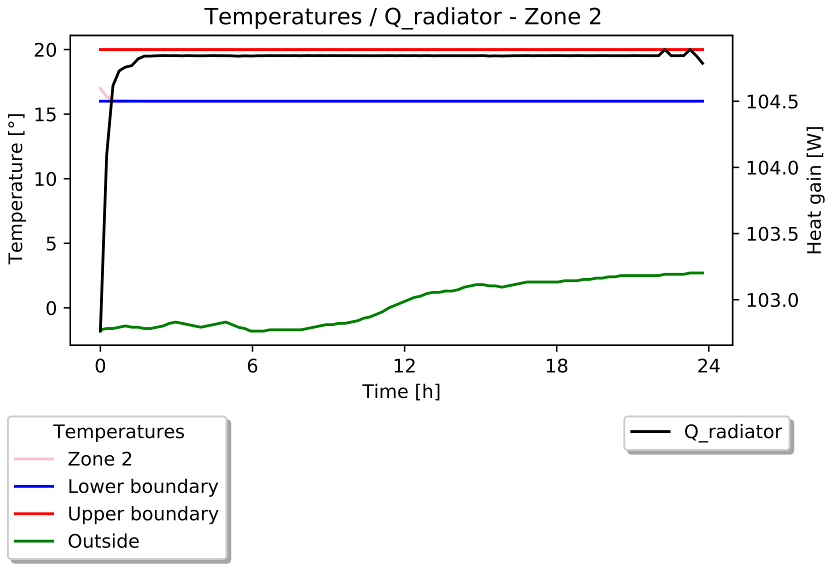

Figure 56: ΔTime 10sec, variable mass flow

References

[1] DIN EN 14511-2:2019-07, Luftkonditionierer, Flüssigkeitskühlsätze und Wärmepumpen für die Raumbeheizung und -kühlung und Prozess-Kühler mit elektrisch angetriebenen Verdichtern_- Teil_2: Prüfbedingungen; Deutsche Fassung EN_14511-2:2018. Technical report, Beuth Verlag GmbH, . URL https://www.beuth.de/de/-/-/298537580.

[2] DIN EN 14825:2019-07, Luftkonditionierer, Flüssigkeitskühlsätze und Wärmepumpen mit elektrisch angetriebenen Verdichtern zur Raumbeheizung und -kühlung_- Prüfung und Leistungsbemessung unter Teillastbedingungen und Berechnung der jahreszeitbedingten Leistungszahl; Deutsche Fassung EN_14825:2018. Technical report, Beuth Verlag GmbH, . URL https://www.beuth.de/de/-/-/286479610.

[3] DIN 4108-4:2020-11, Wärmeschutz und Energie-Einsparung in Gebäuden_- Teil_4: Wärme- und feuchteschutztechnische Bemessungswerte. Technical report, Beuth Verlag GmbH, . URL https://www.beuth.de/de/-/-/327502903.

[4] Vorlauftemperatur Buderus. URL https://www.buderus.de/de/waermepumpe/vorlauftemperatur.

[5] Schematic floor heating, . URL https://www.alibaba.com/product-detail/Manufacturer-120W-sqft-electric-underfloor-heating_60726552273.html.

[6] Exemplary radiator, . URL https://cdn.hornbach.de/cmsm/de/chke2-d0/c8640d2d7a67e7d07fa3ad7d83bb95/heizkoerper-montieren-anleitung-as-05-768x512.jpg.webp.

[7] Vorlauftemperatur Vaillant. URL http://www.vaillant.de/heizung/heizung-verstehen/tipps-rund-um-ihre-heizung/vorlauf-rucklauftemperatur/.

[8] Fenster-Verglasung: Glas, Glasstärke, Abstandshalter. URL https://www.energiesparhaus.at/gebaeudehuelle/fenster-verglasung.htm.

[9] Abdul Afram and Farrokh Janabi-Sharifi. Review of modeling methods for HVAC systems. *Applied Thermal Engineering*, 67(1-2):507–519, June 2014. ISSN 13594311. doi: 10.1016/j.applthermaleng.2014.03.055. URL https://linkinghub.elsevier.com/retrieve/pii/S1359431114002348.

[10] Byung-Cheon Ahn. Radiant Floor Heating System. *Developments in Heat Transfer*, page 22, 2011.

[11] F. Alamdari and G. P. Hammond. Improved data correlations for buoyancy-driven convection in rooms. *Building Services Engineering Research and Technology*, 4

(3):106–112, August 1983. ISSN 0143-6244. doi: 10.1177/014362448300400304. URL https://doi.org/10.1177/014362448300400304.

[12] Frank Allgöwer and Ernst Dieter Gilles. Nichtlinearer Reglerentwurf auf der Grundlage exakter Linearisierungstechniken. 1993. doi: 10.18419/opus-4405. URL http://elib.uni-stuttgart.de/handle/11682/4422.

[13] Fatima Amara, K. Agbossou, Alben Cardenas, Yves Dubé, and Sousso Kelouwani. Comparison and Simulation of Building Thermal Models for Effective Energy Management. *Smart Grid and Renewable Energy*, 06:95–112, January 2015. doi: 10.4236/sgre.2015.64009.

[14] Erling Andersen. Linear optimization: Theory, methods, and extensions. November 2001.

[15] Carlos Henggeler Antunes, Vahid Rasouli, Maria João Alves, Álvaro Gomes, José J. Costa, and Adélio Gaspar. A Discussion of Mixed Integer Linear Programming Models of Thermostatic Loads in Demand Response. In Valentin Bertsch, Armin Ardone, Michael Suriyah, Wolf Fichtner, Thomas Leibfried, and Vincent Heuveline, editors, *Advances in Energy System Optimization*, pages 105–122. Springer International Publishing, Cham, 2020. ISBN 978-3-030-32156-7 978-3-030-32157-4. doi: 10.1007/978-3-030-32157-4_7. URL http://link.springer.com/10.1007/978-3-030-32157-4_7.

[16] Tilo Arens, Rolf Busam, Frank Hettlich, Christian Karpfinger, and Hellmuth Stachel. *Differenzialrechnung — die Linearisierung von Funktionen*, pages 551–597. Springer Berlin Heidelberg, Berlin, Heidelberg, 2013. ISBN 978-3-8274-2308-5 978-3-8274-2309-2. doi: 10.1007/978-3-8274-2309-2_15. URL http://link.springer.com/10.1007/978-3-8274-2309-2_15.

[17] Araz Ashouri, Samuel Fux, Michael Benz, and Lino Guzzella. Optimal design and operation of building services using mixed-integer linear programming techniques. *Energy*, 59, September 2013. doi: 10.1016/j.energy.2013.06.053.

[18] ASHRAE, editor. *2001 ASHRAE Handbook: Fundamentals. SI Edition*. ASHRAE, Atlanta, Ga, 2001. ISBN 978-1-883413-88-0.

[19] ASHRAE. ANSI/ASHRAE Addendum a to ANSI/ASHRAE Standard 140-2017. 2020.

[20] H. B. Awbi and A. Hatton. Natural convection from heated room surfaces. *Energy and Buildings*, 30(3):233–244, August 1999. ISSN 0378-7788. doi: 10.1016/S0378-7788(99)00004-3. URL https://www.sciencedirect.com/science/article/pii/S0378778899000043.

[21] Hazim B. Awbi. Calculation of convective heat transfer coefficients of room surfaces for natural convection. *Energy and Buildings*, 28(2):219–227, October

1998. ISSN 0378-7788. doi: 10.1016/S0378-7788(98)00022-X. URL https://www.sciencedirect.com/science/article/pii/S037877889800022X.

[22] Benakopoulos, Salenbien, Vanhoudt, and Svendsen. Improved Control of Radiator Heating Systems with Thermostatic Radiator Valves without Pre-Setting Function. *Energies*, 12(17):3215, August 2019. ISSN 1996-1073. doi: 10.3390/en12173215. URL https://www.mdpi.com/1996-1073/12/17/3215.

[23] T. L. Bergman, editor. *Introduction to Heat Transfer*. Wiley, Hoboken, NJ, 6th ed edition, 2011. ISBN 978-0-470-50196-2.

[24] Christian Brembilla, Mohsen Soleimani-Mohseni, and Thomas Olofsson. TRANSIENT MODEL OF A PANEL RADIATOR. page 8, 2015.

[25] Michael Buhl, Oliver Fritsch, and Boris Lohmann. Exakte Ein-/Ausgangslinearisierung für die translatorische Dynamik eines Quadrocopters. *at - Automatisierungstechnik*, 59(6), January 2011. ISSN 0178-2312. doi: 10.1524/auto.2011.0932. URL http://www.degruyter.com/view/j/auto.2011.59.issue-6/auto.2011.0932/auto.2011.0932.xml.

[26] Bundesverband Wärmepumpe e.V. JAZ-Rechner. URL https://www.waermepumpe.de/normen-technik/jazrechner/.

[27] Yunus A. Cengel. *Introduction To Thermodynamics and Heat Transfer*. McGraw-Hill Education - Europe, Boston, 2. edition edition, February 2009. ISBN 978-0-07-128773-9.

[28] Joseph Clarke. *Energy Simulation in Building Design*. Routledge, Oxford, 2. edition edition, September 2001. ISBN 978-0-7506-5082-3.

[29] Joachim Clemens. *Entwicklung Eines Einfachen Modells Zur Abschätzung Der Sommerlichen Überwärmung in Gebäuden*. PhD thesis, Universität Siegen, May 2000.

[30] Borui Cui, Cheng Fan, Jeffrey Munk, Ning Mao, Linda Xiao, Jin Dong, and Teja Kuruganti. A hybrid building thermal modeling approach for predicting temperatures in typical, detached, two-story houses. *Applied Energy*, 236:101–116, February 2019. doi: 10.1016/j.apenergy.2018.11.077.

[31] İbrahim Dinçer and Marc Rosen. *Exergy Analysis of Heating, Refrigerating, and Air Conditioning: Methods and Applications*. Elsevier, Amsterdam ; Boston, 2015. ISBN 978-0-12-417203-6.

[32] John A. Duffie and William A. Beckman. *Solar Engineering of Thermal Processes*. Wiley, New York, 4. ed edition, 2013. ISBN 978-0-470-87366-3.

[33] Baligh El Hefni and Daniel Bouskela. *Modeling and Simulation of Thermal Power Plants with ThermoSysPro: A Theoretical Introduction and a Practical Guide.* Springer International Publishing, Cham, 2019. ISBN 978-3-030-05104-4 978-3-030-05105-1. doi: 10.1007/978-3-030-05105-1. URL http://link.springer.com/10.1007/978-3-030-05105-1.

[34] Joel H. Ferziger and Milovan Perić. *Numerische Strömungsmechanik.* Springer, Berlin Heidelberg, 2008. ISBN 978-3-540-67586-0 978-3-540-68228-8.

[35] Ambros M. Gleixner, Daniel E. Steffy, and Kati Wolter. Improving the accuracy of linear programming solvers with iterative refinement. In *Proceedings of the 37th International Symposium on Symbolic and Algebraic Computation - ISSAC '12*, pages 187–194, Grenoble, France, 2012. ACM Press. ISBN 978-1-4503-1269-1. doi: 10.1145/2442829.2442858. URL http://dl.acm.org/citation.cfm?doid=2442829.2442858.

[36] J. Gustafsson, J. Delsing, and J. van Deventer. Thermodynamic Simulation of a Detached House with District Heating Subcentral. In *2008 2nd Annual IEEE Systems Conference*, pages 1–8, Montreal, QC, Canada, April 2008. IEEE. ISBN 978-1-4244-2149-7 978-1-4244-2150-3. doi: 10.1109/SYSTEMS.2008.4519054. URL http://ieeexplore.ieee.org/document/4519054/.

[37] V.S.K.V. Harish and Arun Kumar. A review on modeling and simulation of building energy systems. *Renewable and Sustainable Energy Reviews*, 56:1272–1292, April 2016. ISSN 13640321. doi: 10.1016/j.rser.2015.12.040. URL https://linkinghub.elsevier.com/retrieve/pii/S1364032115014239.

[38] M. Henson. Chapter 4 Feedback Linearizing Control, 2006.

[39] Winfried Hochstättler. *Lineare Optimierung.* Springer Berlin Heidelberg, Berlin, Heidelberg, 2017. ISBN 978-3-662-54424-2 978-3-662-54425-9. doi: 10.1007/978-3-662-54425-9. URL http://link.springer.com/10.1007/978-3-662-54425-9.

[40] Jörg Hoffmann. *Informationssystem-Architekturen produzierender Unternehmen bei software-definierten Plattformen.* PhD thesis, 2018.

[41] Raad Homod. Review on the HVAC System Modeling Types and the Shortcomings of Their Application. *Journal of Energy*, 2013, May 2013. doi: 10.1155/2013/768632.

[42] Ipseng Iu and D E Fisher. Application of Conduction Transfer Functions and Periodic Response Factors in Cooling Load Calculation Procedures. *ASHRAE Transactions*, 2004.

[43] V O Kaledin, E S Viachkin, A E Gileva, E A Viachkina, D A Galgin, and A D Ulyanov. Model of heat and mass transfer in the heating system pipe. *Journal*

of Physics: Conference Series, 1382:012197, November 2019. ISSN 1742-6588, 1742-6596. doi: 10.1088/1742-6596/1382/1/012197. URL https://iopscience.iop.org/article/10.1088/1742-6596/1382/1/012197.

[44] N. Karmarkar. A new polynomial-time algorithm for linear programming. *Combinatorica*, 4(4):373–395, December 1984. ISSN 1439-6912. doi: 10.1007/BF02579150. URL https://doi.org/10.1007/BF02579150.

[45] Anthony Kelman and Francesco Borrelli. Bilinear Model Predictive Control of a HVAC System Using Sequential Quadratic Programming. *IFAC Proceedings Volumes*, 44(1):9869–9874, January 2011. ISSN 1474-6670. doi: 10.3182/20110828-6-IT-1002.03811. URL http://www.sciencedirect.com/science/article/pii/S1474667016451979.

[46] Abdul-Jabbar N Khalifa. Natural convective heat transfer coefficient - a review II. Surfaces in two- and three-dimensional enclosures. *Energy Conversion and Management*, page 13, 2001.

[47] Hassan K. Khalil. *Nonlinear Systems*. Prentice Hall, Upper Saddle River, N.J, 3rd ed edition, 2002. ISBN 978-0-13-067389-3.

[48] Ken-ichi Kimura. *Scientific Basis of Air Conditioning*. December 2016. ISBN 978-4-9907042-3-0.

[49] Anand Kushwah, Krishna Dutta Pandey, Ankur Gupta, and Gaurav Saxena. Thermal Modeling of Heat Exchanger: A Review. *International Journal of Advance Research in Engineering, Science & Technology*, 4:30–35, January 2017.

[50] T. Kusuda and P. Achenbach. Earth Temperature and Thermal Diffusivity at Selected Stations in the United States. 1965. doi: 10.6028/NBS.RPT.8972.

[51] Moritz Lauster, Peter Remmen, Marcus Fuchs, Jens Teichmann, Rita Streblow, and Dirk Müller. Modelling long-wave radiation heat exchange for thermal network building simulations at urban scale using Modelica. In *The 10th International Modelica Conference, March 10-12, 2014, Lund, Sweden*, pages 125–133, March 2014. doi: 10.3384/ecp14096125. URL http://www.ep.liu.se/ecp/article.asp?issue=096%26article=13.

[52] Catherine Lewis. Linear Programming: Theory and Applications. page 66, 2008.

[53] Xiang Qian Li, Youming Chen, J. D. Spitler, and D. Fisher. Applicability of calculation methods for conduction transfer function of building constructions. *International Journal of Thermal Sciences*, 48(7):1441–1451, July 2009. ISSN 1290-0729. doi: 10.1016/j.ijthermalsci.2008.11.006. URL https://www.sciencedirect.com/science/article/pii/S1290072908002299.

[54] Xiwang Li and Jin Wen. Review of building energy modeling for control and operation. *Renewable and Sustainable Energy Reviews*, 37:517–537, September 2014. ISSN 13640321. doi: 10.1016/j.rser.2014.05.056. URL https://linkinghub.elsevier.com/retrieve/pii/S1364032114003815.

[55] Benjamin Y. H. Liu and Richard C. Jordan. The interrelationship and characteristic distribution of direct, diffuse and total solar radiation. *Solar Energy*, 4 (3):1–19, July 1960. ISSN 0038-092X. doi: 10.1016/0038-092X(60)90062-1. URL http://www.sciencedirect.com/science/article/pii/0038092X60900621.

[56] Benjamin Y.H. Liu and Richard C. Jordan. The long-term average performance of flat-plate solar-energy collectors. *Solar Energy*, 7(2):53–74, April 1963. ISSN 0038092X. doi: 10.1016/0038-092X(63)90006-9. URL https://linkinghub.elsevier.com/retrieve/pii/0038092X63900069.

[57] Xiaoshu Lü. Modelling of heat and moisture transfer in buildings: I. Model program. *Energy and Buildings*, 34(10):1033–1043, November 2002. ISSN 0378-7788. doi: 10.1016/S0378-7788(02)00021-X. URL http://www.sciencedirect.com/science/article/pii/S037877880200021X.

[58] Jack Macki and Aaron Strauss. *Introduction to Optimal Control Theory*. January 1995. ISBN 978-1-4612-5673-1. doi: 10.1007/978-1-4612-5671-7.

[59] Uwe Mayer. Heizflächen. Technical report, Beuth Verlag GmbH, 2005. URL https://www.beuth.de/de/-/-/28818252.

[60] M. Mirsadeghi, D. Cóstola, B. Blocken, and J. L. M. Hensen. Review of external convective heat transfer coefficient models in building energy simulation programs: Implementation and uncertainty. *Applied Thermal Engineering*, 56(1):134–151, July 2013. ISSN 1359-4311. doi: 10.1016/j.applthermaleng.2013.03.003. URL https://www.sciencedirect.com/science/article/pii/S1359431113001543.

[61] Jana Mižáková and Ján Pitel'. An analytical dynamic model of heat transfer from the heating body to the heated room. *MATEC Web of Conferences*, 125: 02047, 2017. ISSN 2261-236X. doi: 10.1051/matecconf/201712502047. URL http://www.matec-conferences.org/10.1051/matecconf/201712502047.

[62] Saman Mostafavi, Robert Cox, Benjamin Futrell, and Roshanak Ashrafi. Calibration of White-Box Whole-Building Energy Models Using a Systems-Identification Approach. pages 795–800, October 2018. doi: 10.1109/IECON.2018.8591845.

[63] National Renewable Energy Laboratory. Saving Energy with Electric Resistance Heating. *DOE/GO-10097-381*, 1997.

[64] Oliver Nelles. Nonlinear Global Optimization. In Oliver Nelles, editor, *Nonlinear System Identification: From Classical Approaches to Neural Networks and*

Fuzzy Models, pages 113–136. Springer, Berlin, Heidelberg, 2001. ISBN 978-3-662-04323-3. doi: 10.1007/978-3-662-04323-3_5. URL https://doi.org/10.1007/978-3-662-04323-3_5.

[65] Henk Nijmeijer and Arjan van der Schaft. Feedback Linearization of Nonlinear Systems. In Henk Nijmeijer and Arjan van der Schaft, editors, *Nonlinear Dynamical Control Systems*, pages 161–192. Springer, New York, NY, 1990. ISBN 978-1-4757-2101-0. doi: 10.1007/978-1-4757-2101-0_6. URL https://doi.org/10.1007/978-1-4757-2101-0_6.

[66] Mohammad Ostadijafari and Anamika Dubey. Linear Model-Predictive Controller (LMPC) for Building's Heating Ventilation and Air Conditioning (HVAC) System. *arXiv:1906.00352 [cs]*, June 2019. URL http://arxiv.org/abs/1906.00352.

[67] Camille Pajot, Nils Artiges, Benoît Delinchant, and Yves Maréchal. Building Reduced Model for MILP Optimization: Application to Demand Response of Residential Buildings. page 9, September 2019.

[68] Damien Picard, Filip Jorissen, and L. Helsen. Methodology for Obtaining Linear State Space Building Energy Simulation Models. pages 51–58, September 2015. doi: 10.3384/ecp1511851.

[69] Damien Picard, Maarten Sourbron, Zdeněk Váňa, Jiří Cigler, Lukáš Ferkl, L. Helsen, and Filip Jorissen. Comparison of Model Predictive Control Performance Using Grey-Box and White-Box Controller Models of a Multi-zone Office Building. July 2016.

[70] Jerson A. Pinzon, Pedro P. Vergara, Luiz C. P. da Silva, and Marcos J. Rider. An MILP model for optimal management of energy consumption and comfort in smart buildings. In *2017 IEEE Power & Energy Society Innovative Smart Grid Technologies Conference (ISGT)*, pages 1–5, Washington, DC, USA, April 2017. IEEE. ISBN 978-1-5386-2890-4. doi: 10.1109/ISGT.2017.8085956. URL http://ieeexplore.ieee.org/document/8085956/.

[71] Aung Pyae. *Linear Programming Formulations (Formulations and Calculations Using R Programming)*. March 2019. doi: 10.13140/RG.2.2.25441.35688.

[72] Erick Ronoh and Thomas Rath. Modelling of longwave radiation exchange at greenhouse surfaces under all-sky conditions. 17:23–35, December 2015.

[73] Ioan Sarbu and Calin Sebarchievici. Performance Evaluation of Radiator and Radiant Floor Heating Systems for an Office Room Connected to a Ground-Coupled Heat Pump. *Energies*, 9(4):228, March 2016. ISSN 1996-1073. doi: 10.3390/en9040228. URL http://www.mdpi.com/1996-1073/9/4/228.

[74] Mark Schulze. Linear Programming for Optimization. September 2000.

[75] Arvid Skartveit and Jan Asle Olseth. A model for the diffuse fraction of hourly global radiation. *Solar Energy*, 38(4):271–274, January 1987. ISSN 0038-092X. doi: 10.1016/0038-092X(87)90049-1. URL `http://www.sciencedirect.com/science/article/pii/0038092X87900491`.

[76] Paweł Skruch. A thermal model of the building for the design of temperature control algorithms. *Automatyka/Automatics*, 18(1):9, 2014. ISSN 1429-3447. doi: 10.7494/automat.2014.18.1.9. URL `http://journals.bg.agh.edu.pl/AUTOMAT/2014.18.1/9.php`.

[77] Dawid Taler and Jan Taler. Simple heat transfer correlations for turbulent tube flow. *E3S Web of Conferences*, 13:02008, 2017. ISSN 2267-1242. doi: 10.1051/e3sconf/20171302008. URL `http://www.e3s-conferences.org/10.1051/e3sconf/20171302008`.

[78] Teschl. *Mathematik für Informatiker*. eXamen.press. Springer Berlin Heidelberg, Berlin, Heidelberg, 2008. ISBN 978-3-540-77431-0 978-3-540-77432-7. doi: 10.1007/978-3-540-77432-7. URL `http://link.springer.com/10.1007/978-3-540-77432-7`.

[79] Armin Teskeredzic and Rejhana Blazevic. Transient Radiator Room Heating—Mathematical Model and Solution Algorithm. *Buildings*, 8(11):163, November 2018. ISSN 2075-5309. doi: 10.3390/buildings8110163. URL `http://www.mdpi.com/2075-5309/8/11/163`.

[80] C. P. Underwood and F. W. H. Yik. *Modelling Methods for Energy in Buildings*. Blackwell Science, Oxford ; Malden, MA, 2004. ISBN 978-0-632-05936-2.

[81] Thomas Unger and Stephan Dempe. *Lineare Optimierung: Modell, Lösung, Anwendung*. Studienbücher Wirtschaftsmathematik. Vieweg + Teubner, Wiesbaden, 1. aufl edition, 2010. ISBN 978-3-8351-0139-5.

[82] VDI-Fachbereich Energietechnik. *VDI 4650 Blatt 2 - Kurzverfahren zur Berechnung der Jahresheizzahl und des Jahresnutzungsgrads von Sorptionswärmepumpenanlagen - Gas-Wärmepumpen zur Raumheizung und Warmwasserbereitung*. 2013. URL `https://www.vdi.de/richtlinien/details/vdi-4650-blatt-2-kurzverfahren-zur-berechnung-der-jahresheizzahl-und-des-jahres`

[83] VDI-Fachbereich Energietechnik. *VDI 4650 Blatt 1 - Berechnung der Jahresarbeitszahl von Wärmepumpenanlagen - Elektrowärmepumpen zur Raumheizung und Trinkwassererwärmung*. 2019. URL `https://www.vdi.de/richtlinien/details/vdi-4650-blatt-1-berechnung-der-jahresarbeitszahl-von-waermepumpenanlagen-elekt`

[84] H. P. Williams. *Model Building in Mathematical Programming*. Wiley, Hoboken, N.J, 5th ed edition, 2013. ISBN 978-1-118-44333-0.

[85] Siyu Wu and J. Q. Sun. A physics-based linear parametric model of room temperature in office buildings, April 2012.

[86] Mehry Yazdanian and Joseph Klems. Measurement of the Exterior Convective Film Coefficient for Windows in Low-Rise Buildings. *ASHRAE Transactions*, 100, Part 1, 1993.

[87] Ryohei Yokoyama, Yuji Shinano, Syusuke Taniguchi, Masashi Ohkura, and Tetsuya Wakui. Optimization of energy supply systems by MILP branch and bound method in consideration of hierarchical relationship between design and operation. *Energy Conversion and Management*, 92:92–104, March 2015. ISSN 01968904. doi: 10.1016/j.enconman.2014.12.020. URL `https://linkinghub.elsevier.com/retrieve/pii/S0196890414010498`.